

Syracuse University

SURFACE

Dissertations - ALL

SURFACE

December 2020

Atmospheric Chemistry of Outdoor and Indoor Environments: Physical and Chemical Characterization of Urban Grime and Measurements of Oxidants in Vehicle Cabins

Corey Richard Kroptavich
Syracuse University

Follow this and additional works at: <https://surface.syr.edu/etd>



Part of the [Physical Sciences and Mathematics Commons](#)

Recommended Citation

Kroptavich, Corey Richard, "Atmospheric Chemistry of Outdoor and Indoor Environments: Physical and Chemical Characterization of Urban Grime and Measurements of Oxidants in Vehicle Cabins" (2020). *Dissertations - ALL*. 1234.
<https://surface.syr.edu/etd/1234>

This Dissertation is brought to you for free and open access by the SURFACE at SURFACE. It has been accepted for inclusion in Dissertations - ALL by an authorized administrator of SURFACE. For more information, please contact surface@syr.edu.

Abstract

This work investigates chemistry in two distinct environments in urban atmospheres. The first is the coatings found on urban surfaces often referred to as urban grime. Urban grime may serve as an important medium for photochemical and heterogeneous reactions in cities. This study characterized the composition and physical state of urban grime collected from two American cities. Wavelength-resolved extinction spectra of urban grime samples were also analyzed to improve our understanding of urban grime's role in photochemistry. The research showed that the grime from the American cities was similar in composition to previous studies conducted in Europe and Canada, but with significant variations in particular ions, such as sulfate in the European samples and chloride in the North American samples. The grime also showed the ability to absorb sunlight which could indicate it may play a role in photochemical reactions.

The second focus of this research is quantifying oxidant concentrations in vehicle cabins. Recent research has investigated the oxidative capacity of indoor environments such as homes and commercial buildings, but vehicles are typically overlooked as an indoor environment. However, based on the amount of time people spend in vehicles they are still an important area to study. This research will work to understand how vehicle's cabin atmosphere compare to both indoor and outdoor environments under several conditions, and thereby understand the kinds of chemical interactions that can be taking place. One of the early findings was that the oxidant levels within the vehicle are more closely aligned with the composition seen in residences compared to commercial buildings or the outdoor environment. Additionally, the level of sunlight that enters the vehicle during the day is significant enough for photochemistry of select oxidants to potentially take place within the cabin.

ATMOSPHERIC CHEMISTRY OF OUTDOOR AND INDOOR ENVIRONMENTS:
PHYSICAL AND CHEMICAL CHARACTERIZATION OF URBAN GRIME AND
MEASUREMENTS OF OXIDANTS IN VEHICLE CABINS

by

Corey Kryptavich

B.S., University of Scranton, 2014
M.P.S., Pennsylvania State University, 2016

Dissertation

Submitted in partial fulfillment of the requirements for the degree of
Doctor of Philosophy in Chemistry.

Syracuse University
December 2020

Copyright © Corey Kryptavich 2020

All Rights Reserved

Acknowledgements

First, I would like to thank my advisor, Dr. Tara Kahan. You have been instrumental to my success at this stage of my academic career; I don't believe anyone else would have been able to help make this internationally collaborative, multi-time zone research work quite as well as you.

Next, thank you to my friends and family for ceaselessly supporting me through what, to some, must have looked like seemingly endless years of schooling. You were always there when I needed to focus on my work, but moreso when I needed a relaxing distraction. I especially want to thank my amazing wife, Abby, for your steadfast presence. If there was one thing, I could rely on even during my most demanding weeks, it was your strength and encouragement.

Thank you as well to the members of the Kahan group; your questions and feedback on my research throughout our group collaborations have been enlightening. Your contributions and our discussions have challenged me as a researcher and scientist, greatly expanding the depth of my understanding in our field.

Lastly, I'd like to thank Syracuse University, the Syracuse University Chemistry Department, the Syracuse University Graduate Student Organization, and the Alfred P. Sloan Foundation for funding my research, providing me with teaching and research assistantships, and travel grants to attend national conferences.

Table of Contents

List of Tables	vii
List of Figures	viii
Chapter 1: Introduction	1
1.1 Urban Environments	2
1.2 Urban Grime	3
1.2.1 Urban Grime Composition	5
1.2.2 Urban Grime Compared to Suburban and Rural Grime	7
1.2.3 Urban Grime Growth	8
1.2.4 Urban Grime and Surface Chemistry	9
1.2.4.1 Partitioning	10
1.2.4.2 Reactivity	11
1.2.5 Predictive Models	14
1.2.6 Summary of Current Work	16
1.3 Indoor Air/Vehicle Air	16
1.3.1 Indoor Air Composition Compared to Outdoor Air	18
1.3.2 Indoor Chemistry	19
1.3.2.1 Oxidation	21
1.3.2.2 Heterogeneous Chemistry	22
1.3.2.3 Photolysis	23
1.3.3 Vehicle Analysis	24
1.3.3.1 External Analysis	24
1.3.3.2 Internal Analysis	25
1.3.4 Human Factors of Oxidants	27
1.3.5 Summary of Current Work	28
1.4 References	29
Chapter 2: Physical and Chemical Characterization of Urban Grime Sampled from Two Cities	34
2.1 Abstract	35
2.2 Introduction	35
2.3 Methods	39
2.4 Results	41
2.4.1 Physical Characterization	41
2.4.2 Bulk Characterization	45
2.4.3 Ionic Composition	47
2.4.4 Correlation between Ionic Species	49
2.4.5 Seasonal Variations	51
2.4.6 Optical Properties	53
2.5 Implications	59
2.6 Acknowledgements	62
2.7 References	62
Chapter 3: Measurements of Oxidants in Vehicle Cabins	66
3.1 Abstract	67
3.2 Introduction	67
3.3 Methods	70

3.4 Results	73
3.4.1 Oxidant* Mixing Ratios and Air Exchange Rates	73
3.4.2 Photochemistry	80
3.5 Environmental Implications	84
3.6 References	85
Appendix	88
A.1. Supplementary Information for Chapter 2	88
Curriculum Vitae	98

List of Tables

Table 3.1: Average air exchange rates and indoor/outdoor ratios of Ozone and NO_x in vehicles under different conditions. Reported AERs are from this work unless otherwise noted.

Table 3.2: Photolytic rate constants and steady-state concentration of OH in the vehicle compared to other indoor environments

List of Figures

Figure 2.1. Optical microscope image (10× magnification) of a glass plate exposed to ambient outdoor air for 10 weeks in Syracuse, NY.

Figure 2.2 Raman spectra of (a) a clean quartz surface, and (b) a particle on a quartz surface.

Figure 2.3 A $192 \times 230 \mu\text{m}$ optical image of a quartz plate placed outdoors for 30 days (top panel), and the corresponding intensity map (bottom panel). Grey pixels correspond to spectra identified as quartz based on relative intensity at 500 cm^{-1} and 650 cm^{-1} . Red pixels correspond to spectra containing fluorescence from urban grime based on relative intensity at 2050 cm^{-1} and 650 cm^{-1} .

Figure 2.4 Compositional breakdown of grime based on mass percentage from (a) Syracuse, NY and (b) Scranton, PA

Figure 2.5 Average ionic composition based on percent ionic mass for (a) Syracuse and (b) Scranton

Figure 2.6 Correlation curves for (a) sodium-chloride, (b) sodium-magnesium, and (c) sodium-nitrate ion pairs from Syracuse samples. The inset within each figure excludes the three high concentration samples (White1, MacNaughton1, and Almond1).

Figure 2.7 Time series for ion ratios in samples from Syracuse.

Figure 2.8 (a) Measured light extinction at 300 nm as a function of urban grime mass concentration in aqueous solution for samples collected from Syracuse and Scranton. Data fitting was performed using the orthogonal distance regression. (b) City-averaged light extinction normalized to total grime mass as a function of wavelength. Shades bound the standard deviation. Colored dashed lines were determined by fitting the mean with a power law equation. The λ^{-1} trend line (black dashed line) expected for black carbon is shown for comparison.

Figure 3.1 Schematic of the tubing setup for testing with MILOS

Figure 3.2 Time series of concentrations for O₃, HONO, NO₂, and NO for select conditions recorded a) May 17 and b) May 18, 2019. c) Box and whisker plots of analyte mixing ratios outside of the vehicle and inside during the tested conditions from all days except from the trials in February. The plots show the median (line), mean (marker), upper and lower quartiles (box), and 10th and 90th percentiles (whiskers). Outdoor and direct fan values for HONO are not reported due to possible artifacts.

Figure 3.3 (a) Transmittance of driver-side windows in a 2013 Honda CRV, a 2006 Pontiac G6 sedan, and a 2016 Mazda 3 hatchback. Transmittance of windows in an office building and a house are also shown for reference. (b) Transmittance of various windows in the Honda CRV.

Figure 3.4 Time series of solar irradiance taken on May 18th, 2019

Chapter One:

Introduction

1.1 Urban Environments

Atmospheric chemistry seeks to understand the various factors that control the concentrations of chemical species found within the earth's atmosphere through chemical and physical analyses.¹ Atmospheric studies often examine the atmosphere on large scales including dust transport from deserts, smoke plumes from wildfires, and ozone depletion events in the poles. But analyzing the atmosphere on a smaller scale can lead to better understanding of the complexities between the environment and humankind. Urban areas create unique matrices for atmospheric chemistry. This is due to the differences in the atmospheric chemical composition of cities compared to non-urban environments. Cities contain a large number of primary pollutant sources that can generate unique and complex gradients in the concentrations of pollutants such as particulate matter and nitrogen oxides within the atmosphere.² The concentration gradients are generally highest closest to the emission sources such as highways and will gradually become diluted the further away from the source. The increased levels of these types of pollutants causes the chemistry within urban environments to take on different paths compared to non-urban locations such as farms and forests.² Compounds such as ammonia, black carbon, particulate matter, and BTEX compounds (benzene, toluene, ethylbenzene, and xylene) have been investigated as they are considered common anthropogenic pollutants.³⁻⁵ The general observed trend for ammonia levels in urban areas was higher compared to suburban locations showing a distinct difference between the air quality of the two.³ Urban locations possess higher levels of surface area both in terms of solid surfaces with the presence of buildings, but the surface area is also connected to the concentration of particulate matter in the air.² The number of buildings and their close proximity to one another lead to high surface to volume ratios.⁶ Urban locations have been shown to have faster reaction rates for atmospheric species compared to rural locations, and

as a result chemical species generally have shorter average lifetimes.² This is due to both the higher concentrations and the effect of mixing due to wind fluctuations created by the increased heat found in urban zones. With the increased impervious surface area, ranging between 33-56% of urban surfaces and rising as high as 98% in downtown areas, and the complex mix of atmospheric pollutants, urban environments lead to the prevalence of heterogenous chemical reactions.⁷ These reactions play an important role in removing certain compounds from the environment or resulting in the creation of more toxic species.^{2, 8}

Atmospheric chemistry is not just limited to the outside world but can also involve chemical interactions within indoor environments. Reactions in the indoor atmosphere can occur between a variety of different kinds of compounds though most of the highly examined ones are organics and oxidative pollutants.⁹⁻¹¹ It has also been recently discovered that indoor emissions of volatile organic compounds can affect the outdoor environment.¹² These emissions come from a variety of sources including adhesives, printing inks, personal care products, and cleaning agents which are used in everyday routines. They are considered an emerging source of urban volatile organic compounds especially as emissions derived from transportation sources have declined following stricter regulations.¹² Further discussion of indoor chemistry will be discussed in section 3 of the Introduction.

1.2 Urban Grime

Diamond et al indicate that the urban environments possess a high proportion of impervious surfaces on which coatings referred to as urban grime or urban films can form.⁶ These coatings are of interest as they form an extensive media within urban environments. This media can make previously impervious surfaces a new location for reactions to potentially occur

and compounds to settle into. The makeup and reactivity of the grime is only beginning to be understood. Urban grime was long believed to have been an organic film that formed on nearly all surfaces within urban environments. These films were most commonly observed by their formation on clear surfaces such as windows. The concern over the role of these surfaces came as a result of analyses looking into the concentrations polycyclic aromatic hydrocarbons, PAHs, and polychlorinated biphenyls, PCBs, in urban atmospheres.¹³ These compounds are widely understood to be toxic to human health and can lead to cardiovascular disease and various cancers.^{14, 15} But it is their prevalence in the environment that leads individuals to want to understand the composition of urban grime and the role it might play in the lifecycle of these particular compounds and other chemical species that are damaging to health. Two potential roles were theorized for urban grime to play. The first is that it can be a possible sink for these molecules and second can it serve as an important substrate for reactions.^{16, 17}

The large surface to volume ratio in urban environments makes heterogeneous reactions more important than in other environments.² Heterogeneous atmospheric reactions typically follow the Langmuir-Hinshelwood mechanism in which reactants adsorb to the surface and react to create a new product which may or may not desorb from the surface back into the atmosphere.¹⁸ Ozone is a common reactant on surfaces, and its uptake onto different surfaces has been widely studied.¹⁹ Ozone's uptake is slowest on glass surfaces compared to other building materials with the fastest uptake occurring on wood.¹⁹ Ozone uptake to concrete falls between the two previous materials, but can be affected by the relative humidity.²⁰ However, in urban environments these materials and their surfaces are rarely left in a pristine manner. As they are exposed to the environment, other materials will adsorb and collect on the surface.⁶ This is where urban grime as a reaction matrix comes into the discussion. The coating creates a new surface on

which heterogeneous reactions can occur and depending on its composition could change the rates of adsorption for common gaseous species.⁶ This initiated the research into the potential composition and interactions that the surface films could have.⁶

1.2.1 Urban Grime Composition

Research has determined that urban grime is not just an organic film but is mostly inorganic in composition.²¹ These discoveries also led to the postulation that urban grime is formed by the deposition of aerosols onto impervious surfaces. The urban grime would then build up over time as more and more material was deposited onto these surfaces which would form complex substrates.²² The grime would remain for chemistry to occur until it was removed by natural or artificial means. The only natural method for removing the grime was understood to be through precipitation which would more often remove the grime through physical means rather than through dissolution of the material. The artificial means of removing the grime is through the application of cleaners and wiping away the solution and grime. However, as the investigation into urban grime increased so too did the understanding of what urban grime consisted of. Research conducted by Lam et al used multiple techniques including nuclear magnetic resonance (NMR), organic/elemental carbon analysis (OC/EC), ion chromatography (IC), and inductively coupled plasma optical emission spectroscopy (ICP-OES).²¹ The analysis found that inorganic component made up approximately 95% of the tested grime which included metals (18%), nitrate (7%), and sulfate (8%).²¹ The vast majority of the inorganic component however was undetermined by this research. The research also determined that only 5% of the urban grime consisted of organic carbon while less than 1% of the grime was elemental carbon.

The organic carbon was further determined to consist predominately of aliphatic carbons, aromatics, carbohydrates, and carbonyls.²¹

Following Lam et al's work on grime from Toronto, Canada, Favez et al studied the composition of urban grime located in several European cities. This group collected urban grime samples from London, United Kingdom, Krakow, Poland, Athens, Greece, Prague, Czech Republic, Troyes, France, and Montelibretti, Italy. The study focused on identifying carbon, organics, and ionic species using total carbon and elemental carbon analysis, and ion chromatography.²³ A difference between the two studies showed a higher percentage of carbon based mass within the European samples (11-48%) compared to the Canadian samples (5%).^{21, 23}

The ionic composition of the regional samples showed similar concentrations for sulfate and nitrate. Another similarity between the datasets showed calcium as the major metal component followed by sodium.^{21, 23} Toronto samples were also analyzed for their ionic content which showed a high concentration of sodium, chloride, calcium, and nitrate.²⁵ Samples collected from Leipzig showed similar results to the previous European samples collected with regard to their ionic composition.²⁶ Sulfate, nitrate, and calcium once again made up the majority of the ionic mass.²⁶ A third group analyzed grime and surface films in the Brisbane Australia. Duigu et al sought to characterize the elemental composition of the grime.²⁷ In comparison to the previous studies, the Brisbane study saw calcium and magnesium being the dominant metals detected in the analysis followed by iron, aluminum, and zinc.²⁷ Among the metals analyzed by Liu et al., iron was the most abundant metal in both locations though significantly higher in concentration in the urban environment compared to the suburban.²⁹ Iron was followed in abundance by zinc, barium, strontium, and zirconium. The research however did not show the abundance of calcium or sodium within the collected grime which in other studies were

consistently shown as the most abundant metals in grime samples.²⁹ They examined both urban and suburban films within the Baltimore areas and determined that the concentrations of organic molecules such as PAHs and PCBs were higher in the urban environment compared to the suburban.²⁹ The work completed by the previous groups show variation within the study of urban grime composition, and the need to further research the topic.

1.2.2 Urban Grime Compared to Suburban and Rural Grime

Composition analysis for different environment zones was conducted by Lombardo et al. The group looked at the compositional differences for urban, rural, and industrial zones. All three showed similar distribution of components between the three site types though variations were present for specific sites. A major difference observed was the mass density of the grime collected from rural sites was significantly smaller than those for the industrial and urban sites.²⁸ The rural areas also typically show more particulate organic matter (POM) species attributed to biologic sources such as plant spores and biologic volatile organic carbons (BVOCs) than POMs observed in urban and industrial regions which generally have more anthropogenic sources.

Lombardo et al further expanded on the characterization of soiling of glass and loss visibility with regard to different types of environments. They looked at the soiling of glass in three environment zones classified as urban, rural, and industrial.²⁸ The zones were divided by the atmospheric concentrations of NO₂, SO₂, and PM₁₀ (Particulate matter with diameters 10 μm and smaller). Rural zones were classified as having low concentrations of all three common pollutants. Urban zones have moderate to high levels of NO₂ and PM₁₀ and moderate levels of SO₂. Industrial zones have medium to high rates of NO₂ and PM₁₀ and high levels of SO₂.²⁸ All three types of sites saw high variability with both mass deposition on the surface and the

visibility of the glass referred to as haze values, but variation between the different locations showed little evidence for unique patterns. Their conclusions were that the type of location does not lead to a conclusive indication about how much soiling is possible, but instead the levels of ambient pollution in the atmosphere is a better indicator for soiling on glass surfaces.²⁸

1.2.3 Urban Grime Growth

While determining the composition of urban grime, other groups took it upon themselves to quantify the growth rates of grime and the physical and chemical means by which it forms. An early group to study the accumulation of materials on surfaces in urban environments was Liu et al. Following the work and their analysis of the formation of urban films, the Diamond group decided to continue to analyze the growth of these films through accumulation.²⁹ They determined the thickness of the grime based on the total inorganic and organic mass, and for only the organic component of the film. The bulk film had an approximated thickness ranging from 4.0 to 476 nm while the organic film measured 0.6 to 75 nm in thickness, which showed once more that the majority of the material was inorganic in nature.²⁹ The group also determined that the rate of dry deposition of fine particles from the atmosphere to surfaces was greater for surfaces with films already present compared to clean surfaces. The rate of deposition ranged from 1.4 to 94 times higher for windows already possessing a film compared to those without one present.²⁹

Ionescu et al followed in the same vein of study by analyzing the soiling of glass over time in five European cities. They tested the growth in multiple cities to determine if a standard best fit could be applied to other cities for future work.³⁰ The group analyzed the increase of particle mass per surface area of the tested glass alongside haze, which was based on percent transmittance of light by the glass. The research found a cumulative trend for particle deposition

onto their tested glass surfaces as well was a gradual increase in haze over the tested twenty-eight month period. The largest increases in mass over time were recorded in Athens, Greece, Krakow, Poland, and London, United Kingdom while slower increases were seen in the other three tested cities, Paris, France, Prague, Czech Republic, and Rome, Italy.³⁰ The increase in haze followed a similar trend as the mass growth for all six cities with London and Athens being the highest and Rome being the lowest.

Following the data collection by Ionescu et al., two separate papers were published detailing models for glass soiling utilizing the same dataset and the effect on the optical properties, such as visibility of the glass.^{31, 32} The first paper focused the increase of haze as a function of time and the deposition of material. The model determines that haze forms in two distinct phases.³¹ The first phase sees the haze increase progressively over time on a clean surface until a complete layer of particles has formed. The second phase follows a saturation point where the mass accumulated has little further effect on the quality of the haze. The second phase also has slower growth of the soiling compared to the first.³¹ The second paper utilized the data collected by Ionescu in addition to data parameters for atmospheric species such as SO₂, NO₂, and PM₁₀. They identified that the rate of soiling and haze formation was based on the concentrations of these three species in the atmosphere.³² All of the groups found that various equations explained the growth of the grime, but each saw the same general trends.

1.2.4 Urban Grime and Surface Chemistry

Understanding the composition of urban grime proved useful in future work that involved understanding the chemistry that takes place in the surface coatings. These new experiments led to determining the partitioning potential of the grime in addition to the grime's potential as a

reaction matrix.^{33, 34} These various projects would work on understanding the grime's role as a source and sink for other environmental and atmospheric species.

1.2.4.1 Partitioning

Octanol is typically used, alongside water, to understand the solubility of persistent organic pollutants within the environment with octanol serving as a representation for the organic phases. Furthermore, the partitioning coefficients of K_{ow} , K_{aw} , and K_{ao} representing where analytes can be found between different matrices in specifically octanol and water, air and water, and air and octanol are often used in models to predict the behavior of organic pollutants within all three phases. The group of Wu et al determined that urban grime had the ability to partition out PCBs from the atmosphere. This would illustrate the role urban grime plays to remove pollutants and other compounds from the atmosphere. The group studied the differences in partitioning of several PCB congeners and discovered that different congeners had differing levels of affinity for the urban grime. The group compared this to the partition factors of octanol and ethylene vinyl acetate (EVA). They determined that EVA was a better surrogate for the urban grime compared to octanol.³⁴ This was attributed to the acetate being closer in composition to the organic components in the grime.³⁵ According to the results of the study, PCB congeners showed varying levels of affinity for the urban grime compared to the EVA films and this was attributed to the potential changes in the surface film's composition.³⁴ The researchers did also note that other factors could be at play regarding changes over time including precipitation resulting in component wash-off and regrowth and effects due to ambient temperature.³⁴

The Liu group compared the composition of both urban and suburban grime and determined significant differences in the concentration of organic molecules such as PAHs and

PCBs.²⁹ PAH concentrations were significantly higher in grime collected from urban areas compared to suburban areas and were mostly attributed to vehicle emissions.²⁹ Likewise PCBs were more highly concentrated in the grime sampled from urban environments, and different PCB distributions were observed in urban and suburban samples. In urban environments, the study found that penta- and hexa-PCBs were among the most dominant congeners while in the suburban environment they found nona- and deca-PCBs as the most dominant congeners though at very low concentrations.²⁹

1.2.4.2 Reactivity

Many initial tests involving ozone uptake experiments involved the use of mock organic films often made from octanol or other organic materials. Among these trials were two papers published by Kwamena et al. The first of these two experiments was the reaction of benzo- α -pyrene (BaP), a PAH, with ozone under different surface conditions.³⁶ The group tested the reactivity of ozone with BaP on both organic-based films and salt-based aerosols. The kinetics and reaction probability of the BaP was determined to be higher on the organic substrate compared to that of the salt substrate since the BaP persisted for only 84 min on the organic substrate but lasted for more than 13 days on the salt substrate.³⁶ This work also tested the differences in the reactivity of the BaP and ozone at different levels of relative humidity (RH) while on the organic substrate.³⁶ The apparent rate increase observed when the humidity increased was not linked to a faster reaction between ozone and BaP. Instead the ozone had a higher affinity to the substrate allowing for increased interactions between the molecules on the surface.³⁶ The second paper tested the kinetics of ozone with anthracene via heterogeneous interactions on glass surfaces and found it follows the Langmuir-Hinshelwood mechanism.³⁷

Unlike the previous experiment changing the RH did not appear to effect of the kinetics between ozone and anthracene in the same way it had with the BaP.^{36, 37}

Further work on the reaction kinetics of ozone and PAHs was conducted by Kahan et al and analyzed multiple PAHs and substrates.⁸ The testing utilized the following PAHs dissolved in either octanol or decanol and applied to a surface; naphthalene, anthracene, fluoranthene, phenanthrene, pyrene, and BaP. In addition, the research looked into the effect of additional materials present in the substrate on the kinetics of ozone and anthracene.⁸ It was determined that adding other hydrocarbons or silicone-based greases did not change the reaction kinetics for anthracene and ozone however the presence of oleic acid and squalene did. The group conducted further testing and determined that the effect of the oleic acid and squalene occurred regardless of the other materials present with the anthracene. This effect was attributed to the unsaturated sites within both compounds and those regions ability to interact with ozone.⁸ It was determined that the other PAHs tested also had slower reaction kinetics compared to anthracene except for BaP.⁸ These experiments were important in understanding the role in which urban grime could be playing in atmospheric chemistry. The tests used simulated proxies with similar organic components as those observed in real urban grime samples in order to predict the possible mechanisms that the grime could be subject to especially regarding atmospheric species such as ozone. Grime samples collected from Leipzig, Germany were also tested for organic contributions predominately looking for OC, EC, and PAHs. It was determined that the concentrations of different PAHs within the samples depended on location and exposure of the sample to light.²⁴

Ozone is not the only atmospheric pollutant that is of interest for interactions with urban grime. NO₂ is another common pollutant and urban grime is believed to be an important source

and sink for the molecule and other nitrogen oxides such as NO and HONO, which are important precursors for other atmospheric pollutants such as ozone and serve as OH radical sources through photochemistry.^{38,39} Ammar et al investigated the photochemical uptake of NO₂ to simulated urban grime with a flowtube coated in a layer of pyrene or pyrene with KNO₃ and a flow of NO₂ was added by an injector. The experiment utilized an UV lamp to simulate sunlight, which is important due to NO₂'s ability to photodissociate.³⁹ The experiment showed little reaction in the dark aside from physical uptake by the pyrene coating. The addition of light saw a drop in NO₂ concentration along with an increase in NO and HONO within the sample flow for both coatings.³⁹ It was also determined that the pyrene is more reactive with the NO₂ when the KNO₃ was not present in the film, resulting in higher uptake coefficients. However, HONO production was increased when KNO₃ was present.³⁹ One additional test was conducted without an inflow of NO₂ on a pyrene coating containing KNO₃. The results of this test showed the formation of HONO from the film due to reactions of the pyrene and the salt under irradiated conditions.³⁹ Liu et al tested the ability of NO₂ to be adsorbed by urban grime and what role relative humidity could play. The group saw NO₂ uptake increase as RH was increased on a glass surface coated with real urban grime compared to no real change for a clean glass surface.³³ The group also looked into the effect of photolysis being a source of atmospheric HONO and the role RH could play in the levels of HONO production. In a dark flowtube, low levels of HONO were detected as NO₂ was added to the flowtube but these would gradually decay over time. When the tube was illuminated, a sharp increase in HONO was observed and the level remained consistent until the illumination was removed indicating that HONO production was a photochemical effect.³³ Lastly the group tested the effect of RH on HONO production. On bare glass there was an increase in HONO from 0% to 35% RH but then remained constant at higher RH values. With

the grime sample, HONO production increased as a function of RH increasing under both light and dark conditions though the HONO concentrations were higher under light conditions.³³

Baergen et al determined that illuminating real urban grime collected from Toronto resulted in the release of NO₂ and HONO from the material. The production of NO₂ was a result of the photolysis of nitrate within the grime. HONO however was postulated to be a result of three possible reactions.³⁸ The first is photolysis of nitrite within the grime while another is the interaction of NO₂ with the organic components within the grime. While a third theory was NO₂ hydrolysis within the grime resulting in HONO production. The processes were tested and it was concluded that the formation of HONO was dependent on the RH within the testing chamber. The group observed higher HONO production as RH was increased up to a level of 35% after which further increases in RH no longer had an impact.³⁸ These results indicated that water and its uptake into grime and evaporation away can be an important factor for reactions within the material.³⁸

1.2.5 Predictive models

To better understand the complex nature of urban environments and the compounds that are both generated and eliminated within them, models are created from existing knowledge in order to apply those concepts to larger scales. One such model developed for understanding the fate of semivolatile organic compounds is the multimedia urban model (MUM) developed by the Diamond et al.⁷ The model consists of six compartments for which the compounds could exist at any given time. These compartments are air, surface water, sediment, soil, vegetation, and organic films on impervious surfaces and all were characterized based on the city of Toronto, Canada.⁷ The model initially measured the emissions and sinks of various PAHs and

polychlorinated dibenzodioxanes and determined that the soil is the net sink for most compounds and that surface films plays an important role for the compounds as well. The films can “reflect” the most volatile compounds back into the air, transport compounds to the surface waters via run-off during precipitation events, and serve as a medium for photolytic degradation to occur.⁷ The model was then modified to show the pathways for PCBs within forested regions in Priemer et al.⁴⁰ The model indicated that most compounds within forested areas are lost through transport through the air, but that some settle into the vegetation and eventually the soil leaving them immobile. The group then compared the results from the forest model back to the urban model and found similar results for the PCBs as initially were determined for the PAHs in the initial work indicating a more dynamic removal of the compounds.⁴⁰ The MUM was next used to measure the heterogeneous reactions of PAHs, specifically anthracene, pyrene, and benzo- α -pyrene within urban environments. Kwamena et al determined once again that most PAHs are lost through advection or the transport of compounds by the air, but that ~75% of reactive losses of the PAHs occurred on surface films and atmospheric particulate matters.⁴¹ Work with the MUM continues to expand and has been used to determine the fates of additional compounds such as polybrominated diphenyl ethers and organophosphates all within the original city template of Toronto within the model.^{42, 43} The model has also been applied to the parameters of other locations including Tarragona County in Spain by Dominguez-Morueco et al.⁴⁴ The use and continued evolution of the model as more research comes out is important for understanding the fates of pollutants within the environment, but also shows there are still gaps within the overall understanding of the complex nature of urban environments.

1.2.6 Summary of Current Work

This current work looks at understanding the chemical differences in the grime of different cities and the photochemical properties of the grime. This research is meant to help better understand those differences so that future work can be conducted to understand the different reaction mechanics that may be at play in each unique environment. Grime was formally believed to be a uniform organic film, but both this research and others in the past have indicated that it is not so and that there are mostly inorganic species with many particles on these surfaces. By looking at the composition of grime from different locations, the differences in the locations' environments can be understood. These differences can include concentration of organic species in the grime compared to inorganic and ionic species. Since a city with a larger organic component to its grime could lead to different reactions compared one with less organic matter. Likewise, the differences in ionic concentrations and species ratios can alter the types of chemistry that could be occurring.

1.3 Indoor Air/Vehicle Air

Indoor pollutants have been a concern for human welfare for many decades, but the compounds of concern have often changed over the decades.⁴⁵ These changes have influenced by changes in building materials, the increase in appliance use, increased circulation within indoor environments using ventilation, heating, and air conditioning systems, and decreased exchange with the outdoor environment.⁴⁵ Not only have the environments themselves changed, but so has the scientific community's understanding of the complex nature of indoor environments.⁴⁶

In terms of the changes in pollutant concentrations, there has been a general decrease in the concentrations of inorganic gases such as CO, NO, SO₂, and Radon. Some have been linked a reduction in unventilated combustion within homes and others are associated with a general

decline in the outdoor atmosphere as well.⁴⁵ There has been a mixed result in the concentrations of various aldehydes with formaldehyde and acetaldehyde decreasing but hexanal, decanal, and others seeing an increase. The reduction is explained to have been caused by a change in building materials, but the increase is currently unexplained leaving an opening for future work.⁴⁵ Aromatic compounds have seen a reduction through a decline in their use in solvents, but terpenoids have seen an increase due to their increased use in solvents and scents. Several other classifications of pollutants such as phthalates, biocides, and fungicides have seen increases, but others which have had large notice such as combustion byproducts such as dioxins, smoke particles, and toxic metals, and fibers like asbestos and lead have been on the decline.⁴⁵ As the collective understanding of indoor air quality increases it has shown the need for determining the conditions indoors to better understand its impact on health and comfort of the occupants.⁴⁶ Exposure risk comes in a variety of forms with the most common being inhalation of compounds which can damage the lung tissue.⁴⁷ The exposure comes from both primary pollutants released from cleaning products and also secondary products, which are generated through reactions in the atmosphere. One of these byproducts is hydroxyl radicals which form from the interactions of terpenoids with ozone.⁴⁷ Inhalation is not the only process by which pollutants can enter the body, a second pathway is transdermal penetration. Compounds collect in the lipids on the skin's surface and then can absorb into the dermis either through transcellular transport or through hair follicles and sweat glands in a method of shunt transport.⁴⁸ Based on current estimates some SVOCs can be absorbed through the skin at higher rates than through inhalation.⁴⁸

1.3.1 Indoor Air Composition Compared to Outdoor Air

It is commonly understood that reactions in the air are primarily influenced by the concentrations of radicals and their precursors. The most common radical for atmospheric chemistry is the hydroxyl radical.⁴⁹ In outdoor environments ozone generally plays the part of the precursor for hydroxyl radicals and this is due to the higher levels of ozone present in the atmosphere. However, in indoor environments it has been documented that photolysis of ozone is unlikely to occur due to a lack of wavelengths below 330 nm.⁴⁹⁻⁵¹ With ozone photolysis being less prevalent in indoor environments, other radicals and compounds have been investigated to filling in the role of primary oxidant within the indoor environment. One of these suspected compounds was the nitrate radical.⁵¹ Nitrate radicals form in areas of high O₃ and NO₂, but can be readily eliminated in areas of high NO concentrations.⁵¹ However, based on current observed measurements nitrate radicals are unlikely to be a primary oxidant as Zhou et al showed that indoor levels of NO, NO₂, and O₃ are not conducive to the radical formation.⁵² Instead compounds that can photolyze at longer wavelengths than ozone, such as formaldehyde and HONO may be primary sources of OH radicals indoors.⁵¹ An additional potential oxidant could be chlorine radicals due to the use of chlorine-based cleaning products and the photolability of compounds such as Cl₂, ClNO₂, HOCl, and NCl₃, but are possibly limited due to the uniqueness of their sources.⁵¹ Young et al. also summarized that the current understanding of indoor oxidation chemistry is limited and indicated that indoor environments can be heavily varied in building structure, air exchange rates, location, and sunlight exposure and therefore research along all of these avenues is necessary to understand the chemistry taking place.⁵¹

1.3.2 Indoor Chemistry

Indoor atmospheric chemistry can follow similar reaction pathways to the outdoor atmosphere depending on the concentration of the species present. These reactions include oxidation of compound in the air as well as oxidizing materials found on surfaces, the formation of radicals through chemical reactions and photolysis, and adsorption of gaseous components onto surfaces. Several groups have looked into the concentrations of the various species within indoor environments especially regarding ozone and nitrogen species such as NO, NO₂, and HONO.⁵²⁻⁵⁶ The first of these groups looked at measuring the concentrations of ozone both inside and outside of residential buildings.⁵³ In general, the concentrations of ozone were always lower indoors than outdoors regardless of the time of year or during peak pollution events which caused spikes in ozone concentration.⁵³ The next group added NO₂ and HONO into the analysis alongside O₃. This was done to observe the then unknown concentrations of HONO in indoor environments and look at patterns between the three species.⁵⁴ Based on the observations it was concluded that HONO was generally more concentrated in indoor environments compared to those outdoors and generally correlates with the concentration of NO₂.⁵⁴ In addition to the general patterns, the group determined that certain common household appliances had an effect on the various species. Homes with air conditioners and gas stoves had higher NO₂ concentrations while ozone was generally lower in homes with air conditioners.⁵⁴ The decrease in observed ozone was linked to lower air exchange rates in homes with air conditioners, which in turn led to the determination that the same low air exchange rates lead to higher concentrations of HONO and NO₂. This is due to both gases having sources within indoor environments.⁵⁴ Lastly it was observed that HONO concentrations were inversely correlated with the concentrations of ozone.⁵⁴

Several research groups worked together on a campaign of research that was called HOMEChem. This was a large-scale research experiment meant to analyze a large number of different aspects to indoor chemistry. The researchers looked into airborne particulate matter concentrations and concentrations of compounds such as ammonia, VOCs, CO₂, and NO_x.⁵⁷⁻⁵⁹ Ammonia concentrations have been determined to be higher in indoor environments compared to outdoor environments. This has been strongly correlated to tobacco smoke, building materials, humans, and cleanings products.⁵⁸ Ampollini et al as part of the HOMEChem project found that the background for ammonia in the tested home was 32 ppb compared to the general outdoor levels being between 1-5 ppb. They also observed spikes of up to 1592 ppb during cleaning events within the home in addition to lower spikes induced by cooking or occupants.⁵⁸ They also determined that the greatest modulator for ammonia levels were the HVAC systems within the home.⁵⁸ Another partner within the same campaign saw that particle levels within the tested home were generally lower than that of the outside air, but that cooking periods greatly increase the particle concentration in the environment.^{57, 59} The particles are predominately related to the cooking oil used in the kitchen, but that the particles become increasingly oxygenated and nitrogenated as food is added to the oils.⁵⁹ The research also highlighted an increase in gas phase emissions during cooking events including hydrocarbons and oxidized organic molecules such as lactic acid. They determined that gas phase organics were generally in higher concentrations indoors compared to the outdoor environment.⁵⁹

In addition to the analyses involving NO_x and ozone, other researchers have focused on the concentrations of other pollutants. These other pollutants were either chlorine containing compounds or volatile organic carbons (VOCs).^{60, 61} HCl emissions were measured during a number of different scenarios within indoor environments including cleaning with bleach, using

chlorine containing detergents in dishwashers, and cooking with foods like garlic and onions which contain high levels of chlorine.⁶⁰ The group determined that there are multiple direct and secondary pathways for the production of HCl in indoor environments.⁶⁰ VOCs are another group of pollutants that are readily observed within indoor environments. Most of these studies deal with the source and production of VOCs, such as from the burning of incense or candles in homes or with the reactivity of VOCs with other atmospheric species such as ozone and hydroxyl radicals.^{61, 62} Manoukian et al determined that most candles and incense sticks will emit VOCs while burning and the concentration will continuously increase until the burning ceases.⁶¹ They also determined that while candles emitted lower concentrations of compounds, incense tended to emit high levels of carcinogenic compounds such as benzene and formaldehyde.⁶¹ However, the concentrations would dissipate after a few hours through ventilation and deposition processes, and it was therefore concluded that the emitted concentrations would be generally safe if a room is properly ventilated.⁶¹

1.3.2.1 Oxidation

The oxidation of organic molecules such as alkenes and alkanes in the atmosphere is facilitated by molecules such as ozone and radicals such as OH and hydroperoxyl radicals (HO₂). These reactions typically modify compounds into forms that are more conducive to dry and wet deposition and removal from the atmosphere. Dry deposition is the adsorption of a compound to a surface that it encounters and is the only form of interest in indoor environments. To fully understand the oxidative capacity within a specific chamber or room there are several factors to take into consideration.^{46, 49} One of these is what is the concentrations of known oxidant species within an environment and the other is what is the potential for these oxidants to oxidize other

compounds or generate more oxidative species such as radicals. The first can be achieved by measuring the relative concentration of oxidative species such as ozone and NO_x, but some species cannot be measured directly. For those species such as OH and OOH radicals, their precursors must be measured along with the mechanisms by which they can be generated.^{46, 51} Further analysis can also be conducted by measuring the products of oxidation chemistry and the rates at which they form.⁵¹

1.3.2.2 Heterogeneous Chemistry

Interactions between the air and surface include both dry deposition as indicated in the sections about grime but also through chemical interactions of gaseous molecules with compounds on the surface and the release of species from the surfaces into the atmosphere. Ozone is one of the molecules known to react with surfaces.⁶³ It has been observed that up to 85% of ozone can deposit on surfaces, and was determined that softer indoor surfaces had higher deposition velocities compared to harder surfaces in the same space.⁶³ It was also determined in the same study that the air exchange rates have a factor in the amount of ozone present to interact with the surfaces. The group measured the concentration of carbonyls within the studied chamber and found that their increase correlated with increased air exchange rates.⁶³ This was interpreted as having higher levels of ozone cycling into the chamber and thereby produce more carbonyls from the surfaces it interacts with. In addition, the group determined higher concentrations of aldehydes in the chamber in the presence of higher concentrations of ozone.⁶³ Schripp et al. studied ozone's interactions with wood surfaces within indoor environments. They choose to study these types of interactions since wooden products were already understood to affect indoor air quality through their emissions.^{64, 65} They determined that chemically treated wood emitted

higher concentrations of VOCs compared to solid untreated wood under the same conditions with aged wood showing the smallest concentrations overall.⁶⁴ However, they determined the fastest deposition rates for ozone was among the solid exotic wood and significantly faster than the treated wood.⁶⁴

1.3.2.3 Photolysis

Oxidation of species in the atmosphere can be facilitated through interaction of atmospheric radicals such as hydroxyl radicals. It has been determined that HONO is a common source for the production of these radicals. Work on determining the absorption cross section of HONO has determined that it absorbs strongly in the UV-range of sunlight that makes it to the earth's surface.⁶⁶ This absorbance range and the intensity of the light at different times of day have led to the interpretation that HONO could serve as a missing source for hydroxyl radicals and thus may be a major contributor to atmospheric reactions.⁶⁶ Hydroxyl and peroxy radicals were determined to originate from the photolysis of multiple compounds and the ability for these precursors to photolyze in indoor environments became the source of future studies. One of those compounds was HONO, and its generation of hydroxyl radicals was first shown by Alvarez Gomez et al.⁶⁷ The research showed a linear correlation between the generation of OH radicals and the rate of photolysis of HONO by sunlight entering the building indicating that HONO could be a source of the radicals within indoor environments.⁶⁷ Kowal et al. looked into the emission of various light sources indoors in addition to sunlight entering rooms through windows to determine if photolysis could be initiated by artificial lights. The group looked into the rates of photolysis for HONO, hydrogen peroxide, ozone, formaldehyde, acetaldehyde, nitrogen dioxide, and nitrate radicals.⁶⁸ The group determined that incandescent, halogen, and CFL light sources

were capable of photolysis in indoor environments but only near the light source itself. Uncovered fluorescent light sources were capable of initiating photolysis up to a meter away from the source for some OH formation and 1.9 m for HO₂ formation.⁶⁸ Hydroxyl radical formation from sunlight and uncovered fluorescent lights were 1.53×10^7 and 1.40×10^6 molecules cm⁻³ s⁻¹ respectively, which supported the idea that HONO is an important source of the radicals in indoor environments.⁶⁸

1.3.3 Vehicle Analysis

Current work on atmospheric analysis involving vehicles typically fall into two categories: external and internal.

1.3.3.1 External Analysis

External analysis typically involves analyzing the atmosphere around the vehicle and the influence the vehicle has on its surroundings. These analyses often examine the exhaust of the vehicle, its components and how these components can harm the environment and people's health. One of these analyses looked into the particulate organic matter emitted from vehicle exhaust.⁶⁹ This early work determined that between 7.5 to 18.3% of exhaust is in the form of organic particles and the ambient concentration in the air peaks during peak traffic periods.⁶⁹ Future work expanded on the analysis of particulate organic matter by looking into links between types of fuel and the production of these particles and how they disperse into the environment.⁷⁰ ⁷¹ It was determined that although the primary aerosols emitted by the exhaust were classified as black carbon, the exhaust was an important source for secondary organic aerosols (SOA).⁷¹ It was also shown that high aromatic fuels, those containing higher concentrations of BTEX and

other aromatics at around 30%, will lead to higher concentrations of black carbon emissions, and that non-oxygenated fuels generated more SOA compared to fuels with higher concentrations of ethanol.⁷¹ An additional branch of external vehicle analysis looked into how the exhaust components disperse into the atmosphere and the concentrations they are present at various distances from the source.⁷⁰

Particulate matter has been a concern for health research as it has been linked to number of different negative health effects. One of the primary concerns is pulmonary and cardiovascular health.⁷²⁻⁷⁴ This includes increased rates of mortality in both China and the Mediterranean due to exposure to PM_{2.5} especially in those 75 and older, while PM₁₀ and PM_{2.5-10} had more effect on younger populations.^{72, 73} Likewise, there has been a link between particulate matter exposure and increased mortality due to chronic obstructive pulmonary disorder (COPD).⁷⁵ Acute exposure of exhaust related gases, CO and SO₂, have been shown to negatively impact blood pressure and heart rate in adults.⁷⁶ This particular research was further expanded and showed an increase in acute myocardial infarction because of exposure to SO₂ and NO₂.⁷⁷ It was also determined that chronic exposure to diesel-emitted exhaust particles could also interfere with spermatogenesis and could lead to future work on the effects of air pollution on male reproductive health.⁷⁸

1.3.3.2 Internal Analysis

Internal analysis describes the atmosphere within the vehicle cabin. One of the earliest papers published on the interior environment of vehicles was on the concentration of HONO.⁷⁹ The research showed higher levels of HONO in the vehicle compared to the external environment with concentrations ranging from 7-29 ppb and <2 ppb respectively.⁷⁹ Therefore it

was determined that drivers and passengers within the vehicle would be exposed at greater rates to the pollutant within the vehicle though the actual impact on health was not determined.⁷⁹ In similar veins of thought, the risk of exposure to other common atmospheric pollutants was also assessed. Work was done looking into the concentrations of carbon monoxide, aldehydes, and BTEX (benzene, toluene, ethyl benzene, and xylene).⁸⁰⁻⁸² The levels of formaldehyde and acetaldehyde in passenger vehicles was determined to be 20.0 and 8.9 ppb respectively.⁸⁰ It was also determined that the levels in public buses were on similar magnitude with concentrations of 21.2 and 9.1 ppb for formaldehyde and acetaldehyde.⁸⁰ They determined that vehicle interiors were an important microenvironment for the exposure to the toxic aldehydes.⁸⁰ Som et al investigated the concentrations of BTEX both inside and in the exterior environments of passenger vehicles.⁸¹ The work was done in the city of Kolkata, India where the emission requirements for vehicles are less strict compared to other nations. The group determined that the concentrations of benzene in the outside atmosphere from vehicles without catalytic converters was 214.8 $\mu\text{g}/\text{m}^3$ compared to 30.8 $\mu\text{g}/\text{m}^3$ for those with converters. The results also indicated that the concentrations of benzene within the vehicles was also higher without a catalytic converter, 721.2 $\mu\text{g}/\text{m}^3$ compared to those vehicles that included one, 252.4 $\mu\text{g}/\text{m}^3$.⁸¹ This pattern was also consistent for the other BTEX compounds, which lead the researchers to conclude that the catalytic converters did reduce the concentrations of the compounds but still posed a risk to the occupants.⁸¹ The examinations into the exposure of CO for occupants was also conducted around this time. The research showed higher levels of CO in the vehicle cabin during periods in which the vehicle's ventilation system was closed or set to recirculating and that these two conditions showed similar concentrations at 37.4 and 30.8 ppm. This was comparatively higher than the concentrations of 18.4 ppm for period the ventilation system pulled in exterior air.⁸²

1.3.4 Human Factors on Oxidants

Surfaces in vehicles as well as in most environments that humans live and work in are typically coated in microscopic debris left by the human occupiers. This debris is typically made up of skin cells and oils that are removed via the process of desquamation. These cells and oils have been shown in chamber studies to impact the levels of ozone observed through the uptake of ozone to these surfaces and the process of ozonolysis.⁸³ Ozonolysis is known to occur with skin oils, such as squalene, which causes the ozone to be depleted and the oils to become semi-volatile compounds.^{84, 85} These compounds can enter the atmospheric environment and have their own effects while the mixing ratio of ozone becomes lessened. It has been observed that human bodies are the most efficient surface at removing ozone within an indoor environment, and in particular the oils on the skin's surface.⁶³ One effect of these interactions between squalene and ozone is the alteration in the chemical makeup of air in the immediate area around individuals compared to the rest of a chamber.⁸⁶ It has been shown that the ozone depletes in the area around an individual due to loss via interactions with both the individual and their clothing. The side effect of the ozone depletion causes a rise in concentrations of ozone reaction products within the immediate area.^{85, 86} The researchers concluded that while ozone is a pollutant in the atmosphere and dangerous for individuals to inhale, the concentrations observed in indoor environments are not necessarily the concentrations in the immediate breathing zone of an individual due to reactions with the individual's skin oils.⁸⁶ However, since the reaction products are also classified as toxic that exposure to the individual from these compounds are increased for the same reason that ozone risk is reduced, and therefore researchers need to look into the concentrations of ozone and the products when determining the potential effect on human health.⁸⁶ In addition to looking at reactions with ozone, work has also been done investigating

the interactions of radicals with squalene.⁸⁷ It has been theorized that squalene can also act as a scavenger for the short lived peroxy radicals as they observed the increase in concentrations of squalene hydroperoxide over time after exposure to ozone.⁸⁷ Researchers have also reported that the number of people in a room can increasingly reduce the levels of ozone within a room and thus reduce the risk of exposure for all individuals.⁸⁸

1.3.5 Summary of Current Work

The second half of this research involves looking at the atmosphere of an often overlooked or ignored indoor environment, vehicles. Most research focuses on the atmospheric makeup inside buildings such as offices, classrooms, and residences. These are the general focus as people typically are spending most of their time indoors, but people also spend a large amount of their time in vehicles. It's been estimated that people spend roughly 6% of their day in vehicles though this number can vary greatly between individuals.⁸⁹ Therefore, it is important to understand the environment that people may be interacting with during these periods.

The current work focuses on understanding the mixing ratios of several oxidants in a vehicle's atmosphere. The work looks to quantifying the concentrations of common oxidants and oxidant precursors under various conditions within the vehicle. In addition to the general composition, it also investigates the potential for photochemistry to occur and for the effect on the environment when an occupant was present. The photochemistry is the primary source of radicals in the atmosphere and since vehicles are sealed environments the work looks at the potential for radical formation within the vehicle from the sunlight entering through the windows.

1.4 References

1. Jacob, D. J., *Introduction to Atmospheric Chemistry*. Princeton University Press: 1999.
2. Harrison, R. M., Urban atmospheric chemistry: A very special case for study. *NPJ Clim. Atmos. Sci.* **2018**, *1*.
3. Pathak, R. K.; Chan, C. K., Inter-particle and gas-particle interactions in sampling artifacts of PM_{2.5} in filter-based samplers. *Atmos. Environ.* **2005**, *39* (9), 1597-1607.
4. Herrmann, H.; Brüggemann, E.; Franck, U.; Gnauk, T.; Loschau, G.; Müller, K.; Plewka, A.; Spindler, G., A source study of PM in Saxony by size-segregated characterisation. *J. Atmos. Chem* **2006**, *55* (2), 103-130.
5. Baltrenas, P.; Baltreinaite, E.; Sereviciene, V.; Pereira, P., Atmospheric BTEX concentrations in the vicinity of the crude oil refinery of the Baltic region. *Environ. Monit. Assess.* **2011**, *182* (1-4), 115-127.
6. Diamond, M. L.; Gingrich, S. E.; Fertuck, K.; McCarry, B. E.; Stern, G. A.; Billeck, B.; Grift, B.; Brooker, D.; Yager, T. D., Evidence for organic film on an impervious urban surface: Characterization and potential teratogenic effects. *Environ. Sci. Technol.* **2000**, *34* (14), 2900-2908.
7. Diamond, M. L.; Priemer, D. A.; Law, N. L., Developing a multimedia model of chemical dynamics in an urban area. *Chemosphere* **2001**, *44* (7), 1655-1667.
8. Kahan, T. F.; Kwamena, N. O. A.; Donaldson, D. J., Heterogeneous ozonation kinetics of polycyclic aromatic hydrocarbons on organic films. *Atmos. Environ.* **2006**, *40* (19), 3448-3459.
9. Elkilani, A.; Bouhamra, W.; Crittenden, B. D., An indoor air quality model that includes the sorption of VOCs on fabrics. *Process Safety and Environmental Protection* **2001**, *79* (B4), 233-243.
10. Ongwandee, M.; Chatsuvan, T.; Ayudhya, W. S. N.; Morris, J., Understanding interactions in the adsorption of gaseous organic compounds to indoor materials. *Environ. Sci. Pollut. Res.* **2017**, *24* (6), 5654-5668.
11. Collins, D. B.; Hems, R. F.; Zhou, S. M.; Wang, C.; Grignon, E.; Alavy, M.; Siegel, J. A.; Abbatt, J. P. D., Evidence for Gas-Surface Equilibrium Control of Indoor Nitrous Acid. *Environ. Sci. Technol.* **2018**, *52* (21), 12419-12427.
12. McDonald, B. C.; de Gouw, J. A.; Gilman, J. B.; Jathar, S. H.; Akherati, A.; Cappa, C. D.; Jimenez, J. L.; Lee-Taylor, J.; Hayes, P. L.; McKeen, S. A.; Cui, Y. Y.; Kim, S. W.; Gentner, D. R.; Isaacman-VanWertz, G.; Goldstein, A. H.; Harley, R. A.; Frost, G. J.; Roberts, J. M.; Ryerson, T. B.; Trainer, M., Volatile chemical products emerging as largest petrochemical source of urban organic emissions. *Science* **2018**, *359* (6377), 760-764.
13. Cotham, W. E.; Bidleman, T. F., Polycyclic aromatic hydrocarbons and polychlorinated biphenyls in air at an urban and a rural site near Lake Michigan. *Environ. Sci. Technol.* **1995**, *29* (11), 2782-2789.
14. Alshaarawy, O.; Elbaz, H. A.; Andrew, M. E., The association of urinary polycyclic aromatic hydrocarbon biomarkers and cardiovascular disease in the US population. *Environ. Int* **2016**, *89-90*, 174-178.
15. Alhamedow, A.; Essig, Y. J.; Krais, A. M.; Gustavsson, P.; Tinnerberg, H.; Lindh, C. H.; Hagberg, J.; Graff, P.; Albin, M.; Broberg, K., Fluorene exposure among PAH-exposed workers is associated with epigenetic markers related to lung cancer. *Occupational and Environmental Medicine* **2020**, *77* (7), 488-495.
16. Hodge, E. M.; Diamond, M. L.; McCarry, B. E.; Stern, G. A.; Harper, P. A., Sticky windows: Chemical and biological characteristics of the organic film derived from particulate and gas-phase air contaminants found on an urban impervious surface. *Arch. Environ. Contam. Toxicol.* **2003**, *44* (4), 421-429.
17. Donaldson, D. J.; Kahan, T. F.; Kwamena, N. O. A.; Handley, S. R.; Barbier, C., Atmospheric Chemistry of Urban Surface Films. In *Atmospheric Aerosols*, American Chemical Society: 2009; Vol. 1005, pp 79-89.

18. Ammann, M.; Poschl, U.; Rudich, Y., Effects of reversible adsorption and Langmuir-Hinshelwood surface reactions on gas uptake by atmospheric particles. *Phys. Chem. Chem. Phys.* **2003**, *5* (2), 351-356.
19. Nicolas, M.; Ramalho, O.; Maupetit, F., Reactions between ozone and building products: Impact on primary and secondary emissions. *Atmos. Environ.* **2007**, *41* (15), 3129-3138.
20. Grontoft, T., Measurements and modelling of the ozone deposition velocity to concrete tiles, including the effect of diffusion. *Atmos. Environ.* **2004**, *38* (1), 49-58.
21. Lam, B.; Diamond, M. L.; Simpson, A. J.; Makar, P. A.; Truong, J.; Hernandez-Martinez, N. A., Chemical composition of surface films on glass windows and implications for atmospheric chemistry. *Atmos. Environ.* **2005**, *39* (35), 6578-6586.
22. Grant, J. S.; Zhu, Z. H.; Anderton, C. R.; Shaw, S. K., Physical and Chemical Morphology of Passively Sampled Environmental Films. *ACS Earth Space Chem.* **2019**, *3* (2), 305-313.
23. Favez, O.; Cachier, H.; Chabas, A.; Ausset, P.; Lefevre, R., Crossed optical and chemical evaluations of modern glass soiling in various European urban environments. *Atmos. Environ.* **2006**, *40* (37), 7192-7204.
24. Styler, S. A.; Baergen, A. M.; Donaldson, D. J.; Herrmann, H., Organic Composition, Chemistry, and Photochemistry of Urban Film in Leipzig, Germany. *ACS Earth Space Chem.* **2018**, *2* (9), 935-945.
25. Baergen, A. M.; Donaldson, D. J., Seasonality of the Water-Soluble Inorganic Ion Composition and Water Uptake Behavior of Urban Grime. *Environ. Sci. Technol.* **2019**, *53* (10), 5671-5677.
26. Baergen, A. M.; Styler, S. A.; van Pinxteren, D.; Muller, K.; Herrmann, H.; Donaldson, D. J., Chemistry of Urban Grime: Inorganic Ion Composition of Grime vs Particles in Leipzig, Germany. *Environ. Sci. Technol.* **2015**, *49* (21), 12688-12696.
27. Duigu, J. R.; Ayoko, G. A.; Kokot, S., The relationship between building characteristics and the chemical composition of surface films found on glass windows in Brisbane, Australia. *Build. Environ.* **2009**, *44* (11), 2228-2235.
28. Lombardo, T.; Chabas, A.; Verney-Carron, A.; Cachier, H.; Triquet, S.; Darchy, S., Physico-chemical characterisation of glass soiling in rural, urban and industrial environments. *Environ. Sci. Pollut. Res.* **2014**, *21* (15), 9251-9258.
29. Liu, Q. T.; Diamond, M. L.; Gingrich, S. E.; Ondov, J. M.; Maciejczyk, P.; Stern, G. A., Accumulation of metals, trace elements and semi-volatile organic compounds on exterior window surfaces in Baltimore. *Environ. Pollut.* **2003**, *122* (1), 51-61.
30. Ionescu, A.; Lefevre, R. A.; Chabas, A.; Lombardo, T.; Ausset, P.; Candau, Y.; Rosseman, L., Modeling of soiling based on silica-soda-lime glass exposure at six European sites. *Sci. Total Environ.* **2006**, *369* (1-3), 246-255.
31. Alfaro, S. C.; Chabas, A.; Lombardo, T.; Verney-Carron, A.; Ausset, P., Predicting the soiling of modern glass in urban environments: A new physically-based model. *Atmos. Environ.* **2012**, *60*, 348-357.
32. Verney-Carron, A.; Dutot, A. L.; Lombardo, T.; Chabas, A., Predicting changes of glass optical properties in polluted atmospheric environment by a neural network model. *Atmos. Environ.* **2012**, *54*, 141-148.
33. Liu, J. P.; Li, S.; Mekić, M.; Jiang, H. Y.; Zhou, W. T.; Loisel, G.; Song, W.; Wang, X. M.; Gligorovski, S., Photoenhanced Uptake of NO₂ and HONO Formation on Real Urban Grime. *Environ. Sci. Technol. Lett.* **2019**, *6* (7), 413-417.
34. Wu, R. W.; Harner, T.; Diamond, M. L.; Wilford, B., Partitioning characteristics of PCBs in urban surface films. *Atmos. Environ.* **2008**, *42* (22), 5696-5705.
35. Liu, Q. T.; Chen, R.; McCarry, B. E.; Diamond, M. L.; Bahavar, B., Characterization of polar organic compounds in the organic film on indoor and outdoor glass windows. *Environ. Sci. Technol.* **2003**, *37* (11), 2340-2349.
36. Kwamena, N. O. A.; Thornton, J. A.; Abbatt, J. P. D., Kinetics of surface-bound benzo- α -pyrene and ozone on solid organic and salt aerosols. *J. Phys. Chem. A* **2004**, *108* (52), 11626-11634.

37. Kwamena, N. O. A.; Earp, M. E.; Young, C. J.; Abbatt, J. P. D., Kinetic and product yield study of the heterogeneous gas-surface reaction of anthracene and ozone. *J. Phys. Chem. A* **2006**, *110* (10), 3638-3646.
38. Baergen, A. M.; Donaldson, D. J., Formation of reactive nitrogen oxides from urban grime photochemistry. *Atmospheric Chem. Phys.* **2016**, *16* (10), 6355-6363.
39. Ammar, R.; Monge, M. E.; George, C.; D'Anna, B., Photoenhanced NO₂ loss on simulated urban grime. *Chemphyschem* **2010**, *11* (18), 3956-61.
40. Priemer, D. A.; Diamond, M. L., Application of the multimedia urban model to compare the fate of SOCs in an urban and forested watershed. *Environ. Sci. Technol.* **2002**, *36* (5), 1004-1013.
41. Kwamena, N. O. A.; Clarke, J. P.; Kahan, T. F.; Diamond, M. L.; Donaldson, D. J., Assessing the importance of heterogeneous reactions of polycyclic aromatic hydrocarbons in the urban atmosphere using the Multimedia Urban Model. *Atmos. Environ.* **2007**, *41* (1), 37-50.
42. Csiszar, S. A.; Daggupati, S. M.; Verkoeyen, S.; Giang, A.; Diamond, M. L., SO-MUM: A Coupled Atmospheric Transport and Multimedia Model Used to Predict Intraurban-Scale PCB and PBDE Emissions and Fate. *Environ. Sci. Technol.* **2013**, *47* (1), 436-445.
43. Rodgers, T. F. M.; Truong, J. W.; Jantunen, L. M.; Helm, P. A.; Diamond, M. L., Organophosphate Ester Transport, Fate, and Emissions in Toronto, Canada, Estimated Using an Updated Multimedia Urban Model. *Environ. Sci. Technol.* **2018**, *52* (21), 12465-12474.
44. Dominguez-Morueco, N.; Diamond, M. L.; Sierra, J.; Schuhmacher, M.; Domingo, J. L.; Nadal, M., Application of the Multimedia Urban Model to estimate the emissions and environmental fate of PAHs in Tarragona County, Catalonia, Spain. *Sci. Total Environ.* **2016**, *573*, 1622-1629.
45. Weschler, C. J., Changes in indoor pollutants since the 1950s. *Atmos. Environ.* **2009**, *43* (1), 153-169.
46. Weschler, C. J., Chemistry in indoor environments: 20 years of research. *Indoor Air* **2011**, *21* (3), 205-218.
47. Nazaroff, W. W.; Weschler, C. J., Cleaning products and air fresheners: exposure to primary and secondary air pollutants. *Atmos. Environ.* **2004**, *38* (18), 2841-2865.
48. Weschler, C. J.; Nazaroff, W. W., SVOC exposure indoors: fresh look at dermal pathways. *Indoor Air* **2012**, *22* (5), 356-377.
49. Gligorovski, S.; Weschler, C. J., The Oxidative Capacity of Indoor Atmospheres. *Environ. Sci. Technol.* **2013**, *47* (24), 13905-13906.
50. Weschler, C. J., Ozone in indoor environments: Concentration and chemistry. *Indoor Air-International Journal of Indoor Air Quality and Climate* **2000**, *10* (4), 269-288.
51. Young, C. J.; Zhou, S.; Siegel, J. A.; Kahan, T. F., Illuminating the dark side of indoor oxidants. *Environ. Sci. Process Impacts* **2019**, *21* (8), 1229-1239.
52. Zhou, S.; Young, C. J.; VandenBoer, T. C.; Kowal, S. F.; Kahan, T. F., Time-Resolved Measurements of Nitric Oxide, Nitrogen Dioxide, and Nitrous Acid in an Occupied New York Home. *Environ. Sci. Technol.* **2018**, *52* (15), 8355-8364.
53. Avol, E. L.; Navidi, W. C.; Colome, S. D., Modeling ozone levels in and around southern California homes. *Environ. Sci. Technol.* **1998**, *32* (4), 463-468.
54. Lee, K.; Xue, X. P.; Geyh, A. S.; Ozkaynak, H.; Leaderer, B. P.; Weschler, C. J.; Spengler, J. D., Nitrous acid, nitrogen dioxide, and ozone concentrations in residential environments. *Environ. Health Perspect.* **2002**, *110* (2), 145-149.
55. Zhou, S.; Young, C. J.; VandenBoer, T. C.; Kahan, T. F., Role of location, season, occupant activity, and chemistry in indoor ozone and nitrogen oxide mixing ratios. *Environ. Sci. Process Impacts* **2019**, *21* (8), 1374-1383.
56. Nazaroff, W. W.; Weschler, C. J., Indoor acids and bases. *Indoor Air* **2020**, *30* (4), 559-644.
57. Patel, S.; Sankhyan, S.; Boedicker, E. K.; DeCarlo, P. F.; Farmer, D. K.; Goldstein, A. H.; Katz, E. F.; Nazaroff, W. W.; Tian, Y. L.; Vanhanen, J.; Vance, M. E., Indoor Particulate Matter during HOMEChem: Concentrations, Size Distributions, and Exposures. *Environ. Sci. Technol.* **2020**, *54* (12), 7107-7116.

58. Ampollini, L.; Katz, E. F.; Bourne, S.; Tian, Y. L.; Novoselac, A.; Goldstein, A. H.; Lucic, G.; Waring, M. S.; DeCarlo, P. F., Observations and Contributions of Real-Time Indoor Ammonia Concentrations during HOMEChem. *Environ. Sci. Technol.* **2019**, *53* (15), 8591-8598.
59. Farmer, D. K.; Vance, M. E.; Abbatt, J. P. D.; Abeleira, A.; Alves, M. R.; Arata, C.; Boedicker, E.; Bourne, S.; Cardoso-Saldana, F.; Corsi, R.; DeCarlo, P. F.; Goldstein, A. H.; Grassian, V. H.; Hildebrandt Ruiz, L.; Jimenez, J. L.; Kahan, T. F.; Katz, E. F.; Mattila, J. M.; Nazaroff, W. W.; Novoselac, A.; O'Brien, R. E.; Or, V. W.; Patel, S.; Sankhyan, S.; Stevens, P. S.; Tian, Y.; Wade, M.; Wang, C.; Zhou, S.; Zhou, Y., Overview of HOMEChem: House Observations of Microbial and Environmental Chemistry. *Environ. Sci. Process Impacts* **2019**, *21* (8), 1280-1300.
60. Dawe, K. E. R.; Furlani, T. C.; Kowal, S. F.; Kahan, T. F.; VandenBoer, T. C.; Young, C. J., Formation and emission of hydrogen chloride in indoor air. *Indoor Air* **2019**, *29* (1), 70-78.
61. Manoukian, A.; Quivet, E.; Temime-Roussel, B.; Nicolas, M.; Maupetit, F.; Wortham, H., Emission characteristics of air pollutants from incense and candle burning in indoor atmospheres. *Environ. Sci. Pollut. Res.* **2013**, *20* (7), 4659-4670.
62. Rai, A. C.; Guo, B.; Lin, C. H.; Zhang, J.; Pei, J.; Chen, Q., Ozone reaction with clothing and its initiated VOC emissions in an environmental chamber. *Indoor Air* **2014**, *24* (1), 49-58.
63. Kruza, M.; Lewis, A. C.; Morrison, G. C.; Carslaw, N., Impact of surface ozone interactions on indoor air chemistry: A modeling study. *Indoor Air* **2017**, *27* (5), 1001-1011.
64. Schripp, T.; Langer, S.; Salthammer, T., Interaction of ozone with wooden building products, treated wood samples and exotic wood species. *Atmos. Environ.* **2012**, *54*, 365-372.
65. Tamas, G.; Weschler, C. J.; Toftum, J.; Fanger, P. O., Influence of ozone-limonene reactions on perceived air quality. *Indoor Air* **2006**, *16* (3), 168-178.
66. Stutz, J.; Kim, E. S.; Platt, U.; Bruno, P.; Perrino, C.; Febo, A., UV-visible absorption cross sections of nitrous acid. *J. Geophys. Res. Atmos.* **2000**, *105* (D11), 14585-14592.
67. Gomez Alvarez, E.; Amedro, D.; Afif, C.; Gligorovski, S.; Schoemaeker, C.; Fittschen, C.; Doussin, J. F.; Wortham, H., Unexpectedly high indoor hydroxyl radical concentrations associated with nitrous acid. *PNAS* **2013**, *110* (33), 13294-13299.
68. Kowal, S. F.; Allen, S. R.; Kahan, T. F., Wavelength-Resolved Photon Fluxes of Indoor Light Sources: Implications for HO_x Production. *Environ. Sci. Technol.* **2017**, *51* (18), 10423-10430.
69. Fraser, M. P.; Cass, G. R.; Simoneit, B. R. T., Particulate organic compounds emitted from motor vehicle exhaust and in the urban atmosphere. *Atmos. Environ.* **1999**, *33* (17), 2715-2724.
70. Deng, B. L.; Chen, Y. Y.; Duan, X. B.; Li, D.; Li, Q.; Tao, D.; Ran, J. Q.; Hou, K. H., Dispersion behaviors of exhaust gases and nanoparticle of a passenger vehicle under simulated traffic light driving pattern. *Sci. Total Environ.* **2020**, *740*, 12.
71. Roth, P.; Yang, J. C.; Stamatis, C.; Barsanti, K. C.; Cocker, D. R.; Durbin, T. D.; Asa-Awuku, A.; Karavalakis, G., Evaluating the relationships between aromatic and ethanol levels in gasoline on secondary aerosol formation from a gasoline direct injection vehicle. *Sci. Total Environ.* **2020**, *737*, 10.
72. Samoli, E.; Stafoggia, M.; Rodopoulou, S.; Ostro, B.; Declercq, C.; Alessandrini, E.; Diaz, J.; Karanasiou, A.; Kelessis, A. G.; Le Tertre, A.; Pandolfi, P.; Randi, G.; Scarinzi, C.; Zauli-Sajani, S.; Katsouyanni, K.; Forastiere, F.; Grp, M.-P. S., Associations between Fine and Coarse Particles and Mortality in Mediterranean Cities: Results from the MED-PARTICLES Project. *Environ. Health Perspect.* **2013**, *121* (8), 932-938.
73. Lin, H. L.; Liu, T.; Xiao, J. P.; Zeng, W. L.; Li, X.; Guo, L. C.; Zhang, Y. H.; Xu, Y. J.; Tao, J.; Xian, H.; Syberg, K. M.; Qian, Z. M.; Ma, W. J., Mortality burden of ambient fine particulate air pollution in six Chinese cities: Results from the Pearl River Delta study. *Environ. Int* **2016**, *96*, 91-97.
74. Delfino, R. J.; Zeiger, R. S.; Seltzer, J. M.; Street, D. H.; McLaren, C. E., Association of asthma symptoms with peak particulate air pollution and effect modification by anti-inflammatory medication use. *Environ. Health Perspect.* **2002**, *110* (10), A607-A617.
75. Li, L.; Yang, J.; Song, Y. F.; Chen, P. Y.; Ou, C. Q., The burden of COPD mortality due to ambient air pollution in Guangzhou, China. *Sci. Rep.* **2016**, *6*, 7.

76. Santos, U. D.; Braga, A. L. F.; Giorgi, D. M. A.; Pereira, L. A. A.; Grupi, C. J.; Lin, C. A.; Bussacos, M. A.; Zanetta, D. M. T.; Saldiva, P. H. D.; Terra, M., Effects of air pollution on blood pressure and heart rate variability: a panel study of vehicular traffic controllers in the city of Sao Paulo, Brazil. *Eur. Heart J.* **2005**, *26* (2), 193-200.
77. Lin, H. L.; An, Q. Z.; Luo, C.; Pun, V. C.; Chan, C. S.; Tian, L. W., Gaseous air pollution and acute myocardial infarction mortality in Hong Kong: A time-stratified case-crossover study. *Atmos. Environ.* **2013**, *76*, 68-73.
78. Yang, W.; Xu, Y. Y.; Pan, H. J.; Tian, F.; Wang, Y. Z.; Xia, M. J.; Hu, J. Y.; Yang, M. J.; Tao, S. M.; Sun, S. F.; Kan, H. D.; Li, R. S.; Ying, Z. K.; Li, W. H., Chronic exposure to diesel exhaust particulate matter impairs meiotic progression during spermatogenesis in a mouse model. *Ecotoxicol Environ. Saf.* **2020**, *202*, 9.
79. Febo, A.; Perrino, C., Measurement of High Concentrations of Nitrous Acid Inside Automobiles. *Atmos. Environ.* **1995**, *29* (3), 345-351.
80. Jo, W.-K.; Lee, J.-W., In-vehicle Exposure to Aldehydes while Commuting on Real Commuter Routes in a Korean Urban Area. *Environ. Res. Sec. A* **2002**, *88*, 44-51.
81. Som, D.; Dutta, C.; Chatterjee, A.; Mallick, D.; Jana, T. K.; Sen, S., Studies on Commuters' Exposure to BTEX in Passenger Cars in Kolkata, India. *Sci. Total Environ.* **2007**, *372*, 426-432.
82. Esber, L. A.; El-Fadel, M.; Nuwayhid, I.; Saliba, N., The effect of different ventilation modes on in-vehicle carbon monoxide exposure. *Atmos. Environ.* **2007**, *41* (17), 3644-3657.
83. Di, Y. W.; Mo, J. H.; Zhang, Y. P.; Deng, J. W., Ozone deposition velocities on cotton clothing surface determined by the field and laboratory emission cell. *Indoor Built Environ.* **2017**, *26* (5), 631-641.
84. Pham, D. M.; Boussouira, B.; Moyal, D.; Nguyen, Q., Oxidization of squalene, a human skin lipid: a new and reliable marker of environmental pollution studies. *Int. J. Cosmet. Sci.* **2015**, *37* (4), 357-365.
85. Zhou, S. M.; Forbes, M. W.; Katrib, Y.; Abbatt, J. P. D., Rapid Oxidation of Skin Oil by Ozone. *Environ. Sci. Technol. Letters* **2016**, *3* (4), 170-174.
86. Rim, D.; Novoselac, A.; Morrison, G., The influence of chemical interactions at the human surface on breathing zone levels of reactants and products. *Indoor Air* **2009**, *19* (4), 324-334.
87. Dessi, M. A.; Deiana, M.; Day, B. W.; Rosa, A.; Banni, S.; Corongiu, F. P., Oxidative stability of polyunsaturated fatty acids: effect of squalene. *Eur. J. Lipid Sci. Technol.* **2002**, *104* (8), 506-512.
88. Lakey, P. S. J.; Wisthaler, A.; Berkemeier, T.; Mikoviny, T.; Poeschl, U.; Shiraiwa, M., Chemical kinetics of multiphase reactions between ozone and human skin lipids: Implications for indoor air quality and health effects. *Indoor Air* **2017**, *27* (4), 816-828.
89. Klepeis, N. E.; Nelson, W. C.; Ott, W. R.; Robinson, J. P.; Tsang, A. M.; Switzer, P.; Behar, J. V.; Hern, S. C.; Engelmann, W. H., The National Human Activity Pattern Survey (NHAPS): a resource for assessing exposure to environmental pollutants. *J. Expo. Anal. Environ. Epidemiol.* **2001**, *11* (3), 231-252.

Chapter Two:

Physical and Chemical Characterization of Urban Grime Sampled from Two Cities

Reproduced with permission from:

Corey R. Kryptavich, Shan Zhou, Shawn F. Kowal, and Tara F. Kahan *ACS Earth and Space Chemistry* **2020** 4 (10), 1813-1822 DOI: 10.1021/acsearthspacechem.0c00192

Copyright © American Chemical Society 2020

2.1 Abstract

Urban grime can be an important substrate for heterogeneous reactions in cities. Studies performed using laboratory-prepared urban grime proxies and urban grime collected from the field indicate that the physicochemical properties of urban grime can greatly affect heterogeneous reaction rate constants. We investigated several properties of urban grime collected from two cities in the north-east region of the United States of America. Optical and Raman microscopy indicated that urban grime collected from these regions consists primarily of particles as opposed to a uniform film. Total carbon analysis and ion chromatography were used to determine the bulk composition of the urban grime from both cities. Comparing these results to reported compositions of urban grime from cities in Canada and Europe showed strong similarities between different locations, with some variations for specific ions, such as higher chloride levels in North American cities and higher sulfate levels in some European cities. Absorbance spectra demonstrated that urban grime can absorb sunlight across the ultraviolet region. It may therefore be able to participate in photochemical reactions (either hindering them via processes such as the inner filter effect or enhancing them via processes such as photosensitization).

2.2 Introduction

Many atmospheric reactions occur in the gas phase, but reactions on surfaces can also greatly affect air and water quality.¹ The high density of three-dimensional structures in cities leads to high surface area to volume ratios.² Many surfaces in cities are coated with a layer containing a complex mixture of organic and inorganic species often referred to as “urban grime”.³ Urban grime may be an important physical sink for pollutants such as polycyclic

aromatic hydrocarbons (PAHs) and polybrominated diphenyl ethers (PBDEs),^{2, 4-6} and also an important substrate for reactions.⁷ Measurements of reaction kinetics on laboratory-prepared urban grime proxies suggest that heterogeneous ozonation at urban grime surfaces could be an important fate for some aromatic pollutants in cities,^{8, 9} and that nitrous acid (HONO) could be generated in urban grime via photolysis of nitrate ions and from dark and photoenhanced uptake of NO₂.¹⁰⁻¹² Recent experiments using urban grime collected from field sites in various cities have also demonstrated HONO generation from nitrate photolysis and photoenhanced NO₂ uptake.^{13, 14} Finally, temporal changes in the ionic composition of urban grime sampled over periods of months to years are consistent with reactions such as chemical chloride and ammonium loss and reactive SO₂ uptake,^{15, 16} and physical processes such as ammonium nitrate volatilization.¹⁵ Additional processes of radical precursor formation, including ClNO₂ production, have been suggested, but to date no studies have tested this hypothesis.¹⁶

The composition of atmospheric substrates can have large effects on heterogeneous and photochemical reaction kinetics. Therefore, the importance of urban grime as an environmental reaction medium will depend in large part on its composition and morphology. For example, photoenhanced NO₂ uptake coefficients were reported to vary greatly depending on the composition of the grime proxy, with coefficients on solid potassium nitrate films increasing by approximately a factor of two when pyrene was incorporated into the film,¹⁰ and with 10× larger photoenhanced NO₂ uptake coefficients reported on real urban grime than on bare glass.¹³ Likewise, nitrate photolysis rate constants have been reported to vary widely depending on the composition of the underlying substrate, with similar rate constants reported in real urban grime and in grime proxies prepared from vacuum grease,¹⁴ but with rates on glass and in aqueous solution at least an order of magnitude lower.^{12, 17} Heterogeneous ozonation rates of pollutants

such as PAHs have also been shown to depend on substrate, with faster rates reported on some surfaces (e.g., soot, solid azelaic acid, ice)¹⁸⁻²⁰ than others (e.g., water, octanol, quartz).⁹ Non-reactive uptake coefficients also depend strongly on chemical composition, so reactant concentrations in urban grime will depend on grime composition.^{2, 21, 22}

Some components of urban grime can undergo chemical reactions, which can affect atmospheric composition as well as the fate of adsorbed atmospheric species. One example is nitrate photolysis. Nitrate is thought to account for ~6% of urban grime mass,^{3, 15, 23} and illuminated urban grime samples have been shown to release NO and HONO to the gas phase.¹² Some components of urban grime such as unsaturated organics are reactive toward ozone. Unsaturated organics in urban grime proxies have been shown to reduce ozonolysis rates of adsorbed species such as PAHs via competitive reactions.⁹ Finally, components of urban grime may increase reactivity of adsorbed atmospheric species by acting as catalysts or photosensitizers, or may decrease reactivity by competitive photon absorbance (the inner filter effect) or by scavenging reactive trace gases such as ozone and hydroxyl radicals. Increased reactivity of a number of atmospheric species has been reported on real and model atmospheric aerosols due to catalytic and photosensitizing properties of substrate components.¹ Competitive photon scavenging has been suggested to be responsible for slower PAH photodegradation on dark aerosols such as soot and coloured fly ash compared to on lighter coloured aerosols,²⁴ and the presence of unsaturated organics in urban grime proxies was reported to reduce PAH ozonation rates by scavenging ozone.⁹

Urban grime morphology could also be important to predicting reaction rates on urban surfaces. One potentially important parameter is the extent to which urban grime coats surfaces (its fractional surface coverage). Both uptake coefficients and reaction kinetics can depend

strongly on substrate composition. For example, as described above, photoenhanced NO₂ reactive uptake coefficients were reported to be 10× larger on urban grime than on bare glass.¹³ Therefore, this process would likely be a more important HONO source in cities if exterior surfaces are nearly completely covered by urban grime than if only a small fraction of available surface area is covered. A second parameter of interest is whether urban grime is a homogeneous film or a collection of particles (or some combination of the two). This could influence surface coverage (with films being more likely to completely coat surfaces than collections of discrete particles), but could also indicate different composition, since large particles may have different sources than films. If urban grime primarily consists of particles, this could also increase the surface area to volume ratio in cities, increasing the importance of heterogeneous processes to local atmospheric composition. Some recent studies have reported a variety of urban grime morphologies, including films and particles.^{25, 26}

Several studies have measured reaction kinetics in proxies for urban grime, and, more recently, in real urban grime collected from the field. Fabricated films of pyrene and potassium nitrate or octanol, and urban grime samples collected from the field were used to investigate various reactions, in particular the photolysis of nitrate ions.^{10-12, 14} This reaction could be a potential source for reactive species such as HONO, NO, and OH radicals.¹⁴ Other research investigated reactions of ozone at the surface of simulated films made of benzophenone or of alcohols such as octanol and decanol,^{9, 27} and of photosensitized NO₂ uptake to urban grime and urban grime proxies.^{10, 13}

Urban grime is often treated as a homogenous film that coats urban surfaces, although some recent studies suggest that urban grime may consist of particles as well as (or perhaps rather than) a film.^{25, 26} The filtrate of urban grime samples has been reported to consist primarily

of inorganic species, with only 6 – 24% of the mass consisting of organic compounds.^{3, 15, 23} Although the majority of urban grime mass remains uncharacterized, a number of reactive species have been identified, including photolabile ions such as nitrate and metals such as iron and aluminum.³ In this work, we investigated physical properties of urban grime using optical and Raman microscopy, and investigated the composition of urban grime collected from two urban centers using Raman microscopy, total carbon analysis, and ion chromatography. We also used absorption spectroscopy to characterize the wavelength-resolved absorbance of urban grime samples.

2.3 Methods

Urban grime samples used for compositional analysis were collected in Syracuse, New York and Scranton, Pennsylvania between February and October 2017. Sample locations are shown in the supplementary information (SI) as tables S1 and S2. Sampling for bulk analysis was performed by wetting exterior windows with methanol then scraping the wetted surfaces with clean 1 cm × 5 cm Teflon strips. The strips and collected grime were stored in glass jars and dried in desiccators. The Teflon strips and jars were weighed before and after grime collection; the difference in mass is reported as the mass of the grime. Twenty-three samples were collected in Scranton and 19 in Syracuse. All but three of the windows were largely protected from rain by overhangs, which prevent washout of the grime by rain.² The 10 cm closest to the window edge was not sampled to prevent contamination from the window frame or surrounding building material. The sampled area differed for each window due to variations in window size. The average area sampled for each window was $0.5 \pm 0.1 \text{ m}^2$.

A portion of the grime was analyzed for total carbon and total nitrogen content using total carbon analysis (TC), and the remaining portion was dissolved in deionized water and analyzed with UV-Visible spectroscopy and ion chromatography. The UV-Visible spectroscopy was performed with a Cary 60 UV-Vis spectrometer. Absorbance was recorded across the full spectral range of the instrument (200 – 800 nm). Some samples had absorbance values greater than 1. In those cases, the solution was diluted and an “ideal” absorbance of the original solution (i.e., the absorbance expected in the absence of deviations from the Beer-Lambert Law) was determined by a linear extrapolation from the absorbance measured in the diluted sample. This was done to enable comparisons between different samples while avoiding artifacts at high concentrations. Deionized water blanks were analyzed between each sample.

Ion chromatography was performed on a dual column ThermoFisher instrument with conductivity detection. A CS-16 column was calibrated for sodium, magnesium, calcium, potassium, and ammonium. An AS-18 column was calibrated for chloride, bromide, nitrate, sulfate, and fluoride. The ion chromatograph’s anion column is capable of detecting carbonate ions, but due to partitioning of atmospheric carbon dioxide into the water-based grime solutions carbonate concentrations could not be quantified. Calibration standards containing all five of the target anions and all five of the target cations were acquired before each batch of grime samples, along with blanks. The ranges for these standards varied by ion and are listed in table S3 in the SI. Measurements of individual standards were followed by quality control standards from the United States Geological Survey which contained known concentrations of the tested ions in the standard. Grime solution samples were then analyzed, with blanks and external standards placed intermittently between the samples. Internal standards were included in each sample. The

internal standard concentration was the same as the third most concentrated external standard for all ions.

Urban grime was collected for *in situ* analysis in Syracuse by placing $\sim 1 \text{ cm}^2$ quartz plates outdoors for ~ 30 days between May and June 2014. The plates were attached to aluminum sheets which were secured vertically to surfaces such as fences and railings. Raman microscopy was performed using a confocal Renishaw *InVia* Basis microscope with a 50 mW 532 nm YAG laser and a Leica DM2500 objective. Raman maps were acquired by collecting spectra over an area of the quartz surface with a step size of $2 \mu\text{m}$.

2.4 Results

2.4.1 Physical Characterization

Urban grime has long been thought to be predominately a film. This view has started to shift as new evidence comes to light. Work conducted by Favez et al. investigated the optical properties of urban grime and found that deposition of more reflective compounds leads to an overall increase in surface reflectance.¹⁵ They also found that both particle reflection and particle absorbance of light leads to the decrease in the light's transmittance through the glass surface.¹⁵ Grant et al. reported that urban grime morphology is very heterogeneous, containing both films and a variety of particles including mineral dust, biogenic organics, and other components.²⁵ Figure 2.1 shows a microscope image of a glass plate that had been exposed to ambient air in Syracuse for 10 weeks. The main features observed in such slides were collections of particles, in agreement with recent findings.

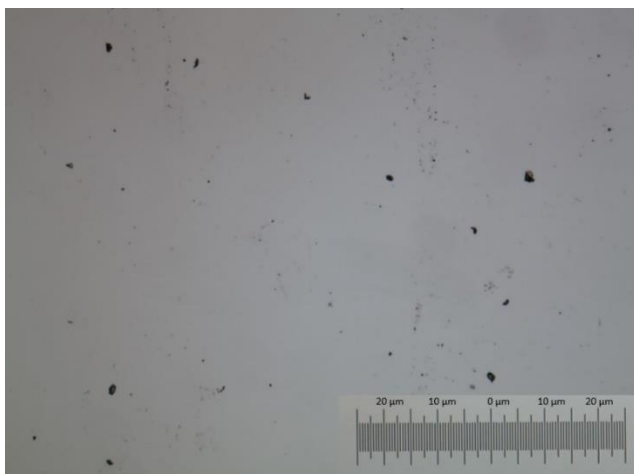


Figure 2.1. Optical microscope image (10× magnification) of a glass plate exposed to ambient outdoor air for 10 weeks in Syracuse, NY.

Figure 2.2 shows the Raman features observed at the surface of quartz plates that had and had not been exposed to outdoor air. Clean plates showed spectral features corresponding to quartz at all locations. Quartz plates that had been exposed to outdoor air showed spectral features corresponding to quartz at locations on the plates that did not contain visible particles. Spectra acquired at locations on the plates with visible particles were characterized by a gradual, generally featureless, increase in intensity with increasing energy. This is consistent with fluorescence, and likely arises from the presence of carbon-containing species. Some particles exhibited an additional feature in the form of two broad overlapping peaks at approximately 1596 cm^{-1} and 1354 cm^{-1} corresponding to graphite and a graphite defect band. The peak area ratio of approximately 0.8 is indicative of atmospheric black carbon as opposed to pure graphite.²⁸ Other spectral features, such as peaks at $2800 - 3000\text{ cm}^{-1}$ corresponding to C-H stretches of organic species, were occasionally but inconsistently detected at locations with visible particles; these are not the focus of this study and were not further analyzed. Figure 2.3 shows an optical image of some particles on a quartz plate, as well as two-component principal component analysis of a Raman map at the same location as the optical image. Grey pixels

indicate Raman emission from quartz, and red pixels indicate fluorescence, with or without contribution from black carbon. In all samples, spectra acquired at locations that did not contain visible particles contained only spectral features from quartz, while most particles exhibited fluorescence.

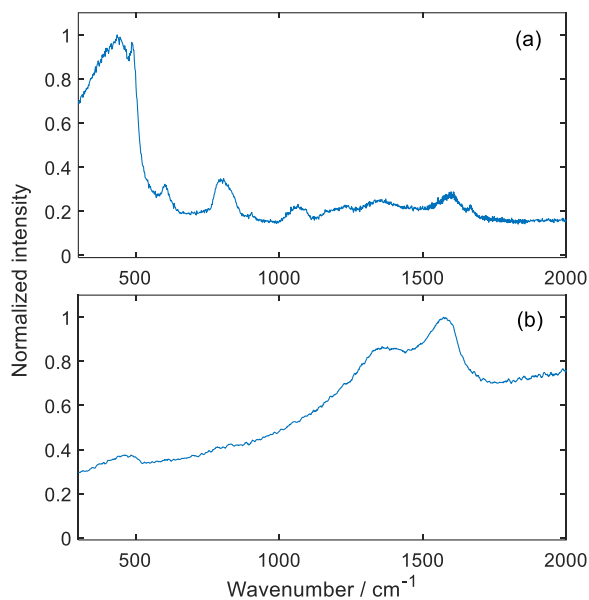


Figure 2.2. Raman spectra of (a) a clean quartz surface, and (b) a particle on a quartz surface.

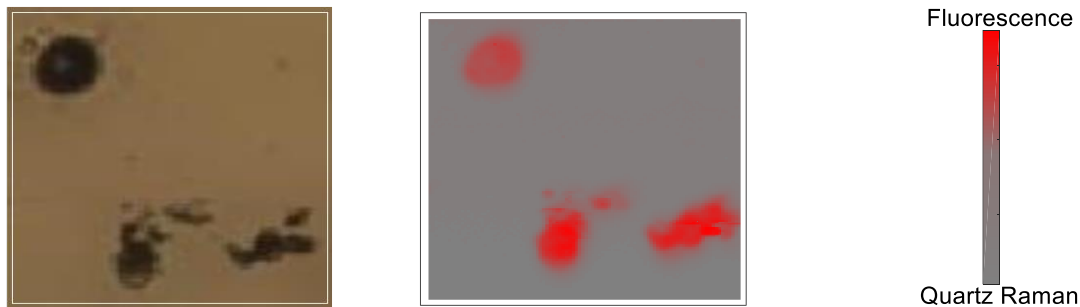


Figure 2.3. A $192 \times 230 \mu\text{m}$ optical image of a quartz plate placed outdoors for 30 days (top panel), and the corresponding intensity map (bottom panel). Grey pixels correspond to spectra identified as quartz based on relative intensity at 500 cm^{-1} and 650 cm^{-1} . Red pixels correspond to spectra containing fluorescence from urban grime based on relative intensity at 2050 cm^{-1} and 650 cm^{-1} .

The above results suggest that urban grime consists of individual particles surrounded by the underlying substrate. A recent study reported the existence of both particles and films based on optical microscopy, atomic force microscopy, and surface-sensitive mass spectrometry.²⁵

Optical microscopy images from that work suggest that particles were detected exclusively for the first two weeks of exposure, with some film (that only covered a small fraction of the surface) detected, in addition to particles, at four weeks of exposure. Near-complete surface coverage was reported for exposure periods of six months or greater. The samples we analyzed using optical microscopy – which were exposed for ~10 weeks – did not show any evidence of film formation. This is likely due in part to the different orientations of the passive samplers used in the two studies. The passive samplers used by Grant et al. were placed horizontally (facing upward), while those used in our study were placed vertically to mimic the sides of buildings.²⁵ A recent model for the growth of indoor surface films suggests that accumulation onto horizontal surfaces will be much more rapid than onto vertical surfaces due to the combined deposition of coarse-mode particles and absorption of semi-volatile organic carbons.²⁹ Since the same principles apply outdoors, it is likely that urban surface films accumulate rapidly on upward-facing surfaces such as roofs and streets, reaching near-complete surface coverage on timescales of approximately 3 months, as reported by Grant et al.,²⁵ but that particles dominate the mass of vertical urban surface coatings such as the sides of buildings for much longer time periods, and that near-complete surface coverage will not be obtained by 3 months time. In fact, many vertical surfaces will likely never be completely coated in urban grime (whether by particles or films) due to rainfall events.

It is possible that a film is present in our samples. However, such a film would be too thin to be detected by optical microscopy, and either would not contain Raman-active components, or these components would be present at concentrations below our detection limit. It is possible that greater surface coverage and film formation would be observed on different substrates – for example, cement is very porous compared to quartz.²⁵ It is also possible that films exist in more

polluted locations; Syracuse has good air quality, with 275 of 283 reported days in 2019 having 24-hour averaged PM_{2.5} levels below 12.0 $\mu\text{g m}^{-3}$.³⁰ We discuss the implications of urban grime fractional surface coverage and conformation (i.e., particles vs. films) in the Implications section.

2.4.2 Bulk Characterization

The surface mass density of urban grime was calculated for each sample by dividing the collected mass by the area of the window scraped. Densities were highly variable in both cities. In Syracuse, the average mass density was $(58 \pm 92) \text{ mg m}^{-2}$, with a median density of 20 mg m^{-2} . The mean was strongly influenced by four samples with densities greater than 100 mg m^{-2} ; all other samples had densities lower than 35 mg m^{-2} . With the outlier samples removed, the mean decreased to $(19 \pm 9) \text{ mg m}^{-2}$. Surface densities were much greater in Scranton than in Syracuse, with a mean of $(78 \pm 79) \text{ mg m}^{-2}$ and a median of 54 mg m^{-2} . Densities generally ranged from 4 mg m^{-2} to 160 mg m^{-2} . Removing two samples with densities of 250 and 320 mg m^{-2} reduced the mean sample density to $58 \pm 47 \text{ mg m}^{-2}$, still much higher than that of the Syracuse samples. Several studies have reported surface mass densities of urban grime or urban grime components in different cities. An average mass density of 67 mg m^{-2} was reported for 15 windows sampled in Toronto;³ this is on the same order of magnitude as the levels we measured in Syracuse and Scranton. Densities averaging $\sim 370 \text{ mg m}^{-2}$ were reported for grime samples collected after approximately 190 days of accumulation in sheltered locations in 6 European cities. Samples collected after more than 800 days of accumulation had surface densities ranging from less than 500 mg m^{-2} (Rome) to $\sim 4 \text{ g m}^{-2}$ (Athens and London).^{15, 31}

Figure 2.4 shows the average composition of urban grime collected from Syracuse and Scranton. Carbon made up a large fraction ($\sim 22\%$) of the total grime mass. Non-ionic nitrogen,

which consists of all measured nitrogen apart from nitrogen in nitrate and ammonia ions, and is likely primarily due to organic nitrogen, accounted for ~2% of the mass in samples from both Syracuse and Scranton. Ionic species account for ~30% of the total mass of samples collected in Syracuse, but only ~9% of the mass from the Scranton samples. The remaining, unidentified, mass of the samples (~44% in Syracuse and ~64% in Scranton) may come from metals, insoluble salts, and other components such as organic oxygen, sulfur, or hydrogen. Previous studies have also reported uncharacterized urban grime mass fractions of 50% or greater.^{3, 15, 32}

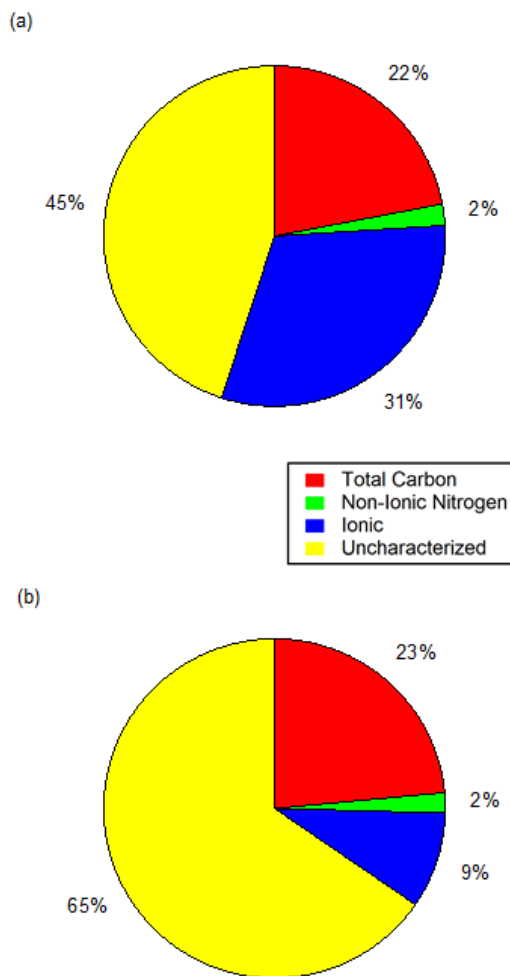


Figure 2.4. Compositional breakdown of grime based on mass percentage from (a) Syracuse, NY and (b) Scranton, PA

Several studies have investigated the fractional composition of urban grime. Urban grime in Toronto, Canada was reported to contain only ~6% carbon by mass,³ while urban grime in six European cities was reported to consist of 24% carbon by mass on average,¹⁵ and another study reported average carbon mass fractions of approximately 19% in four European cities.²³ The carbon mass fraction in urban grime collected from Syracuse and Scranton in this work was ~22% on average, which is similar to that reported in European cities, but larger than that reported in Toronto. Mass fractions of carbon in individual European cities ranged from approximately 11% to 48%, demonstrating the variability in carbon content between different cities and samples.^{15, 23} The reported mass fraction of soluble ionic species in samples collected from European cities ranged from approximately 8 – 30%, with two separate studies reporting an average of ~23%.^{15, 23} The average soluble ionic mass fractions we measured in Syracuse (31%) and Scranton (9%) are at the upper and lower ranges of the measurements in European cities.

2.4.3 Ionic Composition

Figure 2.5 shows the ionic composition of the grime samples. The dominant ion in both cities is sodium (~30%). The relative contributions of other ions to the total mass vary between the two cities. The samples from Scranton show a higher mass contribution from potassium, nitrate, and sulfate, while the Syracuse samples have a higher contribution from chloride, magnesium, and calcium.

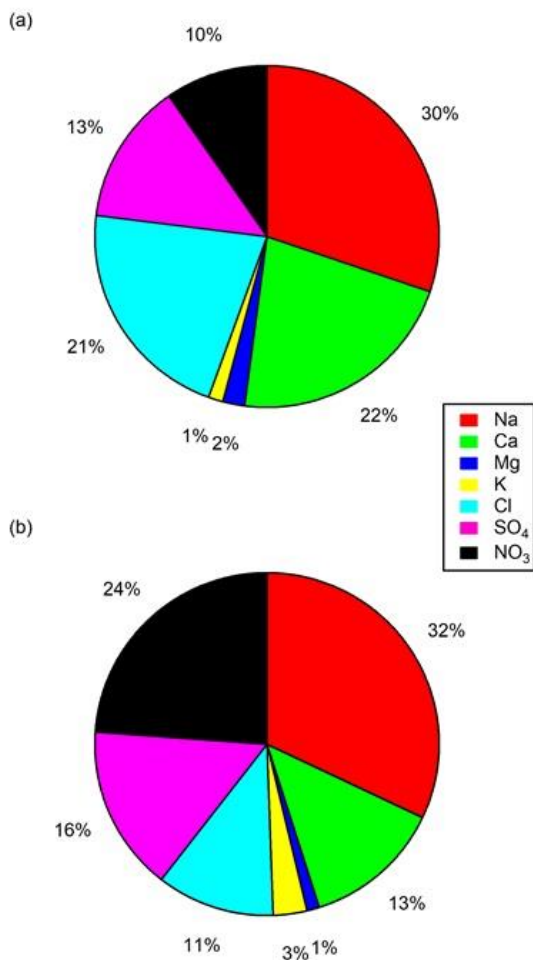


Figure 2.5. Average ionic composition based on percent ionic mass for (a) Syracuse and (b) Scranton

The composition of the ionic fraction of urban grime collected from a city in Canada (Toronto, Ontario) and several cities in Europe has been reported.^{15, 16, 23, 33} Calcium and nitrate fractions were similar in all locations (on the order of 20% of soluble ions for calcium and 26% for nitrate). Syracuse had the lowest relative nitrate concentration at 10% of soluble ions, but it was not greatly different from other locations, which reported nitrated fractions ranging from 13% to 49% of soluble ions. Chloride fractions in 7 European cities averaged only 5%,^{15, 33} while fractions in the North American cities were greater. Chloride accounted for ~11% of measured

soluble ions in Scranton, ~20% in Syracuse, and 29% in Toronto.¹⁶ Sulfate accounted for ~30% of ionic solutes in 7 European cities.^{15, 33} The level was lower in Syracuse and Scranton (13% and 16%, respectively), and still lower in Toronto (~7%).^{3, 16} Magnesium and potassium levels were not reported in the European studies, but our measured contributions of 1 – 3% are in agreement with levels reported in Toronto.¹⁶ Sodium accounted for approximately 30% of soluble ionic species by mass in Syracuse and Scranton. The fraction in Toronto (21%) was higher than that in the 7 European cities (~11%), but still lower than that in our study.^{3, 15, 16, 33} The discrepant sodium and chloride levels in North American and European cities may be due to influences from road salt, which is commonly used in the three North American cities in the winter. The samples were also examined for directional orientation and location, but no statistically significant variation was observed.

2.4.4 Correlations between Ionic Species

Following the determination of the composition by mass, correlations between the various ionic species were investigated. A full description of the method and ion distributions for each sample are provided in the SI. Three of the Syracuse locations (White1, MacNaughton1, and Almond1) had total ion concentrations greater than 360 ppm, while all other locations had total concentrations lower than 60 ppm. In our analysis, we investigated correlations between ion mass including samples from all locations, and also investigated correlations with the high concentration samples removed. Figure 2.6 shows correlation curves for sodium-chloride, sodium-magnesium, and sodium-nitrate ion pairs. Sodium is very highly correlated ($R^2 > 0.95$) with Cl^- both with and without the high concentration samples included. Conversely, Na^+ is only

correlated with Mg^{2+} when the high concentration samples are included, and it is only correlated with NO_3^- when the high concentration samples are removed.

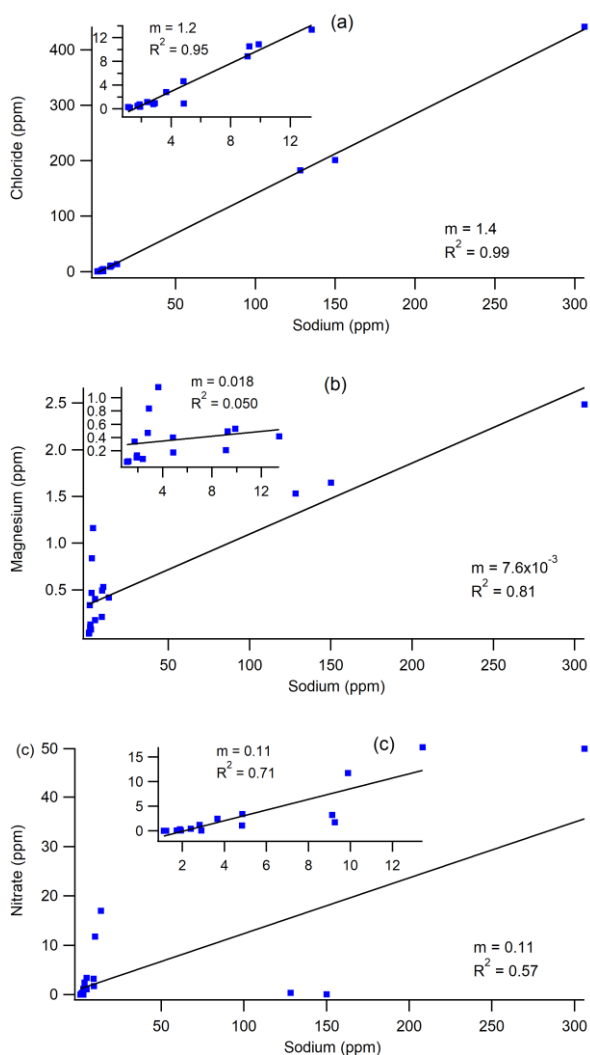


Figure 2.6: Correlation curves for (a) sodium-chloride, (b) sodium-magnesium, and (c) sodium-nitrate ion pairs from Syracuse samples. The inset within each figure excludes the three high concentration samples (White1, MacNaughton1, and Almond1).

The degree of correlation between each ion pair was calculated with and without the high concentration samples included. When the full range of concentrations was considered, all ions except NO_3^- correlated with each other. Nitrate was not correlated with any other ion. When the high concentration samples were not included in the analysis, the majority of ions still correlated

with one another, but Mg^{2+} did not correlate with any ions, and Ca^{2+} only correlated with K^+ . Nitrate, which did not correlate with any ions when all samples were included in the analysis, correlated with all ions except Mg^{2+} and Ca^{2+} when the high concentration samples were not included. These differences suggest that most ions had similar sources, but that Mg^{2+} and Ca^{2+} had different sources than NO_3^- .

As in Syracuse, ion correlations in Scranton samples were investigated with and without high concentration samples included. The low concentration range included ionic concentrations up to 63 ppm; three samples had high ionic concentrations in excess of 100 ppm. Sodium, Mg^{2+} , and NO_3^- were all correlated with one another regardless of whether high ionic concentration samples were included, and SO_4^{2-} correlated with Na^+ and NO_3^- in both concentration ranges. When the full concentration range was considered, K^+ and Cl^- both correlated only with Ca^{2+} (and not with each other), and Ca^{2+} was only correlated with K^+ and Cl^- . When high concentration samples were removed from consideration, Ca^{2+} and K^+ remained correlated with one another, and also correlated with Na^+ and Mg^{2+} , and Cl^- correlated with Na^+ and NO_3^- . These correlations suggest that different urban grime samples in Scranton had similar ion sources, but that the higher ionic concentration samples had different sources of some ions.

2.4.5 Seasonal Variations

The distribution of ionic content in urban grime has been reported to have seasonal variations.^{15, 16} Specifically, the nitrate and sulfate fractions of urban grime sampled in Toronto showed a summer maximum and winter minimum, while sodium and chloride fractions were largest in the winter.¹⁶ We collected grime between February and October 2017, with samples collected in 5 different months in Syracuse (between February and September) and 3 different

months in Scranton (May, June, and October). The temporal trends of ion mass fractions are shown in Figure S1 of the SI. Because we did not sample in December and January, it is difficult to determine whether the seasonal trends observed in Toronto urban grime samples also occur in Syracuse and Scranton. However, temporal trends of ionic mass fractions were generally in agreement with those observed in Toronto over the same time period, with the notable exception of nitrate, which showed a peak in the summer in Toronto, but a decrease in the summer in Syracuse and Scranton. A trend of maximum NO_3^- mass fraction in the winter, similar to our observations, was reported for PM_{10} sampled in Toronto concurrently with urban grime.¹⁶ Given that the urban grime sampled in Syracuse and Scranton appeared to primarily consist of particles, it is not surprising that the temporal variation of composition is similar to that of particulate matter.

More may be learned from the temporal variations of ratios of various ion mass fractions, which are shown in Figure 2.7. For example, the ratio of $\text{Cl}^-:\text{Na}^+$ was generally ~ 1 in Syracuse, with the exception of samples collected in June and September, which had ratios of 0.35 and 0.5 respectively. This is consistent with measurements in Toronto, which showed ratios of ~ 1 between November and May, and lower ratios (~ 0.2) between June and October.¹⁶ Those authors suggested that a ratio close to unity in the winter suggested direct deposition of NaCl from road salt, and that lower values in the summer could suggest chemical loss of chloride.

Baergen et al. also reported $\text{NO}_3^-:\text{Ca}^{2+}$ ratios over the course of their study period.¹⁶ They observed a higher ratio (>2) in the winter (October – February) than in the summer (~ 1 , March – August). Syracuse samples suggested a similar trend, with higher ratios in February and April (0.9 and 2.5) than in the summer (~ 0.2 in May and June, rising to 0.7 in September). The summer decrease in this ratio has been hypothesized to be due to photochemical loss of NO_3^- .¹⁶

Another ratio of interest is $\text{NO}_3^-:\text{SO}_4^{2-}$, which has been reported to show winter minima because of nitrate deposition during the summer and sulfate deposition during the winter.^{15, 16} Baergen and Donaldson reported that an opposite seasonal trend was observed for the $\text{NO}_3^-:\text{SO}_4^{2-}$ ratio in PM_{10} samples, which showed summer minima.¹⁶ As shown in Figure 2.7, this ratio was lowest in the summer in Syracuse. Again, this is consistent with urban grime samples in Syracuse consisting primarily of particles rather than films. At this time it is not clear what drives the development of film vs. particles in urban grime, but it is likely that the composition of the two components can be quite different, as has recently been suggested.²⁵ This deserves further study, as urban grime in different locations may present very different reactive environments and seasonal dependences.

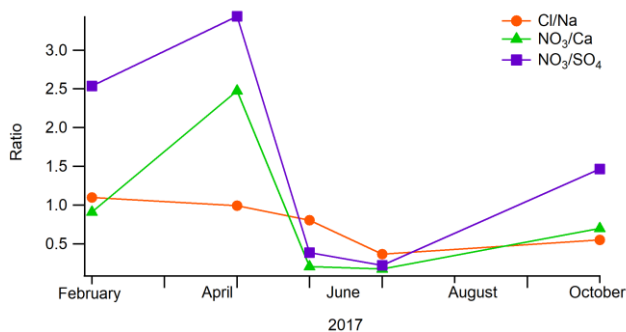


Figure 2.7: Time series for ion ratios in samples from Syracuse.

2.4.6. Optical Properties

Urban grime mass density has been reported to correlate with extinction of visible light (referred to as “haze”) in windows exposed to the outdoor atmosphere in rural, industrial, and urban settings,^{15, 23} but the extent of absorption of ultraviolet light (which initiates the majority of atmospheric photochemistry) has not been reported to our knowledge. Figure 2.8(a) shows the optical extinction of urban grime samples collected at two cities at the wavelength of 300 nm as a function of grime mass concentrations in the aqueous solution. Clear tight increasing trends

between attenuation and total grime mass concentration were observed for samples in both Scranton and Syracuse ($R^2 = 0.78$ and 0.96 , respectively). As suggested by the slopes of the linear fit, Scranton samples appeared to have stronger attenuation than Syracuse samples by approximately 40% (0.57 mL mg^{-1} vs 0.41 mL mg^{-1}) at 300 nm. The city-average normalized extinction (by grime mass concentration) was higher for Scranton samples than Syracuse samples throughout the UV-VIS wavelength range, as shown in Fig. 2.8(b). This suggests that Scranton samples were overall more extinctive than Syracuse samples.

A strong negative wavelength dependence of normalized extinction was observed for all samples in both cities at wavelengths shorter than ~ 475 nm. At longer wavelengths this dependence became very weak. We attribute extinction at longer wavelengths to scattering by particles in the sample. This attribution is supported by spectra of filtered samples (that contain only leachate from urban grime, shown in Figure S2 in the SI), which do not exhibit extinction at long wavelengths, but otherwise have similar extinction profiles to the unfiltered samples. The wavelength dependence observed at shorter wavelengths, along with the observation of extinction at these wavelengths in filtered samples, suggests a significant contribution of absorption at shorter wavelengths in addition to scattering.

The relationship between sample extinction and sample mass was determined to be linear throughout the UV region. This is illustrated in Figure S3 in the SI, which shows relationships between extinction and sample mass at 240 and 270 nm. While only wavelengths longer than ~ 290 nm reach Earth's surface and contribute to atmospheric photochemistry, analyzing shorter wavelengths may be useful for characterizing urban grime samples. Specifically, measuring extinction at shorter wavelengths could enable quantification of smaller sample masses, since urban grime extinction depends negatively on wavelength. While Scranton samples attenuated

light more strongly than Syracuse samples at all wavelengths, the slopes of best fit lines to the data from the individual cities agrees reasonably (within 20%) to the slope of a best fit line through all data points (from both cities combined). This suggests that, at least for samples collected from the two cities in this study, urban grime mass could be estimated using absorbance spectroscopy, perhaps negating the need for the more extensive sample preparation required to directly determine sample mass. This possibility could be explored in future studies.

We plotted extinction against several variables to investigate which urban grime component(s) control extinction. As shown in Figure S3 in the SI, extinction correlated to varying degrees with total urban grime mass, carbon mass, and ionic mass. Correlation was highest for total mass for the Syracuse samples ($R^2 = 0.96$), strong for ionic mass ($R^2 = 0.88$), and weakest for carbon mass ($R^2 = 0.64$). Conversely, extinction of samples from Scranton were most strongly correlated with carbon mass ($R^2 = 0.94$), followed by total mass ($R^2 = 0.78$) and then ionic mass ($R^2 = 0.62$). These disparities are interesting, but we do not wish to over-interpret them. At this point, we simply note their existence, and suggest that further studies into urban grime absorbance are warranted.

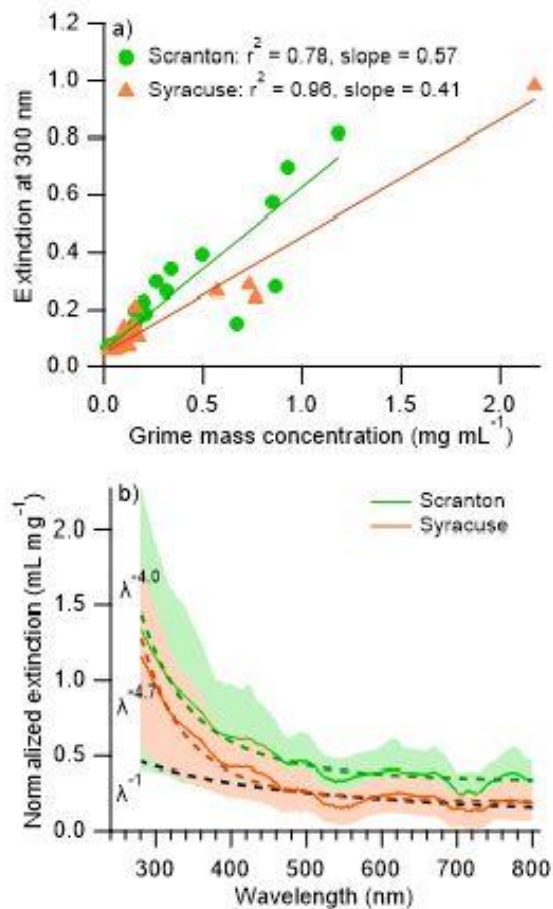


Figure 2.8. (a) Measured light extinction at 300 nm as a function of urban grime mass concentration in aqueous solution for samples collected from Syracuse and Scranton. Data fitting was performed using the orthogonal distance regression. (b) City-averaged light extinction normalized to total grime mass as a function of wavelength. Shades bound the standard deviation. Colored dashed lines were determined by fitting the mean with a power law equation. The λ^{-1} trend line (black dashed line) expected for black carbon is shown for comparison.

Black carbon (BC) and brown carbon (BrC) both absorb strongly in the UV-VIS range.³⁴ The dashed black line in Fig. 2.8(b) suggests particle absorption dominated by BC at longer wavelengths, following a power law of λ^{-1} .³⁵ The strong dependence of extinction on wavelength at shorter wavelengths with characteristic coefficient values, i.e., absorption Angstrom exponent (AAE), in excess of 1 was attributed to absorbing organic carbon (OC), e.g., brown carbon. However, because of multiple effects related to external versus internal mixing to BC, OC, and

BrC in airborne particles, the threshold value that distinguishes BC and BrC is somewhat uncertain. A recent modeling study suggested that an AAE exceeding 1.6 should be classified as BrC.³⁵ Samples collected in this study showed stronger wavelength dependences than BC, with AAE values ranging from 2.0 – 7.4 for Syracuse samples (3.8 ± 1.3) and 1.8 to 7.3 for Scranton samples (mean \pm standard deviation = 3.3 ± 1.5). AAE obtained from the city-average normalized attenuation was 4.7 and 4.0 for Syracuse and Scranton, respectively (Fig. 8b), both substantially greater than that for BC. The city-average normalized attenuation was higher than that of the average of individual samples due to two samples with very high attenuation in both cities. Removing these samples lowered the city average AAEs to 3.2 and 3.1 for Syracuse and Scranton, respectively. The AAE values observed in these samples suggest that the absorbing components of urban grime collected in Syracuse and Scranton were more similar to brown carbon or HULIS (humic-like substances) than to black carbon. The large range of calculated sample AAE in both cities suggest large variabilities in absorptivity. This could relate to the different chemical composition and mass fractional contribution of absorbing organic constituents.

We plotted AAE against carbon mass fraction and ionic mass fraction to investigate whether one of these components controls the observed wavelength dependence of urban grime extinction (Figure S4 in the SI). No correlation was observed with either carbon mass fraction or ionic mass fraction. Given the similarities in the AAE of our samples to those of brown carbon, it is likely that chromophoric organic matter is responsible for the observed wavelength dependence. We don't necessarily expect a correlation between AAE and carbon mass fraction, since relative abundances of organic carbon and black carbon could vary greatly between samples. Extinction spectra of filtered samples (that should not contain black carbon or other particles) had similar

spectral profiles to filtered samples, but overall lower intensity. The mean AAE of filtered samples was 4.8 ± 1.0 for Syracuse samples ($N = 3$) and 3.7 ± 0.8 for Scranton samples ($N = 4$). The fact that AAE were not lower in filtered samples compared to in unfiltered samples suggests that water-soluble species are responsible for a large fraction of the absorbance in urban grime from these two cities. Further analysis would be required to determine the structural similarity of these absorbing moieties to brown carbon or HULIS.

Urban grime is thought to play an important role in gas-phase renoxification in urban centers by providing a substrate for photochemical conversion of NO_3^- to HONO. This was first suggested by Handley et al. based on observations of loss of both nitrate and protons in films comprised of silicone vacuum grease and octanol during exposure to actinic radiation.¹¹ Subsequent studies from the same research group reported rapid photochemical loss of nitrate in illuminated samples of urban grime and urban grime proxies,¹⁴ as well as the formation of gas-phase HONO from irradiated urban grime samples.¹² Our observation of absorbance at wavelengths longer than 290 nm indicates that urban grime can absorb sunlight (Figure 2.8). This suggests that it may participate in photochemistry (e.g., by suppressing photolysis via the inner filter effect or enhancing photolysis via photosensitization or photolyzing to produce reactive species). This supports the observation of Baergen et al. that nitrate photolyzed more rapidly in urban grime than in aqueous solution,¹⁴ and is also consistent with observations that organic particulate matter produce hydroxyl and peroxy radicals in irradiated samples.^{36, 37} Further work is needed to determine the ways in which urban grime affects heterogeneous atmospheric photochemistry.

2.5 Implications

Urban grime has long been known to affect the physical integrity and aesthetics of built materials in cities (contributing to corrosion and visual soiling), and in recent decades has been recognized as an important physical sink for a number of organic pollutants. More recently, the role of urban grime as a reaction medium has been explored. As discussed in the Introduction, a few studies have reported different (and generally faster) reactions on urban grime samples compared to on glass or laboratory-prepared proxies for urban grime, suggesting that urban grime composition plays an important role in its reactivity. However, the reason for this enhanced reactivity is not yet known, and to our knowledge only two reactions have been explored using field-sampled urban grime. Several types of future studies will be required in order to elucidate and quantify the effect of urban grime on heterogeneous atmospheric chemistry in cities. Additional measurements of kinetics of important reactions on real urban grime samples, investigations of composition (both of bulk samples and of individual components such as films and particles), and measurements of surface coverage and conformation (especially particles vs. films) are all needed to improve predictions.

We suggest that fractional surface coverage will be one of the most important variables to constrain in order to improve predictions. At high fractional surface coverages (by either particles or films), most heterogeneous reactions will occur on or within the urban grime, and the physicochemical properties of the underlying material will not be important; predicting heterogeneous reaction kinetics will depend entirely on physicochemical properties of the urban grime. Conversely, at low fractional surface coverages, two environments (urban grime and the underlying substrate) may need to be considered. Under these conditions, the importance of urban grime to heterogeneous reactions will depend on the fractional surface coverage, the

change in specific surface area due to the presence of the urban grime, the composition of the urban grime, and the relative strength of interactions of reactive atmospheric gases with urban grime and the underlying substrate. The importance of fractional surface coverage is intuitive; covering a greater fraction of the underlying substrate will generally increase the likelihood of collisions between gas-phase reactants and urban grime. Increasing the specific surface area (especially if urban grime consists primarily of particles) will increase both the amount of total surface available to gas-phase reactants, as well as the surface area of urban grime relative to that of the underlying substrate. The fact that different reaction kinetics have been reported on real urban grime compared to on other surfaces such as glass and laboratory-prepared proxies strongly suggests that urban grime composition is important to reactivity. Connections between composition and reactivity are sometimes clear – increased photochemical gas-phase NO and HONO production are expected in urban grime samples with high NO_3^- concentrations – but for the most part such connections are not known. Many constituents of urban grime (e.g., ions, metals, organic matter) could affect reactivity, possibly in complex ways. We recommend further investigation of the links between urban grime composition and reactivity. Finally, the composition of urban grime could affect reaction rates, as well as where reactions occur (i.e., on urban grime or on the building material). If partitioning coefficients of reactants to urban grime are much larger than those to the building material, even low surface coverages of urban grime could affect reactivity. Conversely, if partitioning to the building material is greatly favored, very high urban grime fractional surface coverage might be required to affect reactivity.

This work synthesizes the results of several studies that have investigated temporal and spatial variations in urban grime composition. It appears that urban grime composition is generally similar across a number of North American and European cities, with some variations

likely due to local sources of ions such as sulfate and chloride. This observation will help researchers extrapolate results from laboratory experiments using urban grime sampled from a single location to other geographic locations. Our work also builds on previous work showing particles (rather than films) to be a major – and sometime *the* major – component of urban grime. This observation, which is contrary to the common perception of urban grime, but in agreement with some recent studies,^{25, 26} has implications for the extent to which outdoor surfaces are coated with urban grime, and therefore the importance of urban grime as a reaction medium. Grant et al. showed fractional surface coverage of samples in urban areas increasing relatively linearly over the course of ~3 months to a level of ~65%, followed by a slower growth that reached close to 100% coverage by 12 months of exposure.²⁵ The conditions in that study reflect “ideal” urban grime growing conditions (upward-facing surfaces protected from rain). We observed much slower growth, with very low surface coverage even after 10 weeks of exposure. The conditions in our study were more reflective of vertical surfaces. These two sets of results can help us constrain the fractional surface coverage of urban grime in cities. Specifically, the combined results suggest that upward-facing surfaces that are not subject to frequent rain (either due to local weather patterns or physical shelters) may be nearly completely covered with urban grime, whereas vertical surfaces, and especially those exposed to rainfall, may have very little urban grime coverage. Further investigations of urban grime fractional surface coverage under environmentally relevant conditions will be very helpful.

Finally, this work reports the first absorbance spectra of aqueous solutions containing urban grime and urban grime filtrate. Several laboratory studies indicate that heterogeneous photochemical reactions at urban grime surfaces could have large effects on atmospheric composition, especially due to the formation of reactive nitrogen (primarily in the form of

HONO) due to nitrate photolysis and chemical uptake of NO₂.¹⁰⁻¹⁴ We show for the first time that urban grime absorbs sunlight, and therefore may participate in photochemical reactions rather than simply acting as an inert substrate. What form this participation might take (e.g., acting as a photosensitizer, or slowing reactions due to competitive photon absorbance) is not currently known, but is worthy of future study.

2.6 Acknowledgements

This work was funded by an ORAU Ralph E. Powe Junior Faculty Enhancement Award and the Alfred P. Sloan Foundation CIE program (G-2018-11062). Tara Kahan is a Canada Research Chair in Environmental Analytical Chemistry. This research was undertaken, in part, thanks to funding from the Canada Research Chairs program. The authors would like to acknowledge N. Khan and M. Kirich for initial data collection; Dr. C. Junium for assistance with TC analysis; Dr. L. Lautz for assistance with IC analysis; Dr. J. Thomas for use of an optical microscope; Dr. S. Chakraborty for assistance with image preparation and analysis; and Dr. D. J. Donaldson for sharing data on measured ionic composition of urban grime samples in Toronto and Leipzig.

2.7 References

1. George, C.; D'Anna, B.; Herrmann, H.; Weller, C.; Vaida, V.; Donaldson, D. J.; Bartels-Rausch, T.; Ammann, M., Emerging Areas in Atmospheric Photochemistry. In *Atmospheric and Aerosol Chemistry*, McNeill, V. F.; Ariya, P. A., Eds. Springer-Verlag Berlin: Berlin, 2014; Vol. 339, pp 1-53.
2. Diamond, M. L.; Gingrich, S. E.; Fertuck, K.; McCarry, B. E.; Stern, G. A.; Billeck, B.; Grift, B.; Brooker, D.; Yager, T. D., Evidence for Organic Film on an Impervious Urban Surface: Characterization and Potential Teratogenic Effects. *Environ. Sci. Technol.* **2000**, *34* (14), 2900-2908.

3. Lam, B.; Diamond, M. L.; Simpson, A. J.; Makar, P. A.; Truong, J.; Hernandez-Martinez, N. A., Chemical Composition of Surface Films on Glass Windows and Implications for Atmospheric Chemistry. *Atmos. Environ.* **2005**, *39* (35), 6578-6586.
4. Csiszar, S. A.; Diamond, M. L.; Thibodeaux, L. J., Modeling Urban Films Using a Dynamic Multimedia Fugacity Model. *Chemosphere* **2012**, *87* (9), 1024-1031.
5. Simpson, A. J.; Lam, B.; Diamond, M. L.; Donaldson, D. J.; Lefebvre, B. A.; Moser, A. Q.; Williams, A. J.; Larin, N. I.; Kvasha, M. P., Assessing the Organic Composition of Urban Surface Films Using Nuclear Magnetic Resonance Spectroscopy. *Chemosphere* **2006**, *63* (1), 142-152.
6. Hodge, E. M.; Diamond, M. L.; McCarry, B. E.; Stern, G. A.; Harper, P. A., Sticky Windows: Chemical and Biological Characteristics of the Organic Film Derived from Particulate and Gas-Phase Air Contaminants Found on an Urban Impervious Surface. *Arch. Environ. Contam. Toxicol.* **2003**, *44* (4), 421-429.
7. Donaldson, D. J.; Kahan, T. F.; Kwamena, N. O. A.; Handley, S. R.; Barbier, C., Atmospheric Chemistry of Urban Surface Films. In *Atmospheric Aerosols*, American Chemical Society: 2009; Vol. 1005, pp 79-89.
8. Kwamena, N. O. A.; Earp, M. E.; Young, C. J.; Abbatt, J. P. D., Kinetic and Product Yield Study of the Heterogeneous Gas-Surface Reaction of Anthracene and Ozone. *J. Phys. Chem. A* **2006**, *110* (10), 3638-3646.
9. Kahan, T. F.; Kwamena, N. O. A.; Donaldson, D. J., Heterogeneous Ozonation Kinetics of Polycyclic Aromatic Hydrocarbons on Organic Films. *Atmos. Environ.* **2006**, *40* (19), 3448-3459.
10. Ammar, R.; Monge, M. E.; George, C.; D'Anna, B., Photoenhanced NO₂ Loss on Simulated Urban Grime. *Chemphyschem* **2010**, *11* (18), 3956-61.
11. Handley, S. R.; Clifford, D.; Donaldson, D. J., Photochemical Loss of Nitric Acid on Organic Films: A Possible Recycling Mechanism for NO_x. *Environ. Sci. Technol.* **2007**, *41* (11), 3898-3903.
12. Baergen, A. M.; Donaldson, D. J., Formation of Reactive Nitrogen Oxides From Urban Grime Photochemistry. *Atmos. Chem. Phys.* **2016**, *16* (10), 6355-6363.
13. Liu, J. P.; Li, S.; Mekic, M.; Jiang, H. Y.; Zhou, W. T.; Loisel, G.; Song, W.; Wang, X. M.; Gligorovski, S., Photoenhanced Uptake of NO₂ and HONO Formation on Real Urban Grime. *Environ. Sci. Technol. Lett.* **2019**, *6* (7), 413-417.
14. Baergen, A. M.; Donaldson, D. J., Photochemical Renoxification of Nitric Acid on Real Urban Grime. *Environ. Sci. Technol.* **2013**, *47* (2), 815-820.
15. Favez, O.; Cachier, H.; Chabas, A.; Ausset, P.; Lefevre, R., Crossed Optical and Chemical Evaluations of Modern Glass Soiling in Various European Urban Environments. *Atmos. Environ.* **2006**, *40* (37), 7192-7204.
16. Baergen, A. M.; Donaldson, D. J., Seasonality of the Water-Soluble Inorganic Ion Composition and Water Uptake Behavior of Urban Grime. *Environ. Sci. Technol.* **2019**, *53* (10), 5671-5677.
17. Laufs, S.; Kleffmann, J., Investigations on HONO Formation from Photolysis of Adsorbed HNO₃ on Quartz Glass Surfaces. *Phys. Chem. Chem. Phys.* **2016**, *18* (14), 9616-9625.
18. Kwamena, N. O. A.; Thornton, J. A.; Abbatt, J. P. D., Kinetics of Surface-Bound Benzo- α -pyrene and Ozone on Solid Organic and Salt Aerosols. *J. Phys. Chem. A* **2004**, *108* (52), 11626-11634.

19. Kahan, T. F.; Donaldson, D. J., Heterogeneous Ozonation Kinetics of Phenanthrene at the Air-Ice Interface. *Environ. Res. Lett.* **2008**, *3* (4), 6.
20. Poschl, U.; Letzel, T.; Schauer, C.; Niessner, R., Interaction of Ozone and Water Vapor with Spark Discharge Soot Aerosol Particles Coated with Benzo- α -pyrene: O₃ and H₂O Adsorption, Benzo- α -pyrene Degradation, and Atmospheric Implications. *J. Phys. Chem. A* **2001**, *105* (16), 4029-4041.
21. Liu, Q. T.; Chen, R.; McCarry, B. E.; Diamond, M. L.; Bahavar, B., Characterization of Polar Organic Compounds in the Organic Film on Indoor and Outdoor Glass Windows. *Environ. Sci. Technol.* **2003**, *37* (11), 2340-2349.
22. Wu, R. W.; Harner, T.; Diamond, M. L.; Wilford, B., Partitioning Characteristics of PCBs in Urban Surface Films. *Atmos. Environ.* **2008**, *42* (22), 5696-5705.
23. Lombardo, T.; Chabas, A.; Verney-Carron, A.; Cachier, H.; Triquet, S.; Darchy, S., Physico-chemical Characterisation of Glass Soiling in Rural, Urban and Industrial Environments. *Environ. Sci. Pollut. Res.* **2014**, *21* (15), 9251-9258.
24. Behymer, T. D.; Hites, R. A., Photolysis of Polycyclic Aromatic Hydrocarbons Adsorbed on Fly-ash. *Environ. Sci. Technol.* **1988**, *22* (11), 1311-1319.
25. Grant, J. S.; Zhu, Z. H.; Anderton, C. R.; Shaw, S. K., Physical and Chemical Morphology of Passively Sampled Environmental Films. *ACS Earth Space Chem.* **2019**, *3* (2), 305-313.
26. Donaldson, D. J.; Clouthier, J. T.; Morenz, K. J.; Marr, A., Chemical Morphology and Reactivity at Environmental Interfaces. In *Multiphase Environmental Chemistry in the Atmosphere*, American Chemical Society: 2018; pp 193-207.
27. Jammoul, A.; Gligorovski, S.; George, C.; D'Anna, B., Photosensitized Heterogeneous Chemistry of Ozone on Organic Films. *J. Phys. Chem.* **2008**, *112* (6), 1268-1276.
28. Feng, Y. Q.; Liu, L.; Yang, Y.; Deng, Y.; Li, K. J.; Cheng, H. Y.; Dong, X.; Li, W. J.; Zhang, L. W., The Application of Raman Spectroscopy Combined with Multivariable Analysis on Source Apportionment of Atmospheric Black Carbon Aerosols. *Sci. Total Environ.* **2019**, *685*, 189-196.
29. Weschler, C. J.; Nazaroff, W. W., Growth of organic films on indoor surfaces. *Indoor Air* **2017**, *27* (6), 1101-1112.
30. East Syracuse, New York Air Pollution: Real-time Air Quality Index (AQI). <https://aqicn.org/city/usa/newyork/east-syracuse/> (accessed Dec. 17, 2019).
31. Ionescu, A.; Lefevre, R. A.; Chabas, A.; Lombardo, T.; Ausset, P.; Candau, Y.; Rosseman, L., Modeling of Soiling Based on Silica-soda-lime Glass Exposure at Six European Sites. *Sci. Total Environ.* **2006**, *369* (1-3), 246-255.
32. Styler, S. A.; Baergen, A. M.; Donaldson, D. J.; Herrmann, H., Organic Composition, Chemistry, and Photochemistry of Urban Film in Leipzig, Germany. *ACS Earth Space Chem.* **2018**, *2* (9), 935-945.
33. Baergen, A. M.; Styler, S. A.; van Pinxteren, D.; Muller, K.; Herrmann, H.; Donaldson, D. J., Chemistry of Urban Grime: Inorganic Ion Composition of Grime vs. Particles in Leipzig, Germany. *Environ. Sci. Technol.* **2015**, *49* (21), 12688-12696.
34. Laskin, A.; Laskin, J.; Nizkorodov, S. A., Chemistry of Atmospheric Brown Carbon. *Chem. Rev.* **2015**, *115* (10), 4335-4382.
35. Lack, D. A.; Cappa, C. D., Impact of Brown and Clear Carbon on Light Absorption Enhancement,

Single Scatter Albedo and Absorption Wavelength Dependence of Black Carbon. *Atmos. Chem. Phys.* **2010**, *10*, 4207–4220.

36. Bateman, A. P.; Nizkorodov, S. A.; Laskin, J.; Laskin, A., Photolytic Processing of Secondary Organic Aerosols Dissolved in Cloud Droplets. *Phys. Chem. Chem. Phys.* **2011**, *13* (26), 12199-12212.

37. Badali, K. M.; Zhou, S.; Aljawhary, D.; Antinolo, M.; Chen, W. J.; Lok, A.; Mungall, E.; Wong, J. P. S.; Zhao, R.; Abbatt, J. P. D., Formation of Hydroxyl Radicals from Photolysis of Secondary Organic Aerosol Material. *Atmos. Chem. Phys.* **2015**, *15* (14), 7831-7840.

Chapter Three:

Measurements of Oxidants in Vehicle Cabins

3.1 Abstract

This research focuses on quantifying the concentrations of four atmospheric species within the cabin of a vehicle under different conditions. The vehicle was tested under differing settings including variations in the types of ventilation. The interior of vehicle showed concentrations of oxidants namely ozone and nitrogen oxide akin to indoor atmospheres rather than outdoor atmospheres. In this study, the ozone levels in the vehicle measured ~1 ppb within vehicle compared to an average outdoor ozone concentration of ~30 ppb with one exception. When the direct fan setting is used, the ozone levels in the vehicle were observed to increase to ~50% of the levels in the outdoor environment. This is explained due to the ventilation system pulling in air from the external environment. In the case of nitrogen oxide, the opposite trend is observed with the vehicle cabin having higher concentrations around 2 ppb compared to the external environment having on average of around 1 ppb. Lastly, we measured the concentration of NO₂ and HONO within the vehicle along with the transmittance of light entering the vehicle. It was determined that the sunlight entering the vehicle while not able to photolyze ozone is sufficient enough to photolyze HONO. The photolysis of HONO is likely the source of OH radicals within the cabin. The production rate for OH radicals was calculated around 1.08 – 1.81 x 10⁷ molecules cm⁻³ s⁻¹ and the steady state concentration of the radicals was around 29.4 - 49.1 x 10⁵ molecules cm⁻³.

3.2 Introduction

Atmospheric chemistry traditionally looks at the concentrations of various gases and particles interacting in the outdoors. However, as people spend on average closer to 90% of their time indoors,¹ the field has been looking at the composition of these internal environments. Most

research in indoor environments focus on residential and commercial buildings. This research looks into various areas of study which includes volatile organic carbons (VOCs), particulate matter, and gaseous oxidants.²⁻⁴ This last group includes molecules such as ozone and nitrogen oxides,^{5,6} and these oxidants often initiate reactions which can generate the hydroxyl radical, OH·.⁷ OH radicals are the most important reactive species in outdoor environments during the day where they are generated by photolysis of ozone. For indoor environments, the source of OH· is often speculated to be the interaction of ozone with alkenes. However, sunlight that is filtered through windows is often not sufficient to photolyze ozone. Others have postulated that photolysis of nitrous acid (HONO), formaldehydes, and hypochlorous acid (HOCl) can be sources for indoor OH·.^{8,9} Studies on indoor environments have shown that another oxidant, HONO, is the primary precursor for OH radicals rather than ozone.^{7,11} OH· is generated by the photolysis of HONO into the radical and a molecule of NO.¹⁰ Measurements show HONO and nitrogen oxides (NO_x; sum of nitric oxide NO and nitrogen dioxide NO₂) are the more dominant species in residential indoor environments instead of ozone when compared to outdoor environments, and therefore understanding their levels is important in understanding the kinds of chemistry that is occurring in these environments.⁵ However, ozone continues to be a more important oxidant in commercial buildings due to higher air exchange rates with the outside environment.¹²

Aside from these aforementioned locations, vehicles are another environment that can possibly be included as an indoor environment. After all people spend approximately 6% of their time in vehicles and it is not fully understood what they are being exposed to on a daily basis. It is not well understood whether the environment inside the vehicle is more consistent with the general outdoor environment or if the levels of oxidants within are akin to other indoor

environments, but some groups have begun investigating what kinds of compounds can be found within the vehicle cabin.¹ Most exposure in vehicle cabins studied involves common exhaust products or the emissions from the materials the interior is made of. This includes looking at the concentrations of CO both in and outside of the vehicle during different conditions,¹³ and investigating the flow of CO and particulate matter from the engine itself into the cabin.¹⁴ Two groups looked into CO, since it is a toxic compound that is commonly emitted by vehicles. They examined the pathways and concentrations to determine the exposure risk to individuals and found that the levels inside the vehicle differed from those outside.^{13, 14}

Other groups have investigated the exposure of passengers and drivers to VOCs, particulate matter, and aldehydes, which are common components of exhaust.¹⁵⁻¹⁷ The study focusing on BTEX (benzene, toluene, ethyl benzene, and xylenes) found that exposure is worse in areas of limited road space like those in Kolkata where the research took place.¹⁶ Meanwhile the group examining the exposure of aldehydes found it was similar in various vehicle types and was higher within the cabins compared to the surrounding environment outdoors.¹⁵ There have been a few groups investigating ozone and NO_x. One group looked into the exposure of passengers and pedestrians to NO₂, but the method used involved passive sampling rather than active real-time sampling that could show changes over time.¹⁸ Lastly, a group in the 1990s looked into the concentrations of HONO in vehicles, but the values measured were much higher than those seen in buildings reading between 10-25 ppb in the vehicle.¹⁹ Current research shows HONO levels in residences to be around 4 ppb.⁵ To better understand the makeup of the oxidant and oxidant precursor species in vehicles (oxidants*), time-resolved measurements of O₃, NO, NO₂, and HONO were conducted inside the cabin. In addition to the mixing ratio measurements,

solar irradiance spectra were collected to determine if HONO photolysis could be a source of OH radicals.

3.3 Methods

The five separate continuous measurement experiments were conducted from May of 2019. The vehicle used for the experiments was a 2012 Toyota Rav4 with a cloth interior. The vehicle was kept immobile throughout the measurement period and in-cabin analyte measurements were made under four different conditions: car off (car off), car on passive ventilation (fan off), car on mechanical ventilation with recirculating fan (recirculation), and car on mechanical ventilation with direct fan (direct fan). Outdoor measurements were taken in between each tested setting.

The time resolved mixing ratios of O₃, NO, NO₂, and HONO were measured using a custom-built mobile analytical laboratory (Mobile Indoor Laboratory for Oxidative Species, MILOS). Ozone was measured using an Ecotech Serinus 10 UV photometric analyzer with an accuracy of 0.5 ppbv. The nitrogen oxide, NO_x, species of NO and NO₂ were measured using an Ecotech Serinus 40 O₃ based chemiluminescence analyzer with an accuracy of 0.4 ppbv. The HONO was measured by a modification to the NO_x analyzer which allowed for simultaneous quantitative measurements through a difference technique. There was placed a line split upstream from the inlet for the NO_x analyzer. One pathway contained an annular denuder coated with sodium carbonate that removed gaseous acids, such as HONO, from the flow. The denuder was coated using a saturated sodium carbonate solution, letting sit for four days, pouring out the excess solution, and dried using zero air. The other line served as a bypass line to detect the sum of NO₂ and HONO. A Teflon solenoid valve was used to alternate between the two lines

every 5 minutes. Data for all four analyzed species was logged every 30 seconds. The first minute of the 5 min intervals for both NO₂ and HONO was excluded due to the response time of the instrument after each switch. The remaining four minutes of data was then averaged.

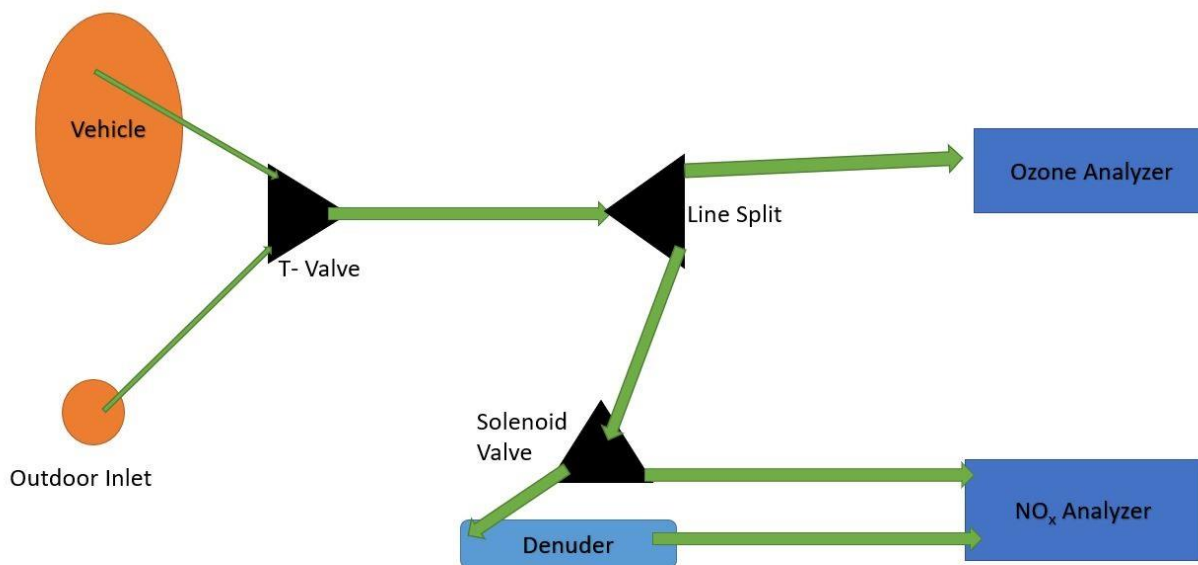


Figure 3.1: Schematic of the tubing setup for testing with MILOS

Calibrations for the two analyzers were performed before and after the testing periods. The calibrations used a dilution calibrator and ozone generator (Ecotech GasCal 1100) and a NO cylinder (19.8 ppmv in N₂, analytical uncertainty of 5%). The 30 sec limit of detections (LODs) for the analytes was determined at 3 times the standard deviations (3σ) of the corresponding signals in zero air. The LODs for O₃, NO, NO₂, and Σ (NO₂ + HONO) were 0.65, 1.2, 1.5, and 1.5 ppbv respectively. The 5 min LOD of HONO was calculated as 0.7 ppbv from the standard deviation of the subtraction of NO₂ from the Σ (NO₂ + HONO). The quality control of the system followed the same method outlined in Zhou et. al.⁵

MILOS was stationed inside the stairwell nearest the parking lot in which the vehicle was located to prevent any potential precipitation damage to the instruments and

reuptake of tested gases into the vehicle. The teflon sampling inlet was put inside the vehicle cabin through the driver side window and placed around the steering wheel. The window was opened wide enough for only the inlet to enter and was then sealed using parafilm. The inlet included a t-valve that would allow switching between air being measured from vehicle and the outdoor air without breaking the seal over the window. The outdoor inlet was placed on the hood of the vehicle in front of the driver. Vent measurements were taken by moving the interior inlet from the position at the steering and placing it into the outflow of the ventilation system approximately 6 cm into the flow. Exhaust measurements were conducted by suspending the outdoor inlet in the path of the exhaust exiting through the tailpipe.

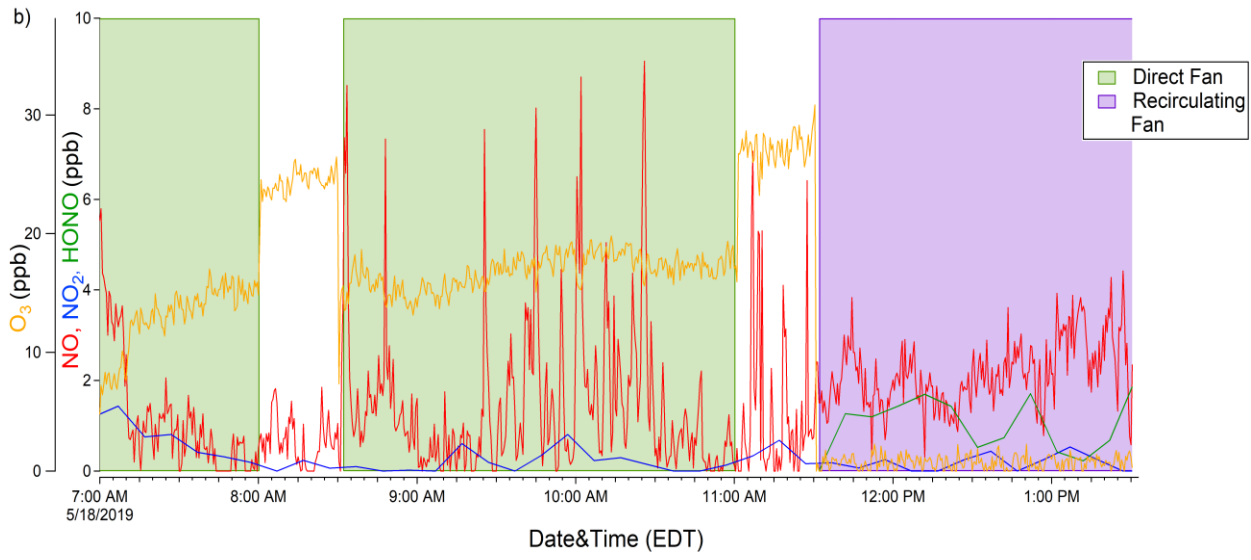
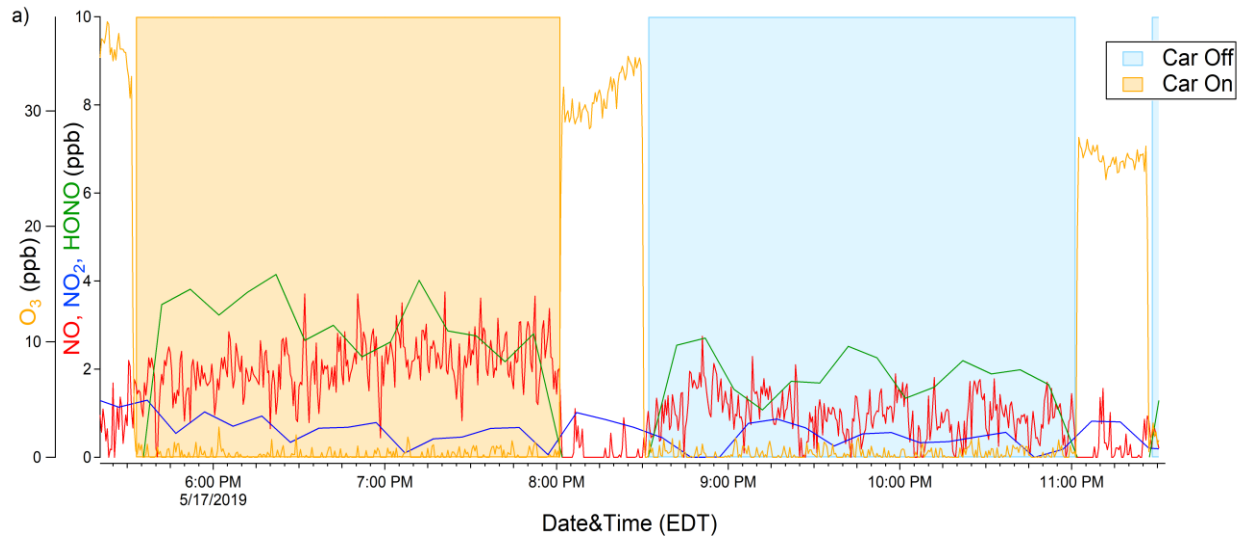
Air exchange rates were measured within the vehicle at each of the fan settings and also with the vehicle off. These measurements were recorded using a TSI IAQ7545, which recorded the decrease in added CO₂ from dry ice over time. Each test used approximately 20 g of dry ice which was broken up and scattered throughout the cabin and allowed to sublimate. Measurements were recorded at 30 sec intervals like the other gases. The CO₂ was measured over 2 hr periods for all settings except the direct fan where 30 min intervals were determined to be sufficient to return to background levels. The collected data was then analyzed and a quantile regression was used to determine the air exchange rate. None of the air exchange tests occurred while an occupant was present in the vehicle.

Wavelength resolved spectra of sunlight was collected through both the driver's side window and the windshield using a calibrated Ocean Optics USB4000 spectrometer coupled to a 1 m fiber optic cable and a cosine corrector. Average spectral irradiances were collected, and photon fluxes were estimated using the same method as Kowal et al.²⁰

3.4 Results

3.4.1 Oxidant* Mixing Ratios and Air Exchange Rates

Figure 2 shows two ~6-hour time series from sampling periods on May 17 and 18, 2019. These periods were selected to illustrate analyte levels under different conditions (car off, car on, recirculating fan, and direct fan, as well as analyte levels outdoors). Ozone levels were consistently much higher outdoors than inside the vehicle. Oxidant* levels over the entire campaign period are summarized in Figure 2c. Ozone in the vehicle was below the detection limit (0.65 ppb) for approximately 60% of all measurements inside the vehicle, with the exception of direct fan conditions, with mean ozone a concentration of 1.14 ± 0.65 . When the direct fan was on, indoor O₃ levels were 15.48 ± 5.05 , approximately 50% of the mean outdoor levels. These findings are very similar to those reported in North American residences, where O₃ levels below 5 ppb are consistently reported when doors and windows are closed, and higher levels reported in non-residential buildings with higher AER or in residential buildings with windows open.^{5, 21} We previously reported indoor O₃ levels of 8.1 ± 6.5 ppb in a Syracuse residence with doors open, and 22.5 ± 8.6 in a Syracuse university building.¹² The levels found in the vehicle under all conditions except the direct were found to be similar to levels measured in residences. The increase in the O₃ concentration when the direct fan is applied shows a similar increase seen when the windows are opened in a residence.



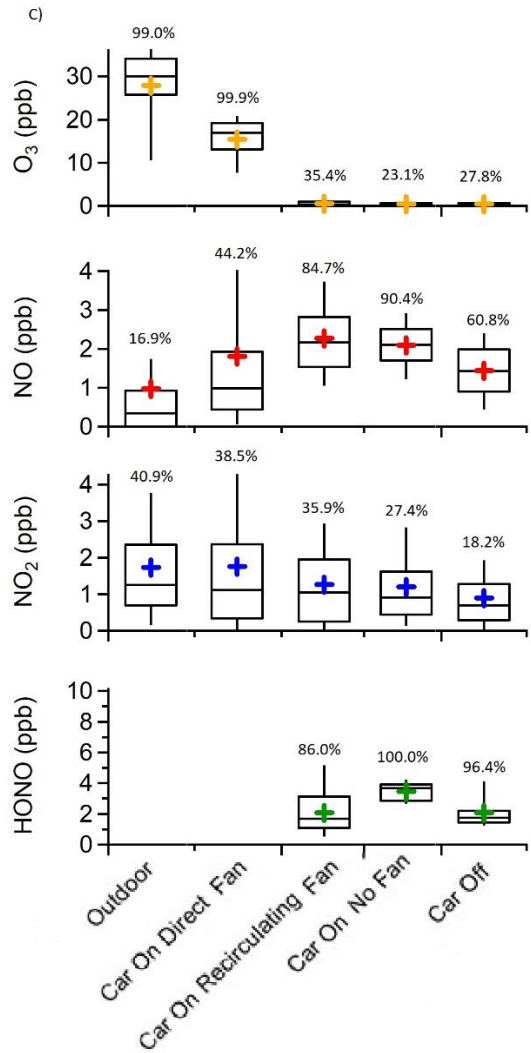


Figure 3.2: Time series of concentrations for O₃, HONO, NO₂, and NO for select conditions recorded a) May 17 and b) May 18, 2019. c) Box and whisker plots of analyte mixing ratios outside of the vehicle and inside during the tested conditions from May tests. The plots show the median (line), mean (marker), upper and lower quartiles (box), and 10th and 90th percentiles (whiskers). Outdoor and direct fan values for HONO are not reported due to possible artifacts. The percentage of samples above detection limit is listed above the plots.

Fig. 2c shows that NO levels in the vehicle were higher than those outdoors under all ventilation conditions. When comparing the three conditions in which there is no influence from

the outdoors (car on, car off, and recirculating fan) to the direct fan which pulls in external air, little difference is at first observed. Average NO levels in the vehicle were 1.87 ± 0.95 ppb, compared to 1.8 ± 3.4 with the direct fan and 0.97 ± 4.3 ppb outdoors. The levels appear similar indoors for all conditions except that the NO time series from May 18 shows several sharp peaks reaching up to 9 ppb when sampling outdoors and in the vehicle with the direct fan running. Similar peaks were observed frequently outdoors and with the direct fan, but not under any other conditions. 36 of these spikes were observed in the testing periods. For 29 of these samples the test vehicle was running at the time of detection, while the remaining 7 were when the vehicle was turned off. We drove a second vehicle (2011 Honda CRV) past the primary reaching ~2 m from the test vehicle at the closest distance. The vehicle passed by 18 times but, no spikes were observed during this test. It is possible that these spikes are caused by variations in wind currents blowing the car's own exhaust into its ventilation system and past the external inlet, but the spikes that occur when the vehicle is off can probably be attributed to other sources such as the nearby road. When these spikes are removed for the direct fan the average drops to 1.5 ± 1.7 and are still generally higher than outdoors. Overall, the in-vehicle mixing ratios are lower than those we previously measured in a Syracuse residence of ~4 ppb but similar to those measured in a university laboratory (~1 ppb) and office (0.5 ppb).¹²

As shown in Figure 2, NO₂ averages were relatively consistent within the vehicle, but somewhat higher under direct fan conditions. The values measured during the on, off, and recirculating periods averaged around 1.09 ± 1.07 ppb but only around 29% of the tested values were above the LOD value of 1.5 ppb. We have previously reported similar indoor NO₂ levels in a Syracuse residence.⁵ Both combustion and infiltration from outdoors are important indoor NO₂ sources.^{6, 22} Based on the indoor:outdoor ratios (I/O) for NO₂ found in Table 1, there is a clearer

picture for the gas's concentration in the cabin. During the direct fan setting, the ratio favors the interior of the vehicle. However, when the engine is off the I/O ratio of NO₂ favor the outdoor environment. During the remaining two settings, car on and recirculating fan the ratios are very close to 1 indicating little difference between the indoor and outdoor concentrations of NO₂.

We do not report HONO levels outdoors or with the direct fan running due to an interference. Mean mixing ratios in the vehicle under other conditions were 2.6 ± 1.3 , with very similar levels observed under all conditions. This is lower than the reported values 4-5 ppb of HONO in residences and laboratories.^{5, 23, 24} It is much lower than the sole reported level in a vehicle of 10-25 ppb.¹⁹ This discrepancy is likely due to the much higher NO₂ levels inside the vehicle studied in that work compared to a mean of 2.5 ppb inside the vehicle in our study. Outdoor NO₂ levels (but not HONO levels) were also much higher in that study than in ours; it is possible that HONO levels in vehicles depend on outdoor NO₂ levels. Further research is needed to quantify and predict HONO levels in vehicles.

One of the key factors affecting indoor oxidant levels is AER. For example, ozone levels in commercial buildings with high AER ($\sim 5 \text{ h}^{-1}$) are often on the order of 30 – 70% of outdoor levels, while levels in residential buildings with low AER ($\sim 0.6 \text{ h}^{-1}$) are generally below 5 ppb, and often below 1 ppb.¹¹ Table 1 reports AER and I/O ratios in the vehicle, residence, laboratory, and office. Air exchange rates in the parked vehicle were the same whether the engine was on or off (0.4 h^{-1}) when no fans were running. This is similar to AERs reported in residences with closed doors and windows (0.5 h^{-1}).^{11, 25} The use of the recirculating fan increases the measured AER by a factor of ~ 3.8 . This is likely due to a shift in the internal pressure caused by the increased air flow velocity in the cabin. With the direct fan, which pulls outdoor air into the car, very large AERs were measured ($\sim 50 \text{ h}^{-1}$). This is significantly higher

than values reported in residences with open windows (2.8-15 h⁻¹).^{26, 27} Air exchange rates have also been measured in a moving vehicle. Ott et al. reported slightly larger AER in a stationary vehicle than that observed in our study (0.92 h⁻¹).²⁸ This increased to ~2 h⁻¹ when the car was in motion, likely due to turbulence outside influencing the air exchange rate. Running the direct fan while the car was in motion increased the AER to 35 h⁻¹, which is within our experimental uncertainty for the AER we measured in a stationary vehicle with the direct fan running.

Table 3.1: Average air exchange rates and indoor/outdoor ratios of Ozone and NO_x in vehicles under different conditions. Reported AERs are from this work unless otherwise noted.

Condition	Number of tests	Air Exchange Rate (h ⁻¹)	Indoor/Outdoor Ratio			Number of Events for I/O Ratio
			O ₃	NO	NO ₂	
Vehicle off	6	0.4 ± 0.1	0.0619	0.9090	0.7424	4
Vehicle on	6	0.4 ± 0.2	0.0340	0.3684	1.0943	2
Vehicle on, recirculating fan	7	1.5 ± 0.3	0.0370	1.1270	0.9546	3
Vehicle on, direct fan	6	50 ± 20	0.5734	1.5193	1.3436	4
Vehicle on, stationary ²⁸	1	0.92				
Vehicle on, in motion ²⁸	3	2.1 ± 0.4				
Vehicle on, in motion, direct fan ²⁸	1	35				
Residence ¹²		0.67				
University Building ¹²		3.8-5.0				

The high AER under direct fan conditions explains the higher O₃ levels compared to other conditions in the vehicle, and also explains why O₃ levels in the vehicle are similar to those in a Syracuse residence with similar AER, but lower than those in a Syracuse university building,

which has higher AER.¹² Nitric oxide is thought to be primarily formed indoors, rather than transported from outdoors.²⁴ Combustion is the major indoor source, but we have reported NO levels of ~4 ppb in a Syracuse residence in the absence of combustion sources.⁵ We and others have reported negative dependences of NO I/O on AER.^{5, 27} We have attributed this to titration by O₃ at higher AER.⁵ A comparison of I/O ratios with AER supports this hypothesis, with NO I/O being inversely proportionate to both AER and O₃ I/O. During the recirculating fan condition a gradual increase in the mixing ratio of NO was observed. This increase was observed in about two-thirds of all recirculating fan testing periods. The source of the NO might be from the engine or through the formation of NO from the photolysis of HONO which typically saw a decrease during the same periods. To further explore the sources of oxidants* in the vehicle, we measured NO, NO₂, and O₃ mixing ratios in the cabin and in the intake vent as well as outdoors near the side of the vehicle and directly in the exhaust flow.

Common sources of indoor NO₂ include transport from outdoors, reaction between O₃ and NO, and direct emission from combustion, while common indoor HONO sources include heterogeneous reactions of NO₂ and physical air-surface partitioning.⁷ For the I/O ratios of NO₂ within the vehicle, are relatively similar for the conditions when the car is on. The I/O of the average for all three conditions is around 1.15. Lee et al measured I/O values of 2.08 within residences, but our own group has previously measured the I/O for NO₂ to be 1.26.^{6, 12} The fact that NO₂ levels are higher than all other indoor conditions and higher than outdoor levels when the direct fan is on suggests chemical formation of NO₂. We previously demonstrated that opening windows in a residence increases indoor NO₂ levels due to reactions between O₃ and NO.¹² Ozone is the limiting reactant for this process in both residences and vehicles. Therefore, increasing O₃ levels in the vehicle by using the direct fan increases the NO₂ production rate and

measured mixing ratios. HONO showed similar concentrations between the three indoor settings of vehicle off, and with the recirculating fan with 2.09 and 2.07 ppb respectively. However, the vehicle running without a fan showed concentrations of 3.47 ppb within the cabin. The concentrations are generally higher than NO₂ during the same periods, but are still lower than what we've previously observed in residences.⁵ Despite the levels being lower, the fact that the concentrations of HONO are higher than NO₂ during the same conditions is similar to the pattern observed in residences.

3.4.2 Photochemistry

Photolysis of HONO has been suggested to be an important indoor OH source.^{10, 29} While windows often attenuate sunlight completely at wavelengths shorter than 330 – 340 nm, HONO remains photo-labile at wavelengths as long as 405 nm,³⁰ and photochemically-formed OH has been reported in sunlit rooms.¹⁰ Given the large surface area of windows in cars, it is possible that OH could also be photochemically formed in cars. We measured solar irradiance in several vehicles in order to predict OH steady-state concentrations in sunlit vehicles. Figure 3(a) shows transmittance of the driver side window of three vehicles. Transmittance was similar in all three windows despite differences in make and age of the vehicles. The wavelength-resolved transmittance profile of each window was characterized by a broad hump centered around 370 nm. This feature is not generally observed in windows used in buildings, as seen in the profiles of windows in a house and an office on the same plot. Transmittance was higher overall in the vehicle windows than in the building windows. Figure 3(b) shows transmittance of four different windows in the Honda CRV. Driver and passenger windows had very similar transmittance, but

the rear passenger window, which was tinted, had much lower transmittance, and the windshield attenuated sunlight almost completely at wavelengths shorter than 390 nm.

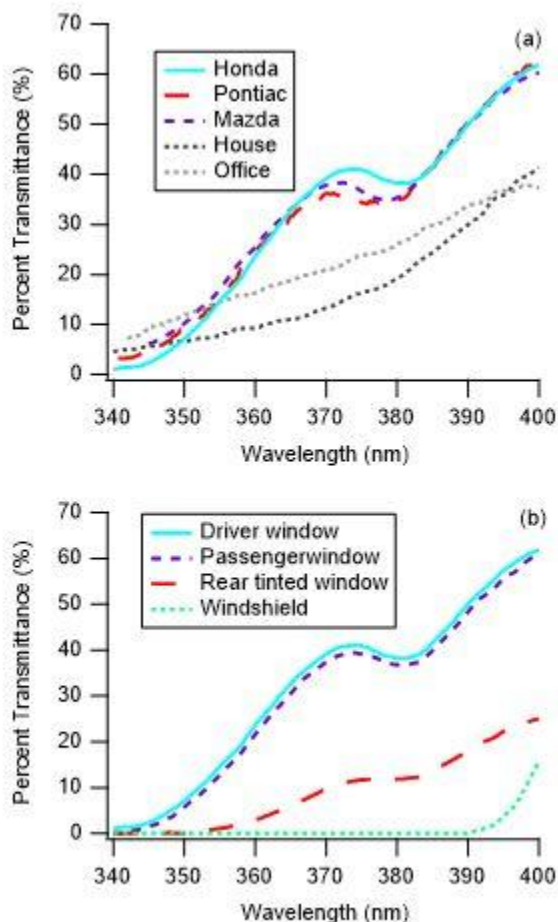


Figure 3.3: (a) Transmittance of driver-side windows in a 2013 Honda CRV, a 2006 Pontiac G6 sedan, and a 2016 Mazda 3 hatchback. Transmittance of windows in an office building and a house are also shown for reference. (b) Transmittance of various windows in the Honda CRV.

The solar irradiance was converted to photon flux as described in Kowal et al and HONO photolysis rate constants were calculated.²⁰ Measured HONO levels were used to calculate OH production rates, and steady-state OH number densities were estimated considering OH reactions with NO, NO₂, and HONO as the major sinks using Eq. 1.³¹

$$\text{Eq. 1} \quad [OH]_{pss} = \frac{J(HONO)[HONO]}{\Sigma(k_{OH+NO}[NO] + k_{OH+NO_2}[NO_2] + k_{OH+HONO}[HONO])}$$

The results of the calculations discussed above are shown in Table 2 for several indoor locations including a vehicle, a home, and a classroom. Photolysis rate constants from sunlight filtered through side windows of a vehicle are similar to those measured in several office and laboratory buildings and in a residence,^{5, 10, 20, 31-33} but calculated OH production rates are lower than in buildings due to lower HONO mixing ratios measured in the vehicle. Despite lower calculated OH production rates in vehicles than in buildings, we predict steady-state OH concentrations in vehicles to be similar to those in residences and higher than those in non-residential buildings due to lower concentrations of OH sinks in vehicles. These concentrations are also similar to those measured and predicted in a variety of residential and non-residential buildings under sunlit conditions.^{12, 29, 31, 32} The OH steady-state concentrations predicted in an illuminated vehicle are similar to those measured outdoors,³⁴ and we conclude that HONO photolysis can be an important OH source in vehicles. We note that the steady-state OH concentrations listed in Table 2 are subject to a large amount of uncertainty. There are few measurements of wavelength-resolved irradiance in the UV in indoor environments (and therefore few calculated HONO photolysis rate constants), and to our knowledge, our measurements are the first performed in vehicles. One previous measurement of HONO concentrations in vehicles has been reported – the levels in that study were 20 ppbv, ten times higher than the 2.1 ppbv measured in this work.¹⁹ If that level is more representative of vehicle interiors than our measurements, we would expect OH production rates of 1×10^8 molecule cm^{-3} s^{-1} , and OH steady-state concentrations of 147×10^5 molecule cm^{-3} , almost 4 times greater than

those in our study. Further measurements in vehicles are necessary to constrain predicted OH levels in vehicles.

Table 3.2: Photolytic rate constants and steady-state concentration of OH in the vehicle compared to other indoor environments

Location - Setting	J_{NO_2} (10^{-4}s^{-1})	J_{HONO} (10^{-4}s^{-1})	HONO mixing ratio (ppb)	OH production rate (10^7 molecule $\text{cm}^{-3} \text{s}^{-1}$)	steady-state OH concentration (10^5 molecule cm^{-3})
Vehicle – On	3.5	2.1 [this work]	3.47 [this work]	1.81	49.1
Vehicle – Off			2.09 [this work]	1.09	29.4
Vehicle – Recirc Fan			2.07 [this work]	1.08	40.7
Office / classroom	8.5	$1.8^{10, 20, 31-33}$	$4.8^{10, 31}$	2.2	8.4
Residence	18.0	2.2^5	4.9^5	2.7	26.2

Indoor solar photon fluxes vary throughout the day, with minimum values at night or in spaces not illuminated by sunlight. The time at which photon fluxes are highest depends both on the intensity of the sun (which generally peaks close to noon), and the orientation of windows. For example, maximum indoor solar intensity in a classroom in France was observed at 6 p.m., when sunlight entered windows directly.²⁹ Figure 4 shows a time-series for the measured spectral irradiance within the parked Toyota. The figure shows the fluctuation of light within the vehicle over time due to influences such as cloud morning and around noon. The figure also shows the observed maximum in irradiance around 11:30 which correlates with the solar maxima on that day. The sharp cut off of light at 13:50 matches the time when the sun moved behind a nearby building and put the vehicle in the building’s shadow.

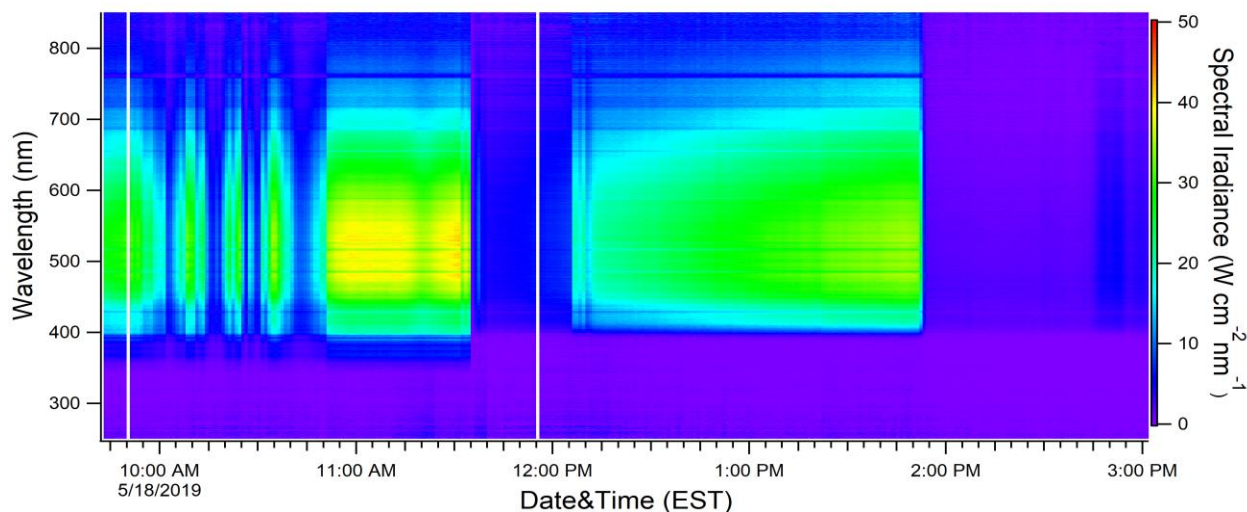


Figure 3.4: Time series of solar irradiance taken on May 18th, 2019

3.5 Environmental Implications

Based on the current observations it appears that the interior atmospheres of vehicles can greatly vary depending on the conditions within the vehicle. During low AER conditions such as those with the recirculating ventilation system or without any fan applied, the interior concentrations of the gases tested appear more like residential environments. However, when the ventilation system pulls in air from outside the vehicle cabin concentrations change rapidly and appear to take on conditions similar to high AER environments such commercial buildings. This dynamic state can greatly change the type of chemistry occurring and alter the dominant oxidizing species depending on relative concentration.

We have observed that HONO photolysis may be occurring based on the observed photon flux within tested vehicles. J_{HONO} values found in this work are within the same range as those previously tested in other environments and the amount of light entering the vehicles is higher than those tested in other indoor environments. This was observed by the increased transmittance of UV light into the vehicle compared to light transmitted through the windows of

residential and commercial buildings. The increased transmittance has the potential to photolyze HONO and be a likely source for OH radicals.

3.6 References

1. Klepeis, N. E.; Nelson, W. C.; Ott, W. R.; Robinson, J. P.; Tsang, A. M.; Switzer, P.; Behar, J. V.; Hern, S. C.; Engelmann, W. H., The national human activity pattern survey (NHAPS): A resource for assessing exposure to environmental pollutants. *J. Expo. Anal. Environ. Epidemiol.* **2001**, *11* (3), 231-252.
2. Yu, C.; Crump, D., A review of the emission of VOCs from polymeric materials used in buildings. *Build. Environ.* **1998**, *33* (6), 357-374.
3. Brauer, M.; Ryan, P. B.; Suh, H. H.; Koutrakis, P.; Spengler, J. D.; Leslie, N. P.; Billick, I. H., Measurements of Nitrous Acid Inside Two Research Houses. *Environ. Sci. Technol.* **1990**, *24* (10), 1521-1527.
4. Koutrakis, P.; Brauer, M.; Briggs, S. L. K.; Leaderer, B. P., Indoor Exposures to Fine Aerosols and Acid Gases. *Environ. Health Perspect.* **1991**, *95*, 23-28.
5. Zhou, S.; Young, C. J.; VandenBoer, T. C.; Kowal, S. F.; Kahan, T. F., Time-Resolved Measurements of Nitric Oxide, Nitrogen Dioxide, and Nitrous Acid in an Occupied New York Home. *Environ. Sci. Technol.* **2018**, *52* (15), 8355-8364.
6. Lee, K.; Xue, X. P.; Geyh, A. S.; Ozkaynak, H.; Leaderer, B. P.; Weschler, C. J.; Spengler, J. D., Nitrous acid, nitrogen dioxide, and ozone concentrations in residential environments. *Environ. Health Perspect.* **2002**, *110* (2), 145-149.
7. Gligorovski, S.; Weschler, C. J., The Oxidative Capacity of Indoor Atmospheres. *Environ. Sci. Technol.* **2013**, *47* (24), 13905-13906.
8. Dawe, K. E. R.; Furlani, T. C.; Kowal, S. F.; Kahan, T. F.; VandenBoer, T. C.; Young, C. J., Formation and emission of hydrogen chloride in indoor air. *Indoor Air* **2019**, *29* (1), 70-78.
9. Weschler, C. J., Ozone in indoor environments: Concentration and chemistry. *Indoor Air-International Journal of Indoor Air Quality and Climate* **2000**, *10* (4), 269-288.
10. Gomez Alvarez, E.; Amedro, D.; Afif, C.; Gligorovski, S.; Schoemaeker, C.; Fittschen, C.; Doussin, J. F.; Wortham, H., Unexpectedly high indoor hydroxyl radical concentrations associated with nitrous acid. *Proceedings of the National Academy of Sciences of the United States of America* **2013**, *110* (33), 13294-13299.
11. Young, C. J.; Zhou, S.; Siegel, J. A.; Kahan, T. F., Illuminating the dark side of indoor oxidants. *Environ. Sci. Process Impacts* **2019**, *21* (8), 1229-1239.
12. Zhou, S.; Young, C. J.; VandenBoer, T. C.; Kahan, T. F., Role of location, season, occupant activity, and chemistry in indoor ozone and nitrogen oxide mixing ratios. *Environ. Sci. Process Impacts* **2019**, *21* (8), 1374-1383.
13. Abi Esber, L.; El-Fadal, M.; Shihadeh, A., Comparison of Trip Average In-vehicle and Exterior CO Determinations by Continuous and Grab Sampling Using an Electrochemical Sensing Method. *Atmos. Environ.* **2007**, *41*, 6087-6094.
14. Abi-Esber, L.; El-Fadel, M., Indoor to outdoor air quality associations with self-pollution implications inside passenger car cabins. *Atmos. Environ.* **2013**, *81*, 450-463.

15. Jo, W.-K.; Lee, J.-W., In-vehicle Exposure to Aldehydes while Commuting on Real Commuter Routes in a Korean Urban Area. *Environ. Res. Sec. A* **2002**, *88*, 44-51.
16. Som, D.; Dutta, C.; Chatterjee, A.; Mallick, D.; Jana, T. K.; Sen, S., Studies on Commuters' Exposure to BTEX in Passenger Cars in Kolkata, India. *Sci. Total Environ.* **2007**, *372*, 426-432.
17. Wheatly, A. D.; Sadhra, S.; Beach, J. R., Exposure to Toxic Gas and Particle Phase Pollutants Evolved During Deployment of Airbags in Vehicles. *Indoor Built Environ.* **1997**, *6*, 134-139.
18. Zak, M.; Melaniuk-Wolny, E.; Widziewicz, K., The Exposure of Pedestrians, Drivers, and Road Transport Passengers to Nitrogen Dioxide. *Atmos. Pollut. Res.* **2017**, *8*, 781-790.
19. Febo, A.; Perrino, C., Measurement of High Concentrations of Nitrous Acid Inside Automobiles. *Atmos. Environ.* **1995**, *29* (3), 345-351.
20. Kowal, S. F.; Allen, S. R.; Kahan, T. F., Wavelength-Resolved Photon Fluxes of Indoor Light Sources: Implications for HO_x Production. *Environ. Sci. Technol.* **2017**, *51* (18), 10423-10430.
21. Avol, E. L.; Navidi, W. C.; Colome, S. D., Modeling ozone levels in and around southern California homes. *Environ. Sci. Technol.* **1998**, *32* (4), 463-468.
22. Willers, S. M.; Brunekreef, B.; Oldenwening, M.; Smit, H. A.; Kerkhof, M.; De Vries, H., Gas cooking, kitchen ventilation, and exposure to combustion products. *Indoor Air* **2006**, *16* (1), 65-73.
23. Leaderer, B. P.; Naeher, L.; Jankun, T.; Balenger, K.; Holford, T. R.; Toth, C.; Sullivan, J.; Wolfson, J. M.; Koutrakis, P., Indoor, outdoor, and regional summer and winter concentrations of PM₁₀, PM_{2.5}, SO₄²⁻, H⁺, NH₄⁺, NO₃⁻, NH₃, and nitrous acid in homes with and without kerosene space heaters. *Environ. Health Perspect.* **1999**, *107* (3), 223-231.
24. Finlayson-Pitts, B. J.; Wingen, L. M.; Sumner, A. L.; Syomin, D.; Ramazan, K. A., The heterogeneous hydrolysis of NO₂ in laboratory systems and in outdoor and indoor atmospheres: An integrated mechanism. *Phys. Chem. Chem. Phys.* **2003**, *5* (2), 223-242.
25. Patel, S.; Sankhyan, S.; Boedicker, E. K.; DeCarlo, P. F.; Farmer, D. K.; Goldstein, A. H.; Katz, E. F.; Nazaroff, W. W.; Tian, Y. L.; Vanhanen, J.; Vance, M. E., Indoor Particulate Matter during HOMEChem: Concentrations, Size Distributions, and Exposures. *Environ. Sci. Technol.* **2020**, *54* (12), 7107-7116.
26. Howard-Reed, C.; Wallace, L. A.; Ott, W. R., The effect of opening windows on air change rates in two homes. *J. Air Waste Manag. Assoc.* **2002**, *52* (2), 147-159.
27. Chao, C. Y. H., Comparison between indoor and outdoor air contaminant levels in residential buildings from passive sampler study. *Build. Environ.* **2001**, *36* (9), 999-1007.
28. Ott, W.; Klepeis, N.; Switzer, P., Air change rates of motor vehicles and in-vehicle pollutant concentrations from secondhand smoke. *J. Expo. Sci. Environ. Epidemiol.* **2008**, *18* (3), 312-325.
29. Gomez Alvarez, E.; Wortham, H.; Streckowski, R.; Zetzsch, C.; Gligorovski, S., Atmospheric Photosensitized Heterogeneous and Multiphase Reactions: From Outdoors to Indoors. *Environ. Sci. Technol.* **2012**, *46* (4), 1955-1963.
30. Stutz, J.; Kim, E. S.; Platt, U.; Bruno, P.; Perrino, C.; Febo, A., UV-visible absorption cross sections of nitrous acid. *J. Geophys. Res. Atmos.* **2000**, *105* (D11), 14585-14592.
31. Liu, J. P.; Li, S.; Zeng, J. F.; Mekic, M.; Yu, Z. J.; Zhou, W. T.; Loisel, G.; Gandolfo, A.; Song, W.; Wang, X. M.; Zhou, Z.; Herrmann, H.; Li, X.; Gligorovski, S.,

Assessing indoor gas phase oxidation capacity through real-time measurements of HONO and NO_x in Guangzhou, China. *Environ. Sci. Process Impacts* **2019**, *21* (8), 1393-1402.

32. Blocquet, M.; Guo, F.; Mendez, M.; Ward, M.; Coudert, S.; Batut, S.; Hecquet, C.; Blond, N.; Fittschen, C.; Schoemaeker, C., Impact of the spectral and spatial properties of natural light on indoor gas-phase chemistry: Experimental and modeling study. *Indoor Air* **2018**, *28* (3), 426-440.

33. Gandolfo, A.; Gligorovski, V.; Bartolomei, V.; Tlili, S.; Alvarez, E. G.; Wortham, H.; Kleffmann, J.; Gligorovski, S., Spectrally resolved actinic flux and photolysis frequencies of key species within an indoor environment. *Build. Environ.* **2016**, *109*, 50-57.

34. Stone, D.; Whalley, L. K.; Heard, D. E., Tropospheric OH and HO₂ radicals: field measurements and model comparisons. *Chem. Soc. Rev.* **2012**, *41* (19), 6348-6404.

Appendix

A.1 Supplementary Information for Chapter Two

A.1.1 Sampling Locations

Table S1: Name, location, collection date, and mass per area of each collected sample.

	Sample Name	Collection Date	Location	Location Type	Mass/Area (mg/m²)
Syracuse, NY	Lafayette1	2/20/2017	North Window #1	Apartment building	8.34
	Lafayette2	4/10/2017	North Window #1	Apartment building	16.95
	CST1	5/31/2017	East Entrance #1	University building	34.01
	CST2	5/31/2017	East Entrance #2	University building	29.28
	LSC1	5/31/2017	East Entrance	University building	13.09
	MacNaughton1	5/31/2017	Causeway Entrance	University building	176.89
	White1	5/31/2017	Causeway Entrance	University building	169.03
	Carrier Dome K1	5/31/2017	K Gate Door	Stadium	27.57
	Irving1	6/13/2017	Ground Level Window #1	Parking garage on busy street	5.17
	Irving2	6/13/2017	Ground Level Window #1	Parking garage on busy street	8.61
	Irving3	6/13/2017	Ground Level Window #2	Parking garage on busy street	16.71
	Irving4	6/13/2017	Ground Level Window #2	Parking garage on busy street	12.23
	White2	6/13/2017	South Window	University building	28.93
	White3	6/13/2017	West Window	University building	26.35
	Jefferson1	9/24/2017	North Window	Commercial building	99.72
	Almond1	9/24/2017	West Window	Commercial building	374.24
	Erie1	9/24/2017	North Window	Commercial building	20.32
	Ainsley1	9/24/2017	South Window	Commercial building	14.53

	Lafayette3	9/24/2017	North Window #2	Apartment building	17.39
Scranton, PA	Dickson1	5/11/2017	North Window #1	Residential building	56.24
	Dickson2	5/11/2017	North Window #2	Residential building	90.96
	Green Ridge1	5/11/2017	South Entrance	Commercial building	3.88
	Foster1	5/11/2017	West Window #1	Residential building	318.07
	Moosic1	5/11/2017	East Window	Residential building	27.44
	Dickson3	6/30/2017	North Window #1	Residential building	53.82
	Dickson4	6/30/2017	North Window #3	Residential building	48.44
	Dickson5	6/30/2017	North Window #4	Residential building	84.77
	Dickson6	6/30/2017	North Window #2	Residential building	64.94
	Marion1	6/30/2017	West Window	Residential building	56.83
	Marion2	6/30/2017	East Window	Residential building	14.64
	Moosic2	6/30/2017	West Window	Residential building	39.94
	Kimberly1	6/30/2017	East Window	Residential building	11.03
	Kimberly2	6/30/2017	West Window	Residential building	20.72
	Main1	6/30/2017	North Entrance	Commercial building	35.79
	Green Ridge2	6/30/2017	West Entrance	Commercial building	36.59
	Foster2	6/30/2017	West Window #2	Residential building	133.20
	Monroe1	10/7/2017	North Window	Shopping Plaza	248.29
	Green Ridge3	10/7/2017	South Window	Shopping Plaza	115.39
	Wyoming1	10/7/2017	East Window	Commercial building	4.31
Vine1	10/7/2017	South Window	Commercial building	21.22	
Keyser1	10/7/2017	South Window	Commercial building	159.65	

	Keyser2	10/7/2017	East Window	Shopping plaza	146.39
--	---------	-----------	-------------	----------------	--------

Table S2. Sample site latitude and longitude

Sample Name	Latitude	Longitude
Lafayette1 & 2	42.998857	-76.127750
CST1	43.037497	-76.130304
CST2	43.037756	-76.130315
LSC1	43.038101	-76.130347
MacNaughton1	43.037717	-76.137489
White1	43.037517	-76.137434
Carrier Dome K1	43.036682	-76.137393
Irving1-4	43.036893	-76.138380
White 2	43.036784	-76.137414
White 3	43.037090	-76.137564
Jefferson1	43.046907	-76.150454
Almond1	43.048875	-76.141864
Erie1	43.053931	-76.099861
Ainsley1	43.011284	-76.131592
Lafayette3	42.998943	-76.129270
Dickson1-6	41.430456	-75.652049
Green Ridge1	41.428156	-75.649634
Foster1&2	41.428003	-75.670334
Green Ridge2	41.428357	-75.649990
Marion1&2	41.426824	-75.651470
Moosic1&2	41.363250	-75.729398
Kimberly1&2	41.341851	-75.773579
Main1	41.371640	-75.733483
Monroe1	41.420887	-75.643314
Green Ridge3	41.432335	-75.655353
Wyoming1	41.422536	-75.650019
Vine1	41.413988	-75.663511
Keyser1	41.428675	-75.692670
Keyser2	41.443965	-75.667738

A.1.2 Ion Chromatography Standards

Table S3: Ion concentrations in ion chromatography standards

Ion	Concentration (ppm)				
	Standard 1	Standard 2	Standard 3	Standard 4	Standard 5
Fluoride	0.05	0.10	0.25	0.50	1.00
Chloride	0.50	2.00	20.00	50.00	150.00
Bromide	0.01	0.03	0.10	0.50	1.00
Sulfate	0.05	0.10	1.00	10.00	50.00
Nitrate	0.01	0.10	1.00	5.00	20.00
Sodium	1.00	10.00	20.00	100.00	150.00
Potassium	0.10	0.50	1.00	2.00	5.00
Calcium	0.10	1.00	10.00	50.00	100.00
Magnesium	0.05	0.10	1.00	5.00	20.00
Ammonium	0.01	0.05	0.10	0.50	1.00

A.1.3 Determination of Ion Outliers

Several samples had much higher grime masses compared to the rest of the samples. These samples were visually much dirtier compared to the others though they only appeared to consist of dirt and grit rather than any biological material. White1 (73.1 mg), McNaughton1 (76.5 mg), Almond1 (217.3 mg) and Jefferson1 (57.9 mg) in Syracuse, and Foster1 (118.2 mg), Monroe (86.5 mg), Keyser1 (92.7 mg) and Keyser2 (85.0 mg) in Scranton.

Table S4: Ionic fractions for both high and low samples

	Low [ion]	High [ion]
Sodium Conc.(ppm)	31.054 ± 10.942	34.913 ± 1.723
Calcium Conc.(ppm)	26.082 ± 13.220	7.145 ± 0.836
Magnesium Conc.(ppm)	2.526 ± 2.135	0.363 ± 0.081

Potassium Conc.(ppm)	1.655 ± 0.966	0.284 ± 0.115
Chloride Conc.(ppm)	15.527 ± 8.916	48.882 ± 0.964
Sulfate Conc.(ppm)	14.286 ± 6.373	6.453 ± 0.227
Nitrate Conc.(ppm)	8.709 ± 9.657	1.838 ± 3.084

A.1.4 Ion correlations

Correlations between ion pairs were investigated by plotting ion masses against each other (Figure 6 in the manuscript, and Figures S1 and S2 in the SI). Some samples were determined to be outliers for one or more ions. In Syracuse, the ionic distribution of Jefferson1 was very different from all others. It had the largest ionic contribution from NO_3^- of all samples (47%, compared to a mean (and median) of 9.6% (5.4%)), and the lowest contribution from Na^+ (2.9% vs. mean (median) 30.2% (32.5%)), Ca_2^+ (1.9% vs. 21.8% (18.2%)), Mg_2^+ (0.07% vs. 2.0% (1.3%)), and K^+ (0.08% vs. 1.4% (1.2%)). Jefferson1 was therefore not included in the correlation analysis. Lafayette3 was determined to be an outlier for K^+ , with a contribution of 4.5%, compared to a mean (median) of 1.4 % (1.2%); this sample was not considered for correlations involving K^+ . Ion pairs were classified as being correlated when linear regression line of the correlation plot (Figures S1 and S2) produced $R^2 > 0.75$. The ion pairs that were not correlated (i.e., ion pairs involving NO_3^-) all had $R^2 < 0.60$. The threshold for correlation in the smaller concentration range (that did not include White1, McNaughton1, and Almond1) was $R^2 > 0.60$ for all pairings except those involving SO_4^{2-} . $\text{Na}^+ - \text{SO}_4^{2-}$ and $\text{K}^+ - \text{SO}_4^{2-}$ were considered correlated despite having R^2 of 0.58 and 0.51, respectively. In both cases, the fit was made worse by high $[\text{SO}_4^{2-}]$ at Carrier Dome K1; removal of this data point increased the fits to $R^2 = 0.85$ for $\text{Na}^+ - \text{SO}_4^{2-}$ and $R^2 = 0.77$ for $\text{K}^+ - \text{SO}_4^{2-}$. Ion pairs that did not correlate in the smaller concentration range had $R^2 < 0.40$.

In Scranton, the ionic distribution of Monroe1 was different from distributions in other samples. It had the lowest contributions from Na⁺ and Cl⁻, and the highest contributions from Ca²⁺ and SO₄²⁻. This sample was not included in the correlation analysis. Keyser1 was determined to be an outlier for K⁺, contributing only 0.4% to ionic mass compared to the mean (median) of 3.2% (2.7%). This sample was not included for correlations involving K⁺. Several ion pairs were only considered correlated after a single data point (from either Keyser1 or Green Ridge3) was removed. Removing the Keyser1 sample improved correlations for Cl⁻ – Ca²⁺ (with R² increasing from 0.66 to 0.91), and Mg²⁺ – SO₄²⁻ (with R² increasing from 0.73 to 0.87). Removing Green Ridge3 from consideration increased R² for correlations of K⁺ with Mg²⁺ (from 0.77 to 0.86), SO₄²⁻ (from 0.74 to 0.81), and NO₃⁻ (from 0.58 to 0.84). Cl⁻ – SO₄²⁻ was considered correlated after the removal of both Keyser1 and Green Ridge3 (with R² increasing from 0.44 to 0.88). Ions that were considered correlated had R² > 0.81. The non-correlating ion pair (K⁺ – Cl⁻) had R² = 0.69.

Table S5: Ionic masses for Syracuse, NY

Sample	Ionic concentration (ppm)							
	Sodium	Calcium	Magnesium	Potassium	Chloride	Sulfate	Nitrate	Total
Irving1	1.12	0.35	0.03	0.033	0.28	0.29	0.005	2.11
Irving2	1.23	0.51	0.04	0.029	0.20	0.47	0	2.48
Ainsley1	1.74	2.14	0.34	0.15	0.49	0.22	0.026	5.12
Irving3	1.89	1.57	0.10	0.066	0.76	1.31	0.26	5.96
Irving4	1.93	1.57	0.13	0.078	0.35	1.26	0.061	5.40
White2	2.40	1.19	0.08	0.061	1.15	0.70	0.41	5.98
Erie1	2.81	10.69	0.47	0.31	0.81	2.33	1.19	18.63
CST2	2.90	4.88	0.84	0.27	0.93	1.78	0.025	11.63
CST1	3.67	7.89	1.16	0.28	2.83	2.42	2.46	20.74
LSC1	4.84	2.72	0.40	0.20	4.63	1.03	1.08	14.90
Lafayette3	4.86	1.58	0.17	0.63	0.87	2.34	3.37	13.86
White3	9.14	5.54	0.21	0.27	8.87	3.82	3.18	31.05
Carrier Dome K1	9.26	5.92	0.49	0.46	10.54	10.54	1.70	38.91

Lafayette1	9.89	12.88	0.53	0.75	10.86	4.63	11.74	51.32
Lafayette2	13.44	6.87	0.41	0.51	13.35	4.94	16.99	56.56
Jefferson1	2.90	1.92	0.066	0.076	27.81	19.93	47.26	100.18
White1	128.22	28.74	1.53	1.47	182.50	23.74	0.36	366.77
MacNaughton1	150.03	30.26	1.65	1.14	200.95	25.47	0.066	409.77
Almond1	306.10	57.35	2.48	1.58	441.58	61.54	49.82	922.86

Table S6: Ionic masses for Scranton, PA

Sample	Ionic concentration (ppm)							
	Sodium	Calcium	Magnesium	Potassium	Chloride	Sulfate	Nitrate	Total
Wyoming1	1.32	0.27	0.022	0.11	0.60	0.16	0.013	2.50
Kimberly1	1.21	0.20	0.0097	0.046	0.41	0.41	0.34	2.62
Main1	1.43	0.60	0.047	0.093	0.43	0.66	0.25	3.50
Vine1	1.64	0.56	0.069	0.14	0.67	0.48	0.14	3.70
Moosic1	1.47	0.83	0.10	0.18	0.29	0.37	0.66	3.89
GreenRidge1	1.17	0.94	0.05	0.30	0.26	0.39	1.16	4.27
GreenRidge2	1.86	0.65	0.046	0.30	0.55	0.93	1.02	5.35
Marion2	1.70	0.53	0.028	0.14	0.43	1.77	0.92	5.50
Moosic2	2.00	0.62	0.047	0.21	0.53	0.99	1.41	5.81
Marion1	3.18	1.90	0.18	0.71	1.30	1.75	0.23	9.24
Dickson3	4.83	2.55	0.21	0.43	0.56	1.61	1.13	11.33
Dickson6	3.97	0.80	0.073	0.50	1.26	2.01	3.12	11.73
Dickson4	4.03	1.26	0.14	0.35	0.90	1.83	5.75	14.25
Kimberly2	4.68	1.65	0.16	0.40	0.55	5.39	4.38	17.21
Dickson5	5.01	2.11	0.29	0.71	1.04	2.11	8.25	19.51
Dickson1	5.81	3.10	0.36	0.65	1.35	1.65	8.05	20.97
Dickson2	12.06	4.88	0.61	0.91	3.08	4.37	20.73	46.64
Keyser2	16.77	3.50	0.37	1.23	1.41	9.13	23.16	55.57
Foster2	16.45	3.27	0.38	0.80	4.04	9.56	28.09	62.59
GreenRidge3	20.17	21.71	0.55	1.82	42.13	9.06	6.48	101.92
Monroe1	15.26	33.85	2.47	1.44	3.43	49.87	41.47	147.79
Foster1	50.90	9.48	2.15	0.75	38.49	15.30	48.63	165.70
Keyser1	44.37	13.61	1.56	2.02	19.53	25.14	69.90	176.12

A.1.5 Seasonal Variations in Ion Content

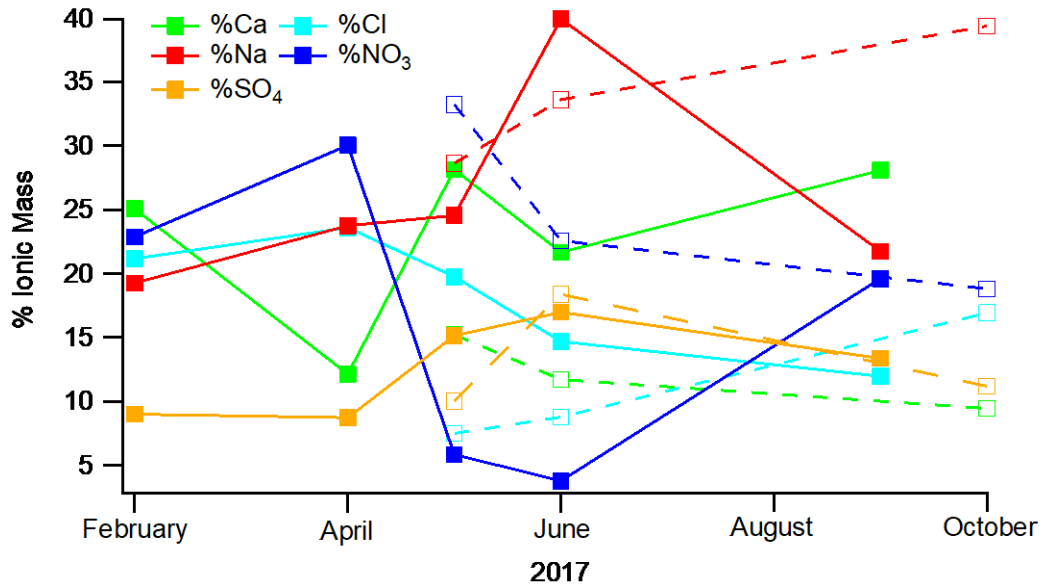


Figure S1: Time series of ionic mass fraction. Syracuse (solid squares), Scranton (open squares)

A.1.6 Absorbance of Grime Solutions

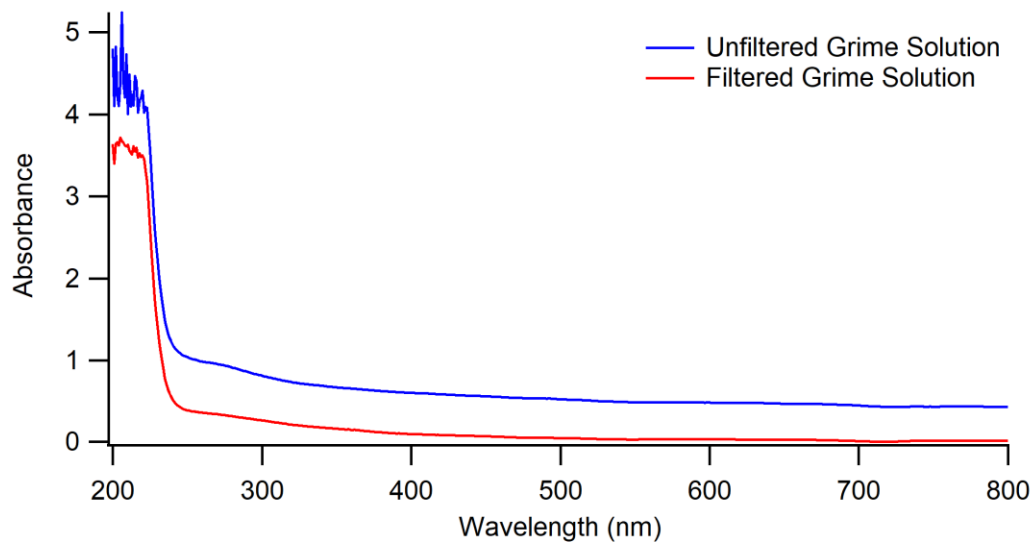


Figure S2: Absorbance plot showing a comparison between filtered and unfiltered measurements of the same sample

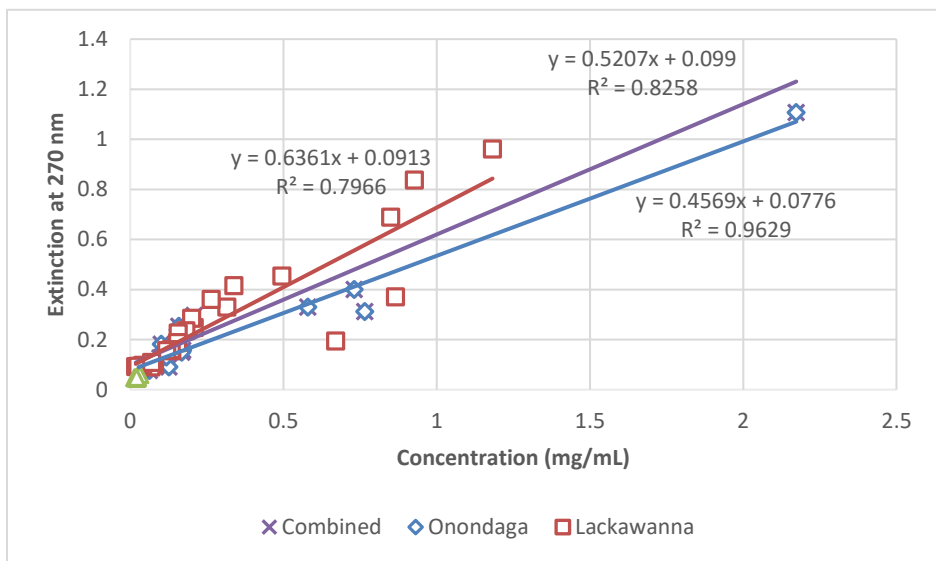
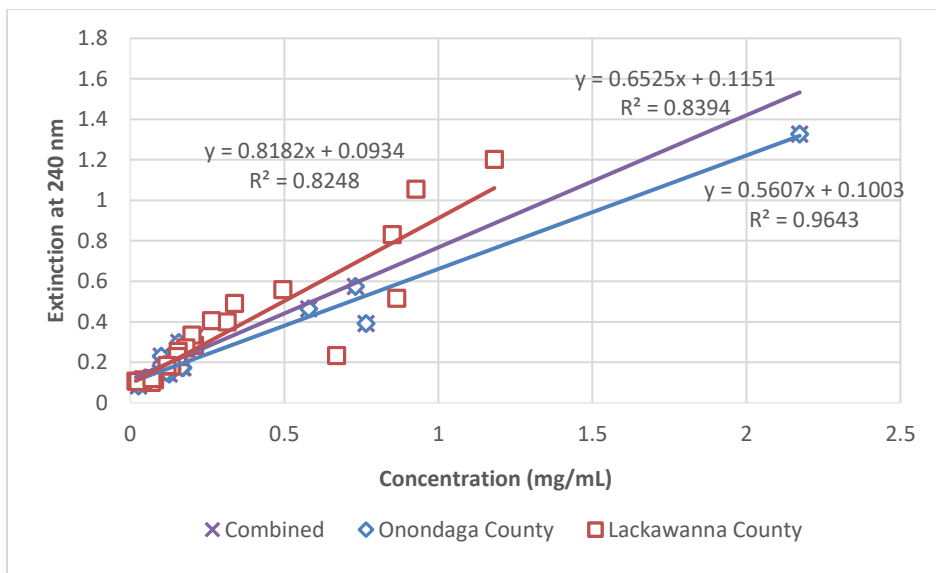


Figure S3: Extinction vs. Concentration plots for samples at 240 and 270 nm

A.1.7 Determination of AAE

Wavelength-resolved light extinction of 19 Syracuse grime samples were averaged; exponential fitting was applied to the mean Syracuse extinction with respect to wavelength. The exponent obtained from curve fitting is referred to as the city-averaged absorption Angstrom exponent (AAE). City-averaged AAE was also derived for Scranton based on 22 grime samples.

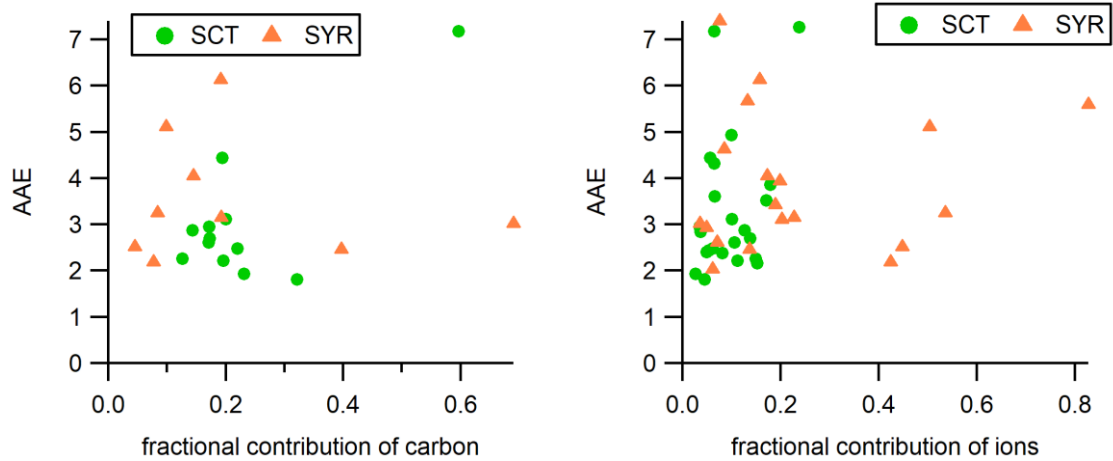


Figure S4: Effect of sample carbon and ionic fractions on absorption Angstrom coefficient (AAE).

COREY R. KROPTAVICH

kroptavichc2@gmail.com | (570)903-0247
67A Ball Road, Syracuse, NY 13215

EDUCATION	Bachelor of Science, Forensic Chemistry, University of Scranton, Scranton, PA <ul style="list-style-type: none">• Minors in Criminal Justice & Arabic• GPA: 3.48 in major, 3.60 overall Coursework Completed: <ul style="list-style-type: none">• General Chemistry and Analytical Chemistry I & II; General Chemistry and Analytical Chemistry Lab I & II; General Biology I & II; General Biology Laboratory I & II; Organic Chemistry I & II; Organic Chemistry Lab I & II; General Physics I & II; General Physics Lab I & II; Biochemistry I; Biophysical Chemistry I & II; Biophysical Chemistry Lab I & II; Inorganic Chemistry; Instrumental Analysis; Instrumental Analysis Lab; Environmental Chemistry; Advanced Inorganic Chemistry; Forensic Chemistry; Forensic Chemistry Lab	June 2014
	Master of Professional Studies, Forensic Science, The Pennsylvania State University, State College, PA <ul style="list-style-type: none">• Forensic chemistry concentration• GPA: 3.29 Coursework Completed: <ul style="list-style-type: none">• Chromatography and Electrochemistry; Scientific Crime Scene Investigation; Crime Scene Investigation Lab; Forensic Science Seminar; Drug Chemistry and Toxicology; Courtroom Proceedings and Testimony; Criminalistics: Trace Evidence; Forensic Chemistry; Criminalistics: Biological Evidence; Ethics in Forensic Science; Forensic Chemistry II; Criminalistics III, Sociology of Deviance	May 2016
RESEARCH	Moorehead Group, Forensic Science Department, Pennsylvania State University, State College, PA <ul style="list-style-type: none">• Principal Investigator: Mr. Wayne Moorehead• Characterized the natural byproducts of smokeless powders due to temporal decay	September 2014 – May 2016

RESEARCH, CONT.	<p>Kahan Group, Chemistry Department, Syracuse University, Syracuse, NY</p> <ul style="list-style-type: none"> • Principal Investigator: Dr. Tara Kahan • Characterized the physical and chemical properties of urban grime, including comparative compositional studies thereof between urban centers • Measured the concentrations of atmospheric oxidant species within vehicle cabins 	January 2017 – Present
PROFESSIONAL DEVELOPMENT	<p>Pittsburgh Conference on Analytical Chemistry and Applied Spectroscopy</p> <ul style="list-style-type: none"> • National meeting attendee; New Orleans, LA; March 2015 <p>Society for Environmental Toxicology and Chemistry North America 40th Annual Meeting</p> <ul style="list-style-type: none"> • Continental meeting attendee; Toronto, ON; November 2019 	
PRESENTATIONS AND PAPERS	<p>Kroptavich, C., Zhou, S., Kowal, S., Kahan, T. (2019, November). <i>The Concentration of Atmospheric Pollutants in Vehicle Cabins</i>. Poster session presented at the annual North American meeting of the Society for Environmental Toxicology and Chemistry, Toronto, ON.</p> <p>Kroptavich, C., Zhou, S., Kowal, S., Kahan, T., <i>Physical and Chemical Characterization of Urban Grime Sampled from Two Cities</i>. ACS Earth and Space Chemistry 2020 4(10), 1813-1822</p>	

- WORK EXPERIENCE** **Course Assistant**, Chemistry Department, Pennsylvania State University, State College, PA August 2014 – May 2016
- CHEM 111: Experimental Chemistry I, Supervisor: Dr. Joe T. Keiser, (814)863-3209
 - Taught basic chemistry laboratory practices, supervised student classwork, and provided guidance where necessary
 - CHEM 425: Chromatography and Electrochemistry, Supervisor: Dr. Dan G. Sykes, (814)863-0796
 - Taught use of gas chromatography, liquid chromatography, capillary electrophoresis, and mass spectroscopy, supervised student classwork, and provided guidance where necessary
 - CHEM 427W: Forensic Chemistry, Supervisor: Dr. Dan G. Sykes, (814)863-0796
 - Taught use of UV-vis spectroscopy, fluorescence spectroscopy, IR spectroscopy, IR microscopy, microcrystal tests, color tests, supervised student classwork, and provided guidance where necessary
- Course Assistant**, Chemistry Department, Syracuse University, Syracuse, NY August 2016 – December 2019
- CHE 106: General Chemistry Lecture I, Supervisor: Dr. Timothy Korter, (315)443-0269
 - Supervised student classwork, and provided guidance where necessary
 - CHE 107: General Chemistry Laboratory I, Supervisor: Mr. Gary Bonomo, (315)443-7500
 - Taught basic chemistry laboratory practices, supervised student classwork, and provided guidance where necessary
 - CHE 347: Physical-Analytical Chem Laboratory, Supervisor: Dr. Joseph Chaiken, (315)443-4285
 - Taught use of UV-vis spectroscopy, fluorescence spectroscopy, IR spectroscopy, Raman spectroscopy, supervised student classwork, and provided guidance where necessary
 - CHE 357: Physical Chemistry Laboratory, Supervisor: Dr. Bruce Hudson, (315)443-4285
 - Taught use of UV-vis spectroscopy, fluorescence spectroscopy, IR spectroscopy, Raman spectroscopy, Gaussian computational software, supervised student classwork, and provided guidance where necessary

WORK EXPERIENCE, CONT. **Research Assistant**, Chemistry Department, Syracuse University, Syracuse, NY January 2020 - Present

- Kahan Research Group, Supervisor: Dr. Tara Kahan
- Conducted characterization studies in atmospheric chemistry, maintained laboratory equipment and instruments, collaborated cross-functionally with extra-departmental research contributors, interfaced with department administration regarding laboratory and research needs